1-1-2011

Functional Comparison Of Immunoglobulin G Versus Oxidized Low-Density Lipoprotien Phagocytic Receptors In Human U937 Macrophages

David T. Vance
Ryerson University

FUNCTIONAL COMPARISON OF IMMUNOGLOBULIN G VERSUS OXIDIZED LOW-DENSITY LIPOPROTEIN PHAGOCYTIC RECEPTORS IN HUMAN U937 MACROPHAGES

by

David Thomson Vance

B.Sc., University of Guelph, 2008

A thesis

presented to Ryerson University

in partial fulfillment of the

requirements for the degree of

Master of Science

in the program of

Molecular Science

Toronto, Ontario, Canada, 2011

Author's Declaration

I hereby declare that I am the sole author of this thesis.

I authorize Ryerson University to lend this thesis to other institutions or individuals for the purposes of scholarly research.

_____

I further authorize Ryerson University to reproduce this thesis by photocopying or by other means, in total, or in part, at the request of other institutions or individuals for the purpose of scholarly research.

_____

FUNCTIONAL COMPARISON OF IMMUNOGLOBULIN G VERSUS OXIDIZED LOW-DENSITY LIPOPROTEIN PHAGOCYTIC RECEPTORS IN HUMAN U937 MACROPHAGES

David Thomson Vance

Master of Science, Molecular Science, Ryerson University, 2011

ABSTRACT

Phagocytic macrophages bind to solid oxidized low-density lipoprotein (oxLDL) deposited on the arterial intima, differentiate into foam cells and cause atherosclerosis —the largest cause of mortality in Canada. The mechanism of oxLDL internalization was examined in vitro using differentiated U937 cells exposed to latex microbeads coated with oxLDL or Immunoglobulin G (IgG). Bead internalization was quantified using immunofluorescent staining and laser confocal assays. IgG-mediated engulfment was more rapid than oxLDL-mediated engulfment indicating a qualitatively different internalization pathway. The filamentous actin inhibitors Cytochalasin D (10µM) and Latrunculin B (5µM) completely inhibited phagocytosis of both oxLDL-coated and IgG-coated beads. The Src and Spleen tyrosine kinase inhibitor 3,4-methylenedioxy-beta-nitrostyrene (20 µM), the phospholipase C inhibitor U73122 (5 µM), and the Janus kinase inhibitor AG 490 (25 µM) displayed significant inhibitory effects on the phagocytosis of both IgG and oxLDL microbeads. The specific isoforms of oxLDL and IgG receptor associated enzymes were determined by nano LC-ESI-MS/MS with an LTQ ion trap.

ACKNOWLEDGEMENTS

I would like to extend my thanks to my supervisor John Marshall for his thorough involvement and guidance throughout every aspect of this project. I consider myself fortunate to have had this opportunity.

I would like to acknowledge the significant contributions of Angelique Florentinus, Peter Bowden and Monika Tucholska and thank them for their adroit assistance.

I would also like to thank my supervisory committee members Roberto Botelho and Marie Killeen for their insight and suggestions, Narendra Tandon for his α-CD36 antibody, the Sergio Grinstein laboratory and Andy Jankowski for his preliminary oxLDL internalization work.

Finally, I would also like to thank my family and friends for their support and understanding.

TABLE OF CONTENTS

INDEX OF TABLES

INDEX OF FIGURES

INDEX OF APPENDICES

LIST OF SELECTED ABBREVIATIONS

acLDL	acetylated low-density lipoprotein
ACN	acetonitrile
ATF2	activating transcription factor 2
CD36	cluster of differentiation 36
CDC42	cell division control protein 42 homolog
CLA-1	CD36 and LIMPII analogous-1
Cy	cyanine
DIC	differential interference contrast
DMSO	dimethyl sulfoxide
dSR-CI	*Drosophila* macrophage scavenger receptor class C type I
EDTA	ethylenediaminetetraacetic acid
Erk	extracellular signal-related protein kinase
FAK	focal adhesion kinase
FBS	fetal bovine serum
$F_c\gamma R$	fragment crystallizable γ receptor
HEPES	N-2-Hydroxyethylpiperazine-N'-2-ethanesulfronic Acid
HMGCR	3-hydroxy-3-methyl-glutaryl-CoA reductase
IgG	immunoglobulin G
ITAM	immunoreceptor tyrosine-based activation motif
Jak	janus kinases
Jnk	c-Jun N-terminal protein kinase
LOX-1	lectin-type oxidized low-density lipoprotein receptor 1
Lyn	V-yes-1 Yamaguchi sarcoma viral related oncogene homolog
MAPK	mitogen activated protein kinase
MARCO	macrophage receptor with collagenous structure
MEKK2	MAPK/ERK kinase kinase 2
NADPH	nicotinamide adenine dinucleotide phosphate
NF-κB	nuclear factor kappa-light-chain-enhancer of activated B cells
nLDL	native LDL
oxLDL	oxidized low-density lipoprotein
p130Cas	Crk-associated substrate p130
PAP1	phosphatidate phosphatase
PBS	phosphate buffered saline
PI3K	phosphoinositide 3-kinase
PKC	protein kinase C
PLC	phospholipase C
PLD	phospholipase D
PMA	phorbol 12-myristate 13-acetate
Pyk	proline-rich tyrosine kinase
Rho GEF	rho guanine nucleotide exchange factor
ROS	reactive oxygen species
RPMI	roswell park memorial institute
SDS-PAGE	sodium dodecyl sulphate polyacrylamide electrophoresis
SH2	Src Homology 2
SHP-1	src homology 1-containing phosphotyrosine phosphatase

LIST OF SELECTED ABBREVIATIONS (CONTINUED)

SRA	scavenger receptor A
STAT	signal transducer and activator of transcription
Syk	spleen tyrosine kinase
Th1	T helper cell 1
Th2	T helper cell 2
TIC	total ion current
TLR	toll-like receptor

INTRODUCTION

The Beginnings of Atherosclerosis

Atherosclerosis is an inflammatory disease of great epidemiological significance. Cholesterol and triglycerides are transported to peripheral tissues from the liver through the blood in phospholipid protein complexes called low-density lipoprotein (LDL). These complexes are manufactured in the liver from lipids obtained from the intestine via chylomycrons.

LDL is approximatey 22 nm in diameter, 3 MDa in mass and composed of triglyceride, esterified and unesterified cholesterol, phosphlipid and apolipoprotein B-100 (ApoB-100) (Figure 1) (Segrest et al., 2001; Mohty et al., 2008). A variety of tissues possess LDL receptors which participate in the normal internalization and use of LDL (Srivastava et al., 1995).

Atherosclerosis is believed to be a result of large amounts of plasma LDL overwhelming the native LDL receptors' ability to internalize it. This is consistent with evidence that high LDL levels constitute a significantly increased risk for cardiovascular disease and the knockout of murine LDL receptors results in lowered LDL uptake and increased levels of LDL and atherosclerosis in response to a high fat diet (Glass and Witztum, 2001; Ishibashi et al., 1993). Additionally, humans with mutations in the LDL receptor or its putative adaptor protein also display hypercholesterolemia (Varret et al., 2008; Garcia et al., 2001).

Excess LDL is capable of crossing the arterial intima and becoming trapped in the subendothelial space—primarily in the large vessels (Glass and Witztum, 2001; Febbraio et al., 2001). Here they can become modified by proteoglycans, lipases or by glycosylating enzymes (Aviram, 1993). Modified LDL is initially bound to the arterial intima in part by proteoglycans. However once this atherosclerotic fatty streak is established the role of LDL attachment is

shifted to macrophage secreted lipoprotein lipase (Pentikainen et al., 2002). The binding of modified LDL to the arterial intima represents the first step in the onset of atherosclerosis.

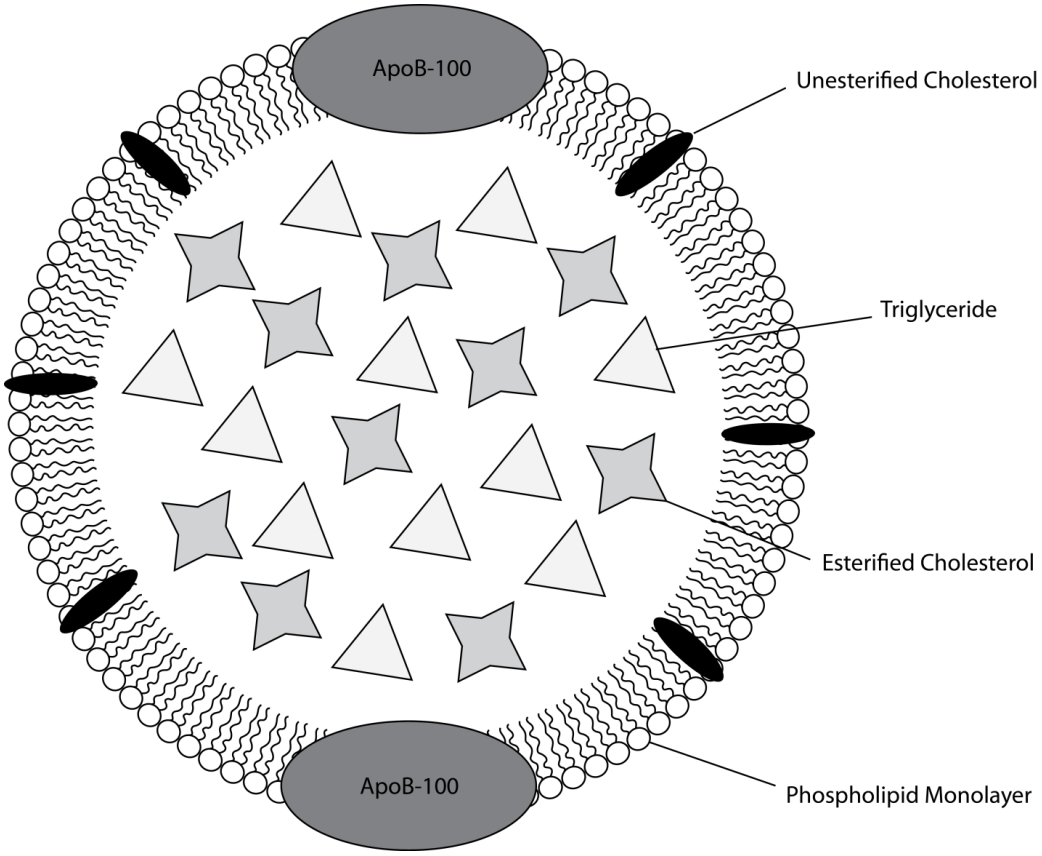

Figure 1: Low-density lipoprotein schematic. Adapted from Milioti et al., 2008.

Oxidized Low-Density Lipoprotein

Of particular interest to the formation of an atherosclerotic lesion is the oxidation of LDL, a process that can be mediated by nitric oxide, myeloperoxide or 7-lipooxygenase (Podrez et al., 2000). Once LDL becomes oxidized it is no longer recognized by the native LDL receptor and gains an affinity for the Class B scavenger receptor CD36 leading to its accumulation in CD36-expressing macrophages (Glass and Witztum, 2001).

It is well established that the internalization of oxLDL by monocyte-derived macrophages is a key event in the progression of atherosclerosis (Glass and Witztum, 2001) (Bobryshev, 2006). In particular, the role of macrophages is also supported by evidence that disrupting the macrophage colony-stimulating factor gene of pro-atherogenic ApoE mice significantly decreases the size and incidence of atherosclerotic lesions while increasing serum cholesterol levels (Smith et al., 1995; Qiao et al., 1997). Additionally, in pig arteries, progressing atherosclerotic lesions sequester monocyte-derived cells whereas they emigrate from improving lesions (Daoud et al., 1981; Llodrá et al., 2004).

Lipids from oxLDL accumulate inside CD36-expressing macrophages but are not adequately metabolized (Glass and Witztum, 2001). This precipitates the cell's differentiation into a foam cell, the characteristic cell type of atherosclerosis, typified by a large vacuolated appearance, low mobility and the release of pro-inflammatory cytokines and reactive oxygen species (ROS) (Bobryshev, 2006). Unable to deal with this lipid-induced stress, foam cells eventually die by necrosis or apoptosis leading to the release of more cytokines and the unprocessed oxLDL.

The release of ROS oxidizes additional LDL and cytokine release attracts other leukocytes such as Th1 and Th2 which secrete additional cytokines that exacerbate inflammation. Cytokine release also attracts monocytes which differentiate into macrophages (Glass and Witztum, 2001). These macrophages attempt to internalize the apoptotic bodies and free lipid and eventually succumb to the same fate as their predecessors thus participating in an inflammatory feedback loop (Figure 2) (Bobryshev, 2006).

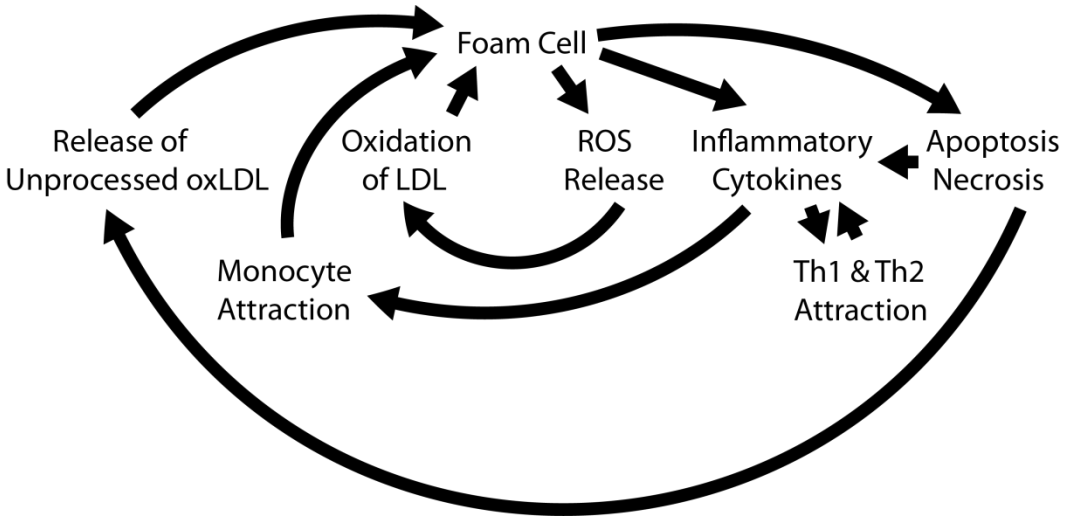

Figure 2: Outline of selected foam cell-related proatherogenic positive feedback loop mechanisms

Complicating proatherogenic mediators include lysophosphatidic acid and platelet activating factor both of which decreased the mobility of monocytes (Llodrá et al., 2004). oxLDL uptake is also enhanced in vitro and in vivo in rat macrophages by C-reactive protein concomitant with increased intracellular accumulation of cholesterol ester and matrix metalloproteinase secretion (Singh et al., 2008). Additionally, there is evidence to suggest that chronic intracellular infection by chlamidia pneumonia may exacerbate this inflammation and the ability of cells to degrade LDL (de Kruif et al., 2005).

Monocytes, macrophages, foam cells, necrotic and apoptotic cell debris and deposited lipid form an atheromatous plaque in the subendothelial space which is eventually covered by a cytokine-induced smooth muscle cell sheath. Inflammatory cytokines spur smooth muscle cells to infiltrate the medial portion of the arterial lumen and secrete extracellular matrix components giving rise to the fibrous plaque (Glass and Witztum, 2001). As the level of inflammation grows by feedback so does the size of the plaque (Ross, 1999).

Narrowing of the arterial lumen caused by the encroachment of atherosclerotic plaque can cause ischemic events, however thrombosis and infarction from plaque rupture is much more common.

This plaque rupture, caused by macrophage-secreted matrix metalloproteinases and neovascularisation-induced destabilization, exposes previously internal plaque tissue factors and lipid leading to platelet recruitment, clotting and the formation of a thrombus which can cause infarction (Glass and Witztum, 2001). This method of pathogenesis has caused heart disease to be recognized as the leading cause of death in the world (Mathers et al., 2009).

Macrophage Scavenger Receptors

oxLDL is recognized by scavenger receptors present on leukocytes. Scavenger receptors, like *N*-formyl methionine mannose receptors and Toll-like receptors (TLR), are inherited non-self surface receptor components of the innate immune system. They are expressed on professional phagocytes but they are also expressed on aortic smooth muscle cells, neuronal cells, keratinocytes, endothelial cells, dendritic cells and Kupfer cells in varying amounts (Zingg et al., 2000).

Scavenger receptors are divided into 6 major classes: classes A-F. Class A consists of MARCO and SR-AI/II, Class B encompasses CD36 and SR-B1/CLA-1, Class C as of yet only encompasses the *Drosophila* protein dSR-CI. Class D contains Macrosialin (gene product of CD68) Class E contains LOX-1 and Class F contains SREC (Zingg et al., 2000).

The Role of CD36 in Atherosclerosis

oxLDL and other modified lipoproteins are known to interact with multiple scavenger receptors. oxLDL can be internalized by scavenger receptor A (SRA) I/II and CD36 but it can also enter the cell via opsonisation with IgG or IgM anti-oxLDL autoantibodies (Kunjathoor et al., 2002; Tsimikas et al., 2007). However, levels of IgG, IgM or apolipoprotein B immune complexes—while possessing univariate divergent correlations with coronary artery disease—were not independently predictive of coronary artery disease among a group of coronary angiography patients (Tsimikas et al., 2007).

Macrophage CD36 has been identified as the primary pro-atherogenic surface receptor of oxLDL (Collot-Teixeira et al., 2007; Silverstein and Febbraio, 2000; Podrez et al., 2000). Three to eleven percent of Japanese blood donors lack a functional CD36 allele compared to 0.2% among American donors and monocyte-derived macrophages from CD36-deficient (aka Nak deficient) humans show a significant decrease in oxLDL internalization (Yamamoto et al., 1990; Tandon et al., 1989; Nozaki et al., 1995; Janabi et al., 2001). Additionally, CD36-deficient patients exposed to oxLDL displayed significantly less activation of NF-Kappa B and other proinflammatory genes (Janabi et al., 2000). Also, macrophages from CD36-deficient humans show marked resistance to foam cell formation in vitro however the anti-atherogenic effect may be mitigated by a higher prevalence of metabolic syndrome that also accompanies this mutation (Hirano et al., 2003).

While knockout of either CD36 or SR A I/II results in the mitigation of atherosclerotic lesions in mice and dual knockout $CD36^{-/-}$/SRA $I/II^{-/-}$ mice show a 75%-90% decrease in acLDL and oxLDL uptake and degradation and do not display modified lipoprotein cholesterol accumulation, knockout of both SRA I/II and CD36 results in no better protection from murine

atherosclerotic lesion development than CD36 alone (Suzuki et al., 1997; Febbraio et al., 2000; Kunjathoor et al., 2002; Kuchibhotla et al., 2008).

Transfection of CD36 into Human Embryonic Kidney 293 cells leads to strong specific binding to oxLDL followed by uptake. Expression of CD36 in CHO hamster cells elicits susceptibility to oxLDL stress (Endemann et al., 1993)(Rusiñol et al., 2000). Also, lightly oxidized LDL (oxidized for only 4 hours) is readily recognized by CD36 transfected murine 293 cells whereas cells transfected with other scavenger receptors known to bind oxLDL (FcγRII-B2 and the acetylated LDL receptor) require significantly more oxidation (Endemann et al., 1993).

Samples of human atherosclerotic aorta obtained from autopsies reveal that CD36 is expressed more strongly on macrophages at the centre of the atheromatous lipid core. Additionally, multiple ex-vivo models demonstrate that foam cell formation appears to be 60-90% dependent on CD36 (Nakata et al., 1999; Febbraio et al., 2001; Silverstein and Febbraio, 2000).

Cross linking of CD36 with a monoclonal antibody elicits release of H_2O_2—a burst that is also observed when macrophages are exposed to a surface coated with oxLDL (Aiken et al., 1990; Maxeiner et al., 1998). α-CD36 antibody treatment also blocks half of oxLDL binding to human THP macrophages and nearly abrogates foam cell formation in human $CD34^+$ progenitor cells (Endemann et al., 1993; Seizer et al., 2010).

Thus it can be concluded that CD36 is the most significant transporter of oxLDL with regards to atherosclerosis.

CD36 Structure

Encoded on band 11.2 of chromosome 7 the class B scavenger receptor, CD36 consists of 472 amino acids. It is a member of the CD36 family of proteins along with LIMP II, SR-BI/CLA-1, and Emp and is expressed by multiple cells lines such as U937, HEL, THP-1 and C32 (Tao et al., 1996; Tandon et al., 1989)

Largely hydrophilic, CD36 contains two hydrophobic domains believed to span the plasma membrane (Figure 3). Both the N- and C- termini are intracellular with the relatively short sequences GCDRNC and SYCACRSKTIK, respectively.

Each tail contains two cysteine residues that are sites of palmitoylation. This is thought to target CD36 to lipid rafts or caveolae (Tao et al., 1996). However, CD36 does not seem to associate with caveolin-1 in Chinese hamster ovary cells or C32 cells while at rest or while internalizing fluid-phase oxLDL. It does, however, reside in lipid rafts and relatively homogenously throughout the membrane in these cells (Zeng et al., 2003a).

At 88 KDa CD36 is highly N-glycosylated compared to 53 KDa unglycosylated (Serghides et al., 2003; Hoosdally et al., 2009). This glycosylation might mediate association with lectins.

CD36 has a high affinity for a conserved group of oxidized choline glycerophospholipids that allow it to bind to oxLDL (Podrez et al., 2002). This binding site is located at 155-183 aa. This region also binds apoptotic neutrophils, the synthetic growth hormone-releasing peptide heraxelin, advanced glycation endproducts and monoclonal antibodies (Collot-Teixeira et al., 2007).

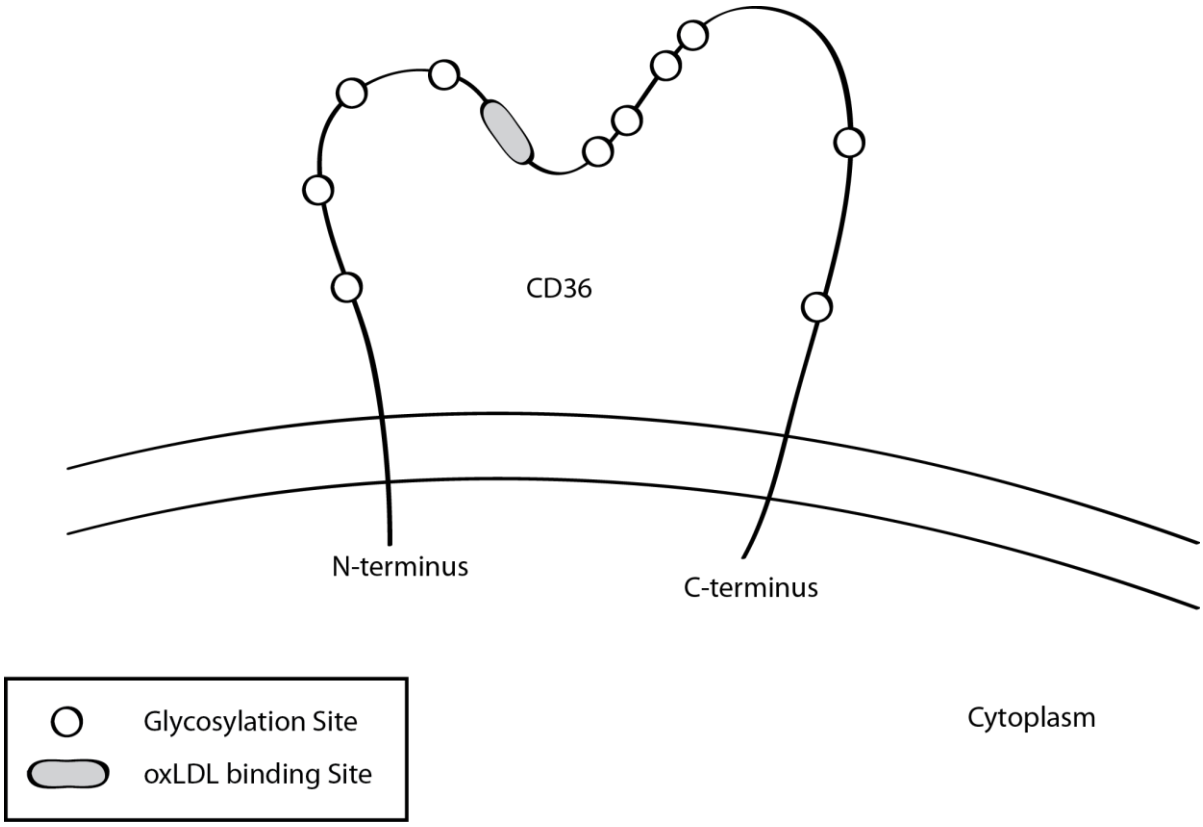

Figure 3: CD36 membrane protein schematic. N-linked glycosylation sites predicted from sequence. Adapted from Collot-Teixeira et al. 2007.

CD36 also binds erythrocytes infected with plasmodium falciparum, collagen, native LDL, vLDL and HDL, β-amyloid fibrils and apoptotic cells (Yamada et al., 1998; Calvo et al., 1998; Coraci et al., 2002). It acts as a fatty acid translocase involved in plasmalemmal fatty acid transport (such as long-chain fatty uptake acids from lipoprotein) as well as a mediator of platelet-platelet binding (van der Vusse et al., 2002; Zingg et al., 2000; Yamada et al., 1998; Tandon et al., 1989). Amino acids 93-120 (CD36 LIMP-II Emp sequence homology binding site) bind thrombospondin 1 and 2 along with a.a. 146-164 or 145-171 which also bind *Plasmodium falciparum* (Collot-Teixeira et al., 2007).

CD36 Signalling

Significant data has been published concerning the signalling mechanisms of CD36. Additionally, CD36 seems to recruit different kinases depending on the cell type in which it is expressed (Rahaman et al., 2006).

Several foam cell-forming oxLDL internalization methods have been proposed including phagoctosis (Chou et al., 2009), endocytosis (Zeng et al., 2003b) and macropinocytosis (Kruth et al., 2005; Jones and Willingham, 1999; Jones et al., 2000). However macropinocytosis and conventional endocytosis theories are contradicted by reports of insensitivity to PI3K or Na/H exchange inhibitors and dominant-negative dynamin transfections, respectively (Collins et al., 2009).

CD36 might regulate binding and activate migration internalization and degradation pathways through spatial association with integrins Rho GEFs and Pyk/Fak kinases and use these molecules to signal (Prieto et al., 1994). It has been demonstrated that members of the Vav family of guanine nucleotide exchange factors become phosphorylated upon exposure to oxLDL in a CD36 dependent manner and deletion of Vav can decrease oxLDL uptake and foam cell formation in murine peritoneal macrophages (Rahaman et al., 2011).

CD36 associates with the tetraspannin CD151 and $\alpha_3\beta_1$ and $\alpha_6\beta_1$ integrins in C32 melanoma cells via the extracellular domain (Thorne et al., 2007; Thorne et al., 2000). It also associates with the tetraspannin CD9 and αIIbβ3 and $\alpha_6\beta_1$ integrins on human platelets (Miao et al., 2001).

While membrane bound CD36 usually exists in a monomeric state, it has been found to dimerize upon exposure to thrombospondin (Daviet et al., 1997). It has also been shown to

associate with other co-receptors such as TLR2 in the binding of *Mycobacterium tuberculosis* and *Staphylococcus* and is necessary for the binding and proper immune recognition of Staphylococcal diacylglycerides via the TLR2/6 heterodimer in murine macrophages (Drage et al., 2009; Hoebe et al., 2005).

CD36 has also been found to participate in the heterodimerization of Toll-like receptors 4 and 6 in response to oxLDL and β-amyloid resulting in sterile inflammation (Stewart et al., 2010). However, CD36 mediated foam cell formation in response to oxLDL does not seem to require TLR2 and deletion of TLR2 or SRA in hyperlipidemic mice had no effect on foam-cell formation (Rahaman et al., 2006).

CD36 expression is regulated by peroxisome proliferator-activated receptor γ, additionally CD36 activates PPAR-γ (Lee et al., 2004; Munteanu et al., 2006). Expression of PPAR-γ and CD36 is highly increased in monocytes by exposure to oxLDL (Kavanagh et al., 2003).

It is hypothesized that the c-terminus is involved in signalling due to homology with several other signalling domains such as those present on CD4 and CD8 (Rahaman et al., 2006). There is evidence of a direct physical association between the carboxy-terminal cytoplasmic tail of CD36 and lyn and MEKK2 within a signalling complex (Rahaman et al., 2006). Additionally, the c-terminus of CD36 is required for oxLDL-mediated tumor necrosis factor-alpha modulation of NF-kappa B (Lipsky et al., 1997).

CD36 from platelets, endothelial and monocytic cell lysate co-precipitates with Fyn Lyn and Yes (Huang et al., 1991; Medeiros et al., 2004; Bull et al., 1994). Lyn's involvement is also consistent with evidence that a lower rate of atherosclerosis is observed in Lyn-deficient mice

and Fyn is activated by thrombospodin-1 via CD36 in microvascular endothelial cells, along with caspase-3 and p38 MAP kinase, leading to a proapoptotic antiangiogenic effect (Miki et al., 2001; Jimenez et al., 2000). Furthermore, oxLDL initiates a platelet activation signalling pathway via CD36 that phophorylates and activates Fyn and Lyn and results in their direct or indirect attachment to CD36 (Chen et al., 2008). Additionally, both (JNK)2 and MKK4 were also phosphorylated in response to oxLDL. Src inhibition reversed this oxLDL-mediated phosphorylation of JNK and both Src and JNK inhibition blocked platelet activation (Chen et al., 2008). Interestingly, Apyrase and RGDS peptide treatment suggested outside-in integrin signals were not required for JNK phosphorylation in these platelets (Chen et al., 2008).

Another study reported CD36-mediated phosphorylation of JNK1 and 2 and their downstream effectors c-Jun and ATF2 in murine macrophages upon exposure to oxLDL but not native LDL (nLDL) and that inhibition of JNK or Src blocked oxLDL uptake and foam cell formation. This study also found no correlation between foam-cell formation and the following: Erk1/2, U0126, Jak, PI3K and PKC (Rahaman et al., 2006). Furthermore, JNK activity is significantly upregulated in atheromas and JNK deletion mitigates atherosclerosis in murine models (Ricci et al., 2004; Metzler et al., 2000).

It has been demonstrated that internalization of oxLDL from the fluid phase by CD36 requires src kinases, c-Jun N-terminal kinases and Rac and/or CDC42 but not PI3K (Collins et al., 2009). Fluid-phase oxLDL, but not nLDL, uptake by macrophages also caused membrane ruffling and the formation of large vacuoles containing relatively small amounts of CD36 compared with smaller vesicles (Jones and Willingham, 1999; Collins et al., 2009).

Macrophage exposure to fluid-phase oxLDL activates FAK in a CD36-dependent manner (Park et al., 2009). CD36 is thought to initiate NADPH oxidase ROS production in response to oxLDL leading to oxidative SHP-1 inactivation and thus sustained FAK activation which in turn leads to actin polymerization and spreading. This is thought to contribute to the trapping of macrophages in the arterial intima leading to foam cell formtion (Park et al., 2009). There is also evidence that CD36 signals to the cytoskeleton and initiates actin polymerization using the scaffold protein p130Cas, Pyk2, paxillin and Fyn via a phosphorylation cascade (Stuart et al., 2007). Correspondingly CD36-mediated fluid phase oxLDL uptake in macrophages was inhibited by Cytochalasin D and Latrunculin B (Collins et al., 2009).

CD36 is also known to associate with Syk in human umbilical vein endothelial cells and microglial CD36 forms a receptor complex with $\alpha_6\beta_1$-integrin and integrin-associated protein (CD47) when binding fibrillar amyloid-β which subsequently activates Syk and NADPH oxidase (Kazerounian et al., 2011; Wilkinson et al., 2006; Bamberger et al., 2003).

There is little evidence forming a direct link between PLC and CD36, however, they are both localized in platelet lipid rafts and PLC becomes activated with the tyrosine kinase phosphorylation associated with platelet activation (Gousset et al., 2004). There is no direct evidence for interaction between CD36 and PLD, however, PLD activation is strongly associated with monocyte-derived macrophage-mediated phagocytosis of *Mycobacterium tuberculosis*, which is in part regulated by CD36 (Kusner et al., 1996). There is no direct link between phosphatidate phosphatase (PAP) and CD36 however both participate in phopholipid recruitment, and propranolol, an inhibitior of PAP-1, has been used to successfully treat diseases related to atherosclerosis (Engelmann and Wiedmann, 2010; Olakowska and Olakowski, 2006).

Lovastatin decreases circulating LDL levels by inhibiting the rate-limiting enzyme 3-hydroxy-3-methyl-glutaryl-CoA reductase (HMGCR) needed for LDL biosynthesis (Endo, 1979). It has also been shown to upregulate the expression of CD36 in some cases (Ruiz-Velasco et al., 2004). However, it is not known whether CD36 affects HMGCR levels or activity.

There is little data on the signalling pathways that regulate CD36 mediated adhesion to solid oxLDL deposited on surfaces. Potential oxLDL internalization signalling pathways were tested using a selection of pharmacological inhibitors targeted to a variety of proteins.

The Fc Gamma Receptor

The Fc Gamma receptor is a well studied leukocytic surface protein that binds to the Fragment, crystallisable (Fc) portion of Immunoglobulin G and initiates phagocytosis of the antibody and the infected cell or pathogen to which it is bound. The activated Fcγ receptor complex has been isolated from the surface of live cells and its binding partners have been successfully identified (Jankowski et al., 2008). It will serve as a control receptor in this study.

The Fcγ receptor is a member of the immunoglobulin superfamily and signals to the cytoplasm mainly via phosphorylation using phosphoinositides, PKC and Rho-family GTPases in distinct phases (Swanson and Hoppe, 2004). Binding of ligand allows Src family kinases to phosphorylate tyrosine pairs on immunoreceptor tyrosine-based activation motifs (ITAMs) allowing the binding of the SH2 domains of Syk (Underhill and Goodridge, 2007). Subsequent phophorylation events regulate actin polymerization, myosin activation, membrane fusion and ROS production allowing the formation of a functioning phagosome (Aderem and Underhill, 1999; Etienne-Manneville and Hall, 2002).

PLD is required for certain functions at the cell membrane such as membrane ruffling and cell migration (O'Luanaigh et al., 2002; Santy and Casanova, 2001). In addition, the PLD product phosphatidic acid localizes to the inner leaflet of the plasma membrane in response to FcγR ligation (Groves et al., 2008). Furthermore, inactivation of PLD isoforms 1 and 2 has been reported to partially impair phagocytosis of IgG-opsonized 3 μm latex beads in RAW264.7 murine macrophages (Corrotte et al., 2006).

PI3K and PLC are both involved in the depletion of the actin assembly and remodelling molecule $PI(4,5)P_2$ at the phagosome (Scott et al., 2005). Inhibition of PI3K and PLC blocks

actin depolymerization around the nascent phagosome (Scott et al., 2005). PI3K was also shown to regulate the pseudopod extender protein Myosin X and the phagocytosis-regulating small g-proteins ADP-ribosylation factor 1 and 6 (Groves et al., 2008). Interestingly phagocytosis of IgG-coated beads smaller than 3 μm was not affected by PI3K inhibition by either Wortmannin or LY294002 (Groves et al., 2008).

In murine RAW 264.7 macrophages PKC-α, δ and ε localize to the plasma membrane during phagocytosis but not necissaily PKC-β or ζ (Larsen et al., 2000). Also, the rate of FcR-mediated phagocytosis in RAW 264.7 macrophages is significantly increased upon PKC-ε overexpression (Larsen et al., 2002).

One study found that the PKC inhibitors H7, staurosporine and calphostin C inhibited IgG-coated 3μm bead internalization by human monocytes (Zheleznyak and Brown, 1992). However another study found that the same PKC inhibitors had no effect on the phagocytosis of IgG-opsonized red-blood cells by murine macrophages (Greenberg et al., 1993). Finally, a later study found the phagocytosis of IgG-opsonized erythrocytes by RAW 264.7 was inhibited by staurosporine and calphostin C (general PKC inhibitors) but not by Gö6976 and CGP 41251 (classic/selective inhibitors) (Larsen et al., 2000).

One study found that cross-linking of Fcγ receptors on human macrophages precipitates the rapid yet transient phosphorylation of Fak (Pan et al., 1999). However, another reported no increased tyrosine phosphorylation of p125Fak during FcγR-mediated phagocytosis in murine macrophages (Greenberg et al., 1994).

Previous studies have found partial inhibition of human monocyte phagocytosis of IgG-opsonized sheep red blood cells using lovastatin (Loike et al., 2004). Fluvastatin, a related

inhibitor of HMGCR, inhibited FcγR signal transduction tyrosine kinase activation, although this was hypothesized to be due to disruption of lipid rafts in monocytes (Hillyard et al., 2004).

There has been no study establishing the requirement of Phosphatidate phosphatase in IgG-mediated phagocytosis. However, PAP may play a part in diacylgycerol production and activation of the NADPH oxidase catalyzed ROS production that is concomitant with phagocytosis (Lennartz, 1999).

There has been some evidence of cross-regulation between ITAM motifs and the cytokine receptor Jak-Signal Transducer and Activator of Transcription (STAT) pathway via Proline-rich tyrosine kinase (Pyk2) (Ivashkiv, 2009; Hu et al., 2007). The Jak/Stat pathway is inhibited by binding of immune complexes to FcγR leading to the suppression of interferon gamma activation, however this does not imply a requirement for phagocytosis (Boekhoudt et al., 2007; Feldman et al., 1995).

RATIONALE

The majority of studies examining the internalization of oxLDL use oxLDL in the fluid phase. However, incubation of macrophages with liquid oxLDL induces a slow (48 hr.) differentiation into foam cell morphology (Shen et al., 2008). As oxLDL deposits on the artery wall it would seem more physiologically relevant to examine the uptake of oxLDL from the solid phase. This distinction is emphasized by evidence that macrophages incubated on oxLDL-coated surfaces release three to four times more H_2O_2 than macrophages incubated on acLDL or nLDL coated surfaces in contrast no H_2O_2 was released upon exposure to fluid-phase oxLDL, nLDL or acLDL (Maxeiner et al., 1998).

Polystyrene microbeads can be coated with various types of ligand and added to in vitro macrophage cultures and easily visualized via microscopic examination. Usefully, protein-coated microbeads that are exterior to the cell can be selectively immunofluorescently stained to determine the extent of bead internalization.

Recent data (Jankowski & Marshall, unpublished) has suggested that RAW 264.7 macrophages presented with oxLDL coated on the surface of a polystyrene microbead rapidly differentiate into foam cells within hours, much faster than when presented with fluid phase oxLDL. Also, it has been established that U937 cells can easily be differentiated into foam cells using oxLDL (Yu et al., 2003).

Intact phagocytic receptor complexes can be isolated from live cells by coating polystyrene microbeads with receptor ligand, allowing cell-bead binding, lysing the resulting mixture and extracting the resultant protein-bound microbeads (Jankowski et al., 2008).

These membrane receptors are key targets for disease treatment and might come together in different combinations to form functionally distinct signalling complexes (Davis, 2007). It is already known that CD36 stably associates with kinases tetraspannins and integrins (Huang et al., 1991; Bamberger et al., 2003; Koenigsknecht and Landreth, 2004; Miao et al., 2001)

It is hypothesized that CD36 will co-segregate in membrane sub-domains with its signalling partners as mass spectrometric evidence demonstrates that phagocytic receptors associate with a large group of membrane-bound receptors upon activation (Jankowski et al., 2008; Marshall et al., 2001). The resulting bead binding partners may be analyzed by nano LC-ESI-MS/MS with an LTQ ion trap to identify possible signalling partners including their various splice variants and isoforms (Jankowski et al., 2008).

Central Hypothesis

The central hypothesis of this research is that oxLDL internalization by macrophages can be quantified and differentiated from other types of phagocytosis using bead based assays and that the identities of specific types of enzymes differentially involved in oxLDL internalization such as SRC, SYK, Janus and PLC can be determined via nano LC-ESI-MS/MS.

Materials and Methods

Antibodies

Monoclonal mouse anti-human CD36 immunoglobulin G (IgG) (clone FA6-152) was purchased from Beckman Coulter (Brea, CA, USA). Monoclonal mouse anti-human CD36 immunoglobulin M (IgM) (clone CB38 [NL07]) was purchased from BD Pharmingen (Franklin Lakes, NJ, USA). Monoclonal mouse anti-mouse CD36 immunoglobulin A (IgA) (clone 63) was purchased from Cascade BioScience (Winchester, MA, USA). Monoclonal mouse anti-human IgG (clone 131.2) was generously provided by Narendra N. Tandon. Polyclonal rabbit anti-Cu^{2+}-oxidized human lipoprotein antibody was purchased from Calbiochem (La Jolla, CA, USA). All secondary antibodies were purchased from Jackson ImmunoResearch (West Grove, PA, USA).

Pharmacological Inhibitors and Reagents

Genestein, Cytochalasin D, LY 294 002, Wortmannin, AG 490, Latrunculin B, AG 1879, 3,4-Methylenedioxy-b-nitrostyrene (MNS), PF 573228, Go6983, propranolol, and human IgG were purchased from Sigma Aldrich (St. Louis, MO, USA). U73122, Lovastatin, BAY 61-3606 and Phorbol 12-myristate 13-acetate (PMA) were purchased from Calbiochem. Ethanol was purchased from Caledon Laboratories (Georgetown, ON). All microspheres were purchased from Bangs Laboratories (Fishers, IN, USA). Oxidized low-density lipoprotein (oxLDL) was prepared by the ultracentrifugation of EDTA-treated human plasma, adjusted to a density of 1.30 g/mL with KBr and overlayed with a 1.006 g/mL NaCl solution, in a TLA110 rotor (Beckman Coulter) at 100 000 rpm at 4°C for one hour. The low-density lipoprotein (LDL) band was extracted and extensively dialyzed against PBS containing 0.5 mM EDTA. Oxidation was performed by

incubating LDL with 5 µM $CuSO_4$ for 16 hours in the dark at 37°C (Shen et al., 2008). Oxidized and unoxidized samples were analyzed for purity blot by western blot.

Cell Culture

Human leukemic U937 cells obtained from the American Type Culture Collection (ATCC, Manassas, VA, USA), were cultured at 37°C at 5% CO_2 in RPMI 1640 medium with L-glutamine (Mediatech, Manassas, VA, USA) supplemented with 10% fetal bovine serum (FBS) (Invitrogen, Carlsbad, CA, USA).

Bead Internalization Assay

In order to quantify the extent of internalization of particles of oxLDL, PMA-treated U937 cells were exposed to 2 µm oxLDL-coated or IgG-coated microspheres and examined via fluorescent microscopy. Cells were seeded onto (2.5 cm diameter) sterile microscope cover slips deposited in (3.5 cm diameter) 6-well plates (2 mL of ~25% confluent cell culture per well). PMA was added to each well to a final concentration of 100 nM and plates were incubated for 72 hours. Polystyrene microspheres were opsonized with either oxLDL or human IgG for 30 min. Coverslips were either washed 5-times with PBS and placed in isotonic experimental medium (140 mM NaCl, 1mM $CaCl_2$, 1mM $MgCl_2$, buffered to pH 7.4 with 20 mM HEPES) or left in their original or the media prior to the addition of 1 µL of opsonized 2 µm microspheres (2.091×10^7 beads) per well. Alternatively, in a third group, media was replaced and plates were placed on ice and incubated for 30 min with beads then washed gently three times with PBS to remove unbound beads followed by the addition of fresh media. All three groups were then incubated at 37°C for 15, 30, 60, 120, 180 and 240 min. Control groups consisting of cells with no beads

added, cells with uncoated beads added and cells incubated with beads on ice for 30 min or 270 min were also used. Cells were subsequently washed 3 times in ice-cold PBS and fixed in PBS with 4% paraformaldehyde for 20 min. Fixing was terminated by the addition of PBS with 5% Glycine. Blocking was performed with PBS with 5% skim milk powder and, in the case of IgG-coated beads, 1% donkey serum. Cover slips that were exposed to oxLDL-coated microspheres were incubated in primary rabbit anti-Cu^{2+}-oxidized human lipoprotein antibody (1:25) for 30 min followed by secondary Cy3-conjugated donkey anti-rabbit antibody (1:10 000) for 30 min in the dark. This was followed by a second 30 minute permeabilizing blocking step with 5% skim milk powder and 0.1% Triton X-100 and another round of primary rabbit anti-Cu^{2+}-oxidized human lipoprotein antibody (1:25) followed by secondary Cy5-conjugated donkey anti-rabbit antibody (1:10 000). Cover slips that were exposed to human IgG-coated microspheres were incubated in PBS for 30 min followed by Cy3-conjugated donkey anti-human antibody (1:20 000) for 30 min in the dark. This was followed by a second 30 minute permeabilizing blocking step with 5% skim milk powder, 1% donkey serum and 0.1% Triton X-100 and incubation in Cy5-conjugated donkey anti-human antibody (1:20 000). All antibody incubations were done at room temperature. Wells were washed three times with PBS followed by two five minute washes before removing the cover slips and affixing them to microscope slides with fluorescence mounting medium (Dako, Carpinteria, CA, USA).

Additionally the internalization of non-opsonized microspheres was assessed in the presence of four different buffers to ascertain the degree of background binding. Cells were grown in PMA-treated RPMI as above. After 72 hours the growth medium was either left untouched or removed by washing 5 times with PBS and replaced with RPMI without FBS, PBS with 1 mM $CaCl_2$ and 1 mM $MgCl_2$, or isotonic experimental medium (140 mM NaCl, 1mM

$CaCl_2$, 1mM $MgCl_2$, buffered to pH 7.4 with 20 mM HEPES). 1 µL of 2µm microspheres was added to each well on ice and incubated for 30 min. Wells were then washed gently three times with PBS to remove unbound beads and fresh media was added. Plates were then incubated at 37°C for 60, 120, 180 and 240 min. Cover slips were washed, fixed and mounted as above.

Slides were examined using a Zeiss LSM 510 laser scanning confocal microscope in conjunction with Zeiss LSM Image Browser. Three to five images per treatment, containing an average of 15 cells per frame, were taken using a 63× water immersion objective lens using the excitation wavelengths 488 and 633 nm for statistical analysis. Several fluorescence and differential interference contrast micrographs per slide were also taken using a 100 × oil immersion objective lens. Internalized 2µm microspheres were quantified by manually counting the total number of microspheres per frame and subtracting any microspheres that were deemed extracellular by the presence of Cy3 fluorescence, indicating the presence of extracellular oxLDL or IgG and dividing by the number of cells. Treatments were replicated at least three times for statistical analysis.

Western Blotting

U937 cells were grown in four 70 cm^2 culture flasks in RPMI supplemented with 10% FBS with 100 nM PMA for 72 hours. Cells were scraped, pelleted, washed three times in PBS, treated with 0.1 mM diisopropyl fluorophosphate (Toronto Research Chemicals, Toronto, ON, Canada), pelleted, resuspended in 200 µL 2 × sodium dodecyl sulphate polyacrylamide gel electrophoresis (SDS-PAGE) sample buffer and heated at 95°C for 5 min. Protein content was determined using the method described by Ghosh et al. (Ghosh et al., 1988). Samples were resolved via tricine SDS-PAGE using 500 µg of protein per well, transferred onto a

polyvinylidene fluoride membrane (Millipore, Billerica, MA, USA), stained with 0.05% Coomassie brilliant blue R-250 in 50% methanol, partially destained with 50% methanol, marked with a pencil to record the position of the molecular weight marker, completely destained with 100% methanol and blocked with PBS containing 0.1% tween, 5% skim milk and 1% goat serum for 30 min. Membranes were probed with mouse anti-human CD36 clone FA6-152 (Beckman Coulter, Brea, CA, USA), mouse anti-human CD36 clone CB38 [NL07] (BD Pharmingen, Franklin Lakes, NJ, USA), mouse anti-mouse CD36 clone 63 (Cascade BioScience Winchester, MA, USA) or mouse anti-human CD36 antibody clone 131.2 (N. Tandon) at a dilution of 1:1000, followed by peroxidase conjugated goat anti-mouse secondary antibody at a dilution 1:10 000. Protein was detected by the enhanced chemiluminescece technique using a solution containing 0.1 M Tris/HCl pH 8.8, 0.125 mM luminol, 2 mM 4-iodopheylboronic acid, and 7.7 mM H_2O_2 on HyBlot CL™ autoradiography film (Denville, Metuchen, NJ, USA).

CD36 Immunofluorescent Staining

Permeabilized and non-permeabilized U937 cells were stained with anti-CD36 antibodies to confirm the localization of CD36. Cells were seeded onto cover slips and grown in PMA treated media as above. Cover slips were subsequently washed 3 times in PBS and fixed in PBS with 4% paraformaldehyde for 20 min. Fixing was terminated by the addition of PBS with 5% Glycine. Blocking was performed with PBS with 5% skim milk powder and 1% goat serum with or without 0.1% Triton X-100. Cover slips were incubated in primary monoclonal anti-CD36 antibody (clones: 63, CB38 [NL07], and FA6-152) (Table 1) at 1:25 concentration and in secondary Cy3-conjugated goat anti-mouse IgG or goat anti-mouse IgM antibody (1:10 000) at room temperature in the dark for 30 min each. Wells were washed 3 times with PBS followed by

two five minute washes before removing the cover slips and affixing them to microscope slides with mounting medium. Slides were examined using a Zeiss LSM 510 laser scanning confocal microscope with an excitation wavelength of 543 nm in conjunction with Zeiss LSM Image Browser.

Table 1: List of antibodies used, their respective immunogen, isotype, species of production, clone designation and source

Immunogen	Isotype	Species	Clone	Source
Human CD36	IgG	Mouse	FA6-152	Beckman Coulter
Human CD36	IgG	Mouse	131.2	N. Tandon
Human CD36	IgM	Mouse	CB38 [NL07]	BD Phamingen
Human CD36	IgA	Mouse	clone 63	Cascade Bioscience
Human oxLDL	pAb	Rabbit	pAb	Calbiochem
Mouse IgG/IgA	IgG	Donkey	Secondary	Jackson ImmunoResearch
Mouse IgG/IgA	IgG	Goat	Secondary	Jackson ImmunoResearch
Mouse IgM	IgG	Goat	Secondary	Jackson ImmunoResearch
Rabbit IgG	IgG	Donkey	Secondary	Jackson ImmunoResearch

Pharmacological Inhibition Assay

To test the possibility that 2 μm oxLDL-coated microsphere internalization utilizes a biochemical pathway distinct from that of IgG-coated microsphere internalization cells were exposed to a variety of pharmacological inhibitors prior to and during microsphere internalization. Cells were grown on cover slips and treated with PMA as above. Cells were pretreated with pharmacological inhibitors or DMSO vehicle alone at the indicated concentrations (Table 2) for one hour (except in the case of lovastatin which was applied for 72 hours) coverslips were washed 5 times with PBS and placed in isotonic experimental medium followed by the addition of either IgG-coated or oxLDL-coated 2μm microspheres and incubated for four hours at 37°C. Cells were stained and analyzed as above.

Live-cell affinity receptor chromatography

To determine the interacting members of the oxLDL/CD36 receptor complex, beads were coated with oxLDL or IgG as above. Macrophages were washed in PBS three times and incubated with beads on ice for 30 min in isotonic experimental medium to allow bead binding. Excess beads were washed off and cells were incubated at 37°C for 0 min, 30 min, 1 hr, 2 hr or 4 hr. Cells were then washed three times with PBS and scraped in Homogenization buffer (20 mM Tris-HCl pH 7.4, with 4-(2-Aminoethyl) benzenesulfonyl fluoride hydrochloride, phenylmethanesulfonylfluoride, DNAse I and II and protease inhibitor cocktail (Sigma Aldrich, St. Louis, MO, USA)). All 5 time points were pooled and homogenized in a French pressure cell press. Additionally a cell lysate control was created by preparing cells as above without adding beads until just prior to homogenization. Beads were pelleted resuspended in PBS and layered on top of a 40% sucrose gradient created in a 4 mL Beckman Coulter OptiSeal polyallomer centrifuge tube using a Beckman Coulter Optima Max Ultracentrifuge with a TLA110 fixed angle rotor at 45 000 rpm for 20 min. Beads were centrifuged at 45 000 rpm at 4°C for 10 min, aspirated with a syringe, and washed once with PBS via pelleting in a microcentrifuge. Bead binding partners were then sequentially extracted with a series of NaCl washes of increasing concentration (50, 100, 150, 200, 250, 300, 350, 400, 450, 500, 550, 600, 700, 800, 900 and 1000 mM NaCl) followed by 70% Acetonitrile. Beads and extracts were trypsinized overnight followed by an additional 1 hr trypsinization. Beads were pelleted, resuspended in chloroform and trypsonized once more. Samples were analyzed by nano LC-ESI-MS/MS with an LTQ ion trap.

Table 2: Pharmacological Inhibitors used and their respective final concentrations

Inhibitor	Target	Concentration	Reference
Cytochalasin D	Filamentous actin	10 µM	(Sulahian et al., 2008) (Nikkhah et al., 2009) (Cuschieri et al., 2009)
Latrunculin B	Filamentous actin	5 µM	(Huang et al., 2008) (Sun et al., 2009) (Epstein et al., 1999) (Segal et al., 2001)
LY 294 002	Phosphoinositide 3-kinase	25 µM	(Tatara et al., 2009) (Cho et al., 2009) (Li et al., 2009) (Kim et al., 2009) (Chan et al., 2009)
Wortmannin	Phosphoinositide 3-kinase	0.5 µM	(Zu et al.) (Tripathi and Sodhi, 2008) (Pang et al.) (Huang et al., 2008) (Jing Chen-Roetling et al., 2008)
AG 490	Janus kinases	25 µM	(Ha et al., 2008) (Chiou et al.) (Akifusa et al., 2010) (Han et al., 2010) (Tripathi and Sodhi, 2008)
Genestein	Protein tyrosine kinases	35 µM	(Tripathi and Sodhi, 2008) (Yang et al., 2008) (Bhatt et al., 2010) (Miksa et al., 2007)
AG 1879 (PP2)	Src tyrosine kinases	10 µM	(Maa et al., 2008) (Yang et al., 2008) (Georgakopoulos et al.) (Xue et al., 2010) (Cammer et al., 2009)

continued on next page

continued from previous page

BAY 61 3606	Spleen tyrosine kinases (Syk)	1 µM	(Sanderson et al., 2010) (Stadanlick et al., 2008) (Yang et al., 2008)
MNS	Src and Syk	20 µM	(Wang et al., 2006)
PF 573228	Focal adhesion kinases	1 µM	(Wendt and Schiemann, 2009) (Jones et al., 2009) (Hatta et al., 2009) (Lafrenaye and Fuss, 2010)
Go6983	Protein kinase C	10 µM	(Sulahian et al., 2008)
U73122	Phospholipase C	5 µM	(Fulton et al., 2008) (Mogami et al., 1997) (Roy and Rai, 2008)
Ethanol	Phospholipase D	200 mM (1.2% v/v)	(Kusner et al., 1996a) (Slomiany et al., 2002) (Imagawa et al.)
Propranolol	Phosphatidate Phosphatase-1	100 µM	(Grkovich et al., 2009) (Laitinen et al.) (Mallants et al., 2009)
lovastatin, sodium salt	3-hydroxy-3-methylglutaryl-CoA reductase	10 µM	(Mandal et al.) (Dalvai and Bystricky, 2010) (Gralczyk et al., 2009)

RESULTS

CD36 Western Blot

Four antibodies specific for CD36 were used in the detection of CD36 in PMA-differentiated U937 lysates (Table 1) via immunoblot. Clones FA6-152, 131.2, CB38 [NL07] and 63 of isotypes IgG, IgG, IgM and IgA respectively produced differing banding patterns (Figure 4). Antibody 131.2 from Narendra Tandon produced only one band. All displayed a visible band at CD36's recorded molecular mass of 88 kDa. This band was not visible when membranes were stained with the secondary antibody alone.

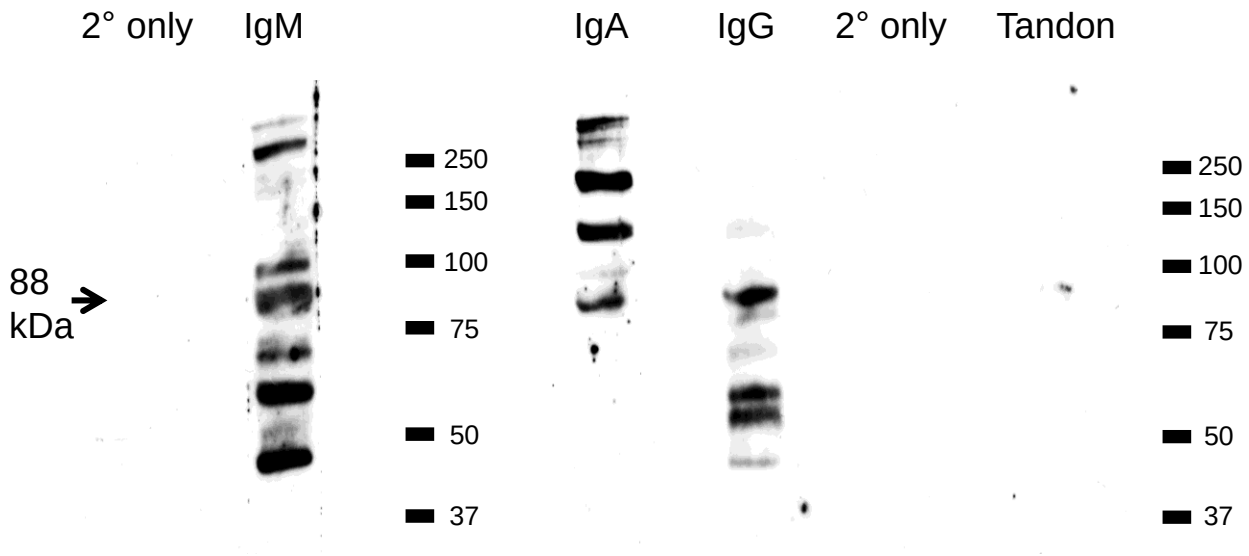

Figure 4: CD36 Immunoblot of PMA-differentiated U937 cells.

Cells were incubated in 100 nM PMA for 3 days and lysed in a French pressure cell press. Lysate was separated via PAGE, blotted onto polyvinyl difluoride membrane, blocked in 5% skim milk with 1% goat serum and treated with mouse IgG, IgM or IgA α-CD36 antibody and peroxidise-conjugated α-IgG or α-IgM secondary antibody. Membranes were developed via enhanced chemiluminescence. Technical assistance: Angelique Florentinus

CD36 Immunofluorescent Staining

Three antibodies specific for CD36 were used in the immunofluorescent staining of CD36 in permeabilized and non permeabilized PMA-differentiated U937 cells (Table 1). Clones FA6-152, CB38 [NL07] and 63 of isotypes IgG, IgM and IgA respectively all produced a bright distinct ring around the membrane of the cell when imaged using a confocal laser scanning microcope (Figure 5). This pattern was not observed when cells were stained with the secondary antibody alone.

Bead Internalization Assay in Isotonic Experimental Medium

To determine the efficacy of the staining procedure polystyrene beads were coated with oxLDL or IgG and incubated with macrophages for 4 hours. The cells were fixed and beads were stained with Cy3 conjugated antibodies, cells were permeabilized and beads were stained a second time (Figure 6). Internalization was ascertained by the presence of Cy5 fluorescence and absence of Cy3 fluorescence.

Once the preliminary assay was completed, a 4 hour internalization time course was performed to examine the progression of internalization. Macrophages were washed 5 times with PBS and incubated in isotonic experimental medium to lower bead contamination from complex medium components with oxLDL or IgG beads for varying times (15 min, 30 min, 1 hr, 2 hr, 3 hr, and 4 hr) and external beads were stained (Figure 7). The average number of internalized beads per cell was quantified with at least three replicates (Figure 8). IgG beads were internalized more quickly and to a greater extent. Over 4 hours an average of approximately 5 IgG beads and 1 oxLDL bead were internalized per cell. Results were analyzed by JMP statistical analysis software (Appendix E).

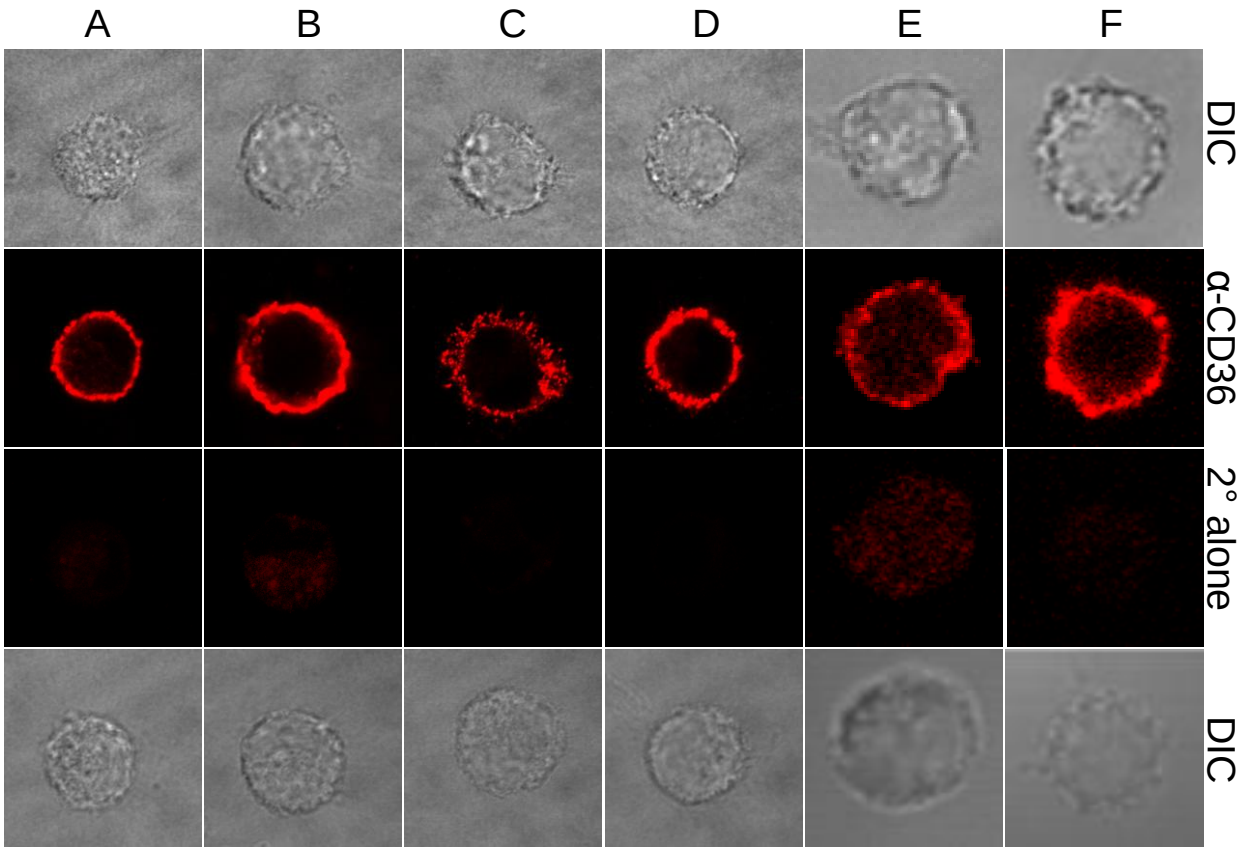

Figure 5: Immunofluorescent staining of PMA-differentiated U937 cells with an α-CD36 antibody with or without a 30 minute 0.1% Triton X-100 permeabilizing step.

To determine presence and distribution all cells were blocked in 5% skim milk with 1% goat serum and stained with an IgG, IgM or IgA α-CD36 antibody followed by a goat Cy3-conjugated α- IgG/IgA or α- IgM secondary antibody. (A) IgG antibody with permeabilization. (B) IgG antibody without permeabilization. (C) IgM antibody with permeabilization. (D) IgM antibody without permeabilization. (E) IgA antibody with permeabilization. (F) IgA antibody without permeabilization. Technical assistance: Angelique Florentinus

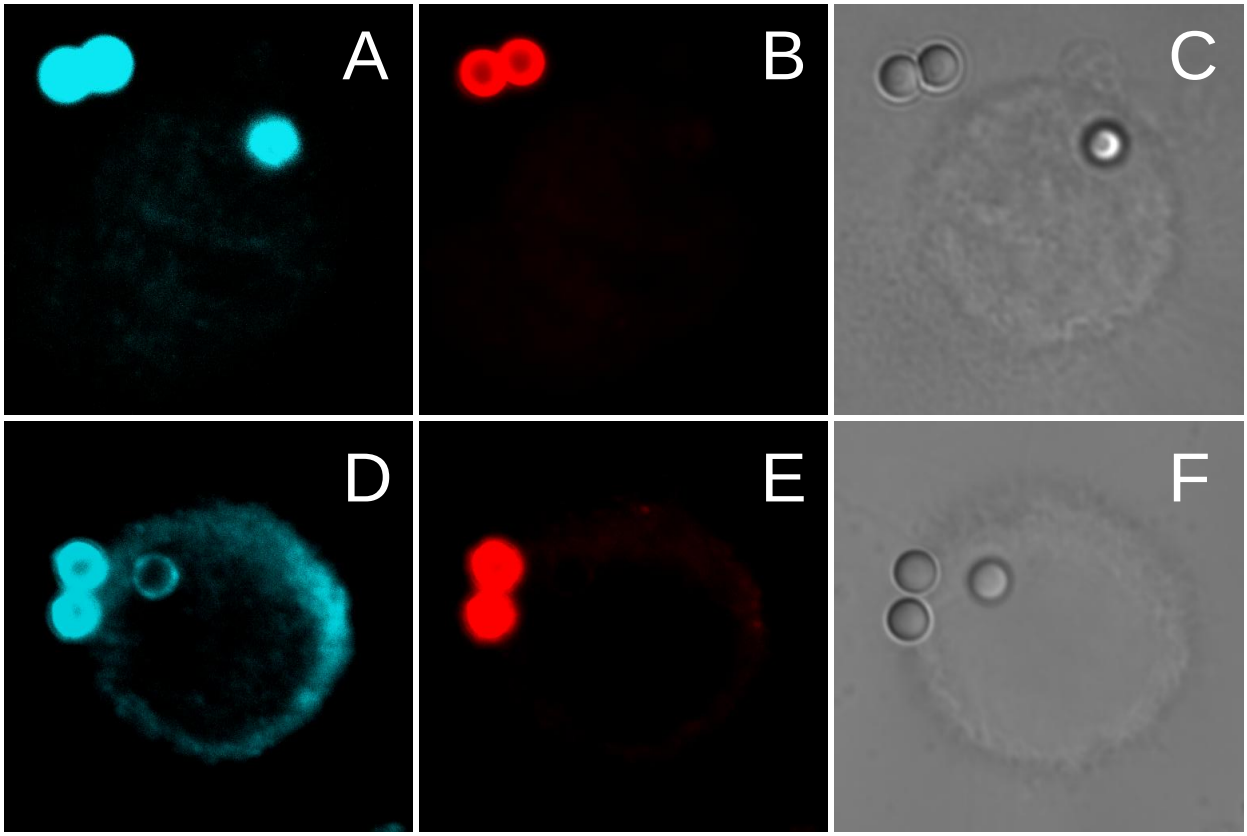

Figure 6: Intracelular and extracellular immunofluorescent bead staining of IgG-coated and oxLDL-coated beads internalized by U937.

Cells were differentiated for 3 days with 100 nM PMA and incubated with oxLDL-coated or IgG-coated beads in isotonic experimental medium. Cells were fixed in a 5% paraformaldehye solution and blocked with 5% skim milk for oxLDLcoated beads and 5% skim milk with 1% donkey serum for IgG coated beads. Beads were subsequently stained with Cy3-conjugated anti-IgG antibody or rabbit polyclonal anti-oxLDL antibody follwed by Cy3-conjugated donkey anti-rabbit antibody to visualize non-internalized beads. All beads were subsequently stained by permeabilizing with a 0.1% Triton X-100 blocking solution followed by Cy5-conjugated anti-IgG antibody or rabbit polyclonal antioxLDL antibody followed by Cy5-conjugated donkey anti-rabbit antibody. (A) External and internal IgG-coated bead Cy5 staining. (B) External IgG-coated bead Cy3 staining. (C) IgG-coated bead DIC. (D) External and internal oxLDL-coated bead Cy5 staining (E) External oxLDL-coated bead Cy3 staining (F) oxLDL-coated bead DIC.

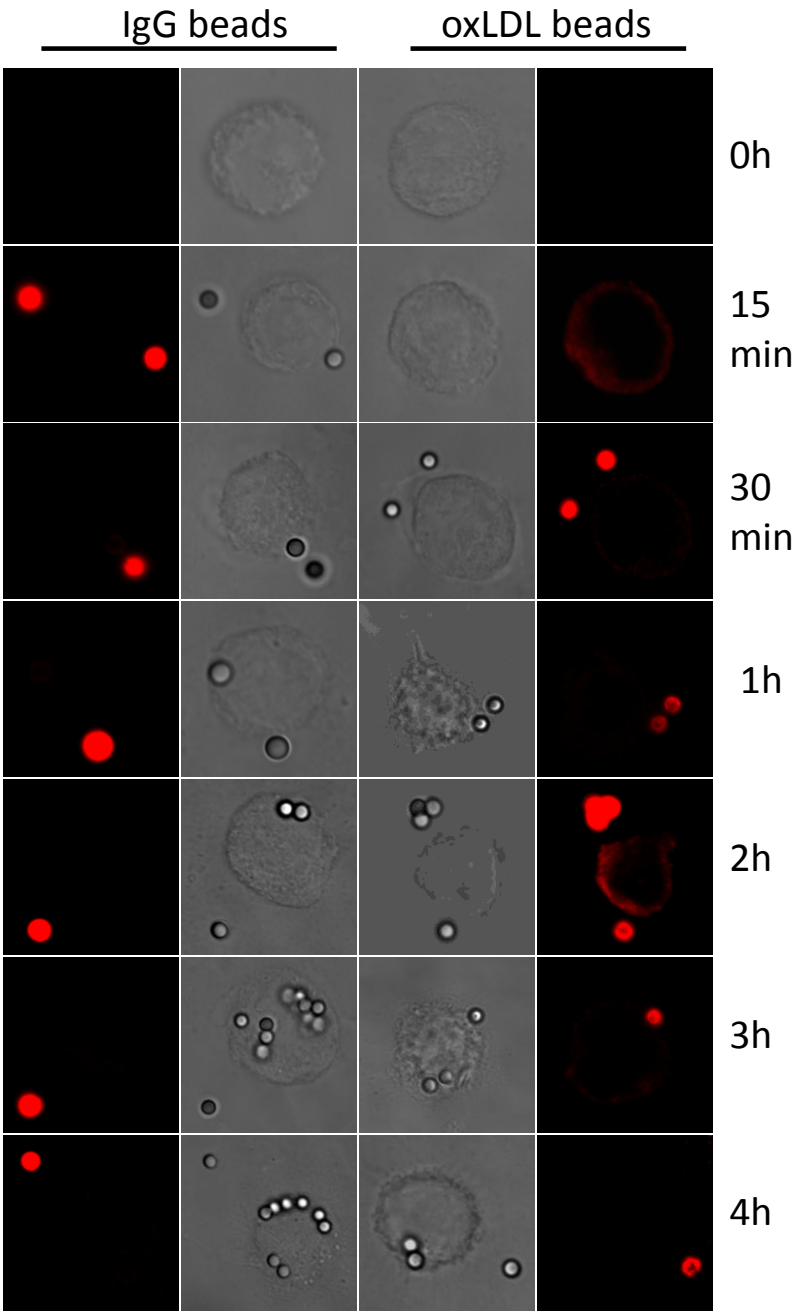

Figure 7: Internalization of IgG-coated and oxLDL-coated Beads by U937 in Saline Experimental Medium over 4 hours

Cells were differentiated for 3 days with 100 nM PMA, washed 5-times with PBS and incubated with oxLDL-coated or IgG-coated beads in isotonic experimental medium. Cells were fixed in a 5% paraformaldehye solution at 15 min, 30 min, 1h, 2h, 3h or 4h. Beads were subsequently stained with Cy3-conjugated anti-IgG antibody or rabbit polyclonal anti-oxLDL antibody followed by Cy3-conjugated donkey anti-rabbit antibody to visualize non-internalized beads. Confocal laser scanning images.

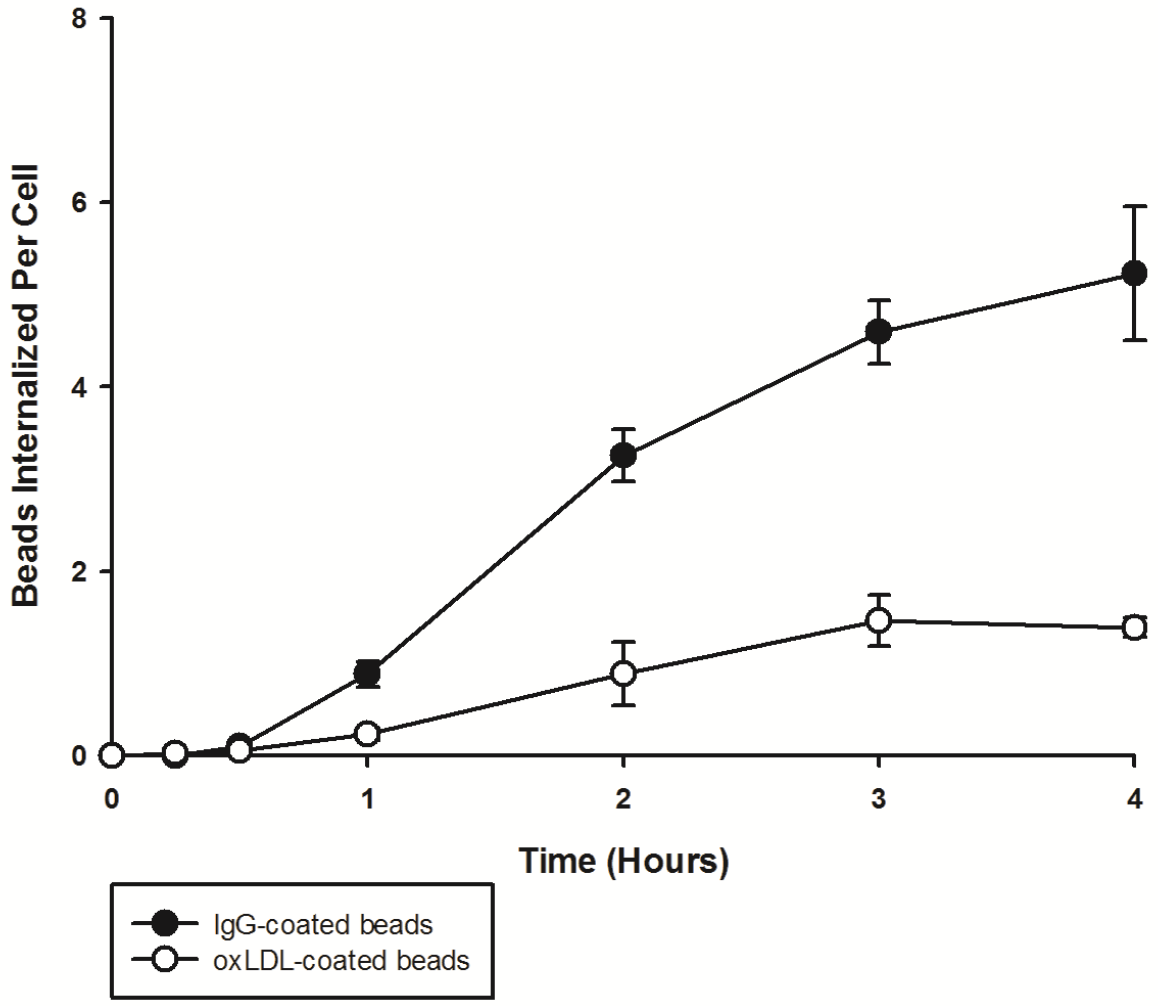

Figure 8: Number of IgG-coated and oxLDL-coated beads internalized by U937 in Saline Experimental Medium over 4 hours.

Cells were differentiated for 3 days with 100 nM PMA, washed 5-times with PBS and incubated with oxLDL-coated or IgG-coated beads in isotonic experimental medium. Cells were fixed in a 5% paraformaldehye solution at 15 min, 30 min, 1h, 2h, 3h or 4h. Beads were subsequently stained with Cy3-conjugated anti-IgG antibody or rabbit polyclonal anti-oxLDL antibody followed by Cy3-conjugated donkey anti-rabbit antibody to visualize non-internalized beads. Quantification of bead internalization of at least 3 replicates with an average of 3 images per treatment and 15 cells per image +/- standard error.

Bead Internalization Assay in RPMI with 10% FBS

oxLDL or IgG beads were incubated with macrophages as above. Cells were not washed beforehand and bead incubation took place in RPMI with 10% fetal bovine serum to be more physiologically relevant to the arterial conditions experienced by macrophages in vivo. The average number of internalized beads per cell was quantified with at least three replicates (Figure 9). IgG beads were internalized more quickly initially, but engulfment plateaued while oxLDL engulfment continued. Over 4 hours an average of approximately 7 IgG beads and 9 oxLDL bead were internalized per cell.

Bead Internalization Assay in RPMI with 10% FBS After a 30 Minute On Ice Incubation

Macrophages were exposed to beads for a 30 minute on ice preincubation period in RPMI with FBS to allow beads to bind without internalization. This was done to remove the element of bead settling time. Excess beads were washed off and cells were then heated to 37° C in RPMI with FBS bead internalization was assayed as above (Figure 10). IgG beads were internalized more quickly initially but engulfment plateaued while oxLDL engulfment continued. Over 4 hours an average of approximately 0.5 IgG beads and 1 oxLDL bead were internalized per cell.

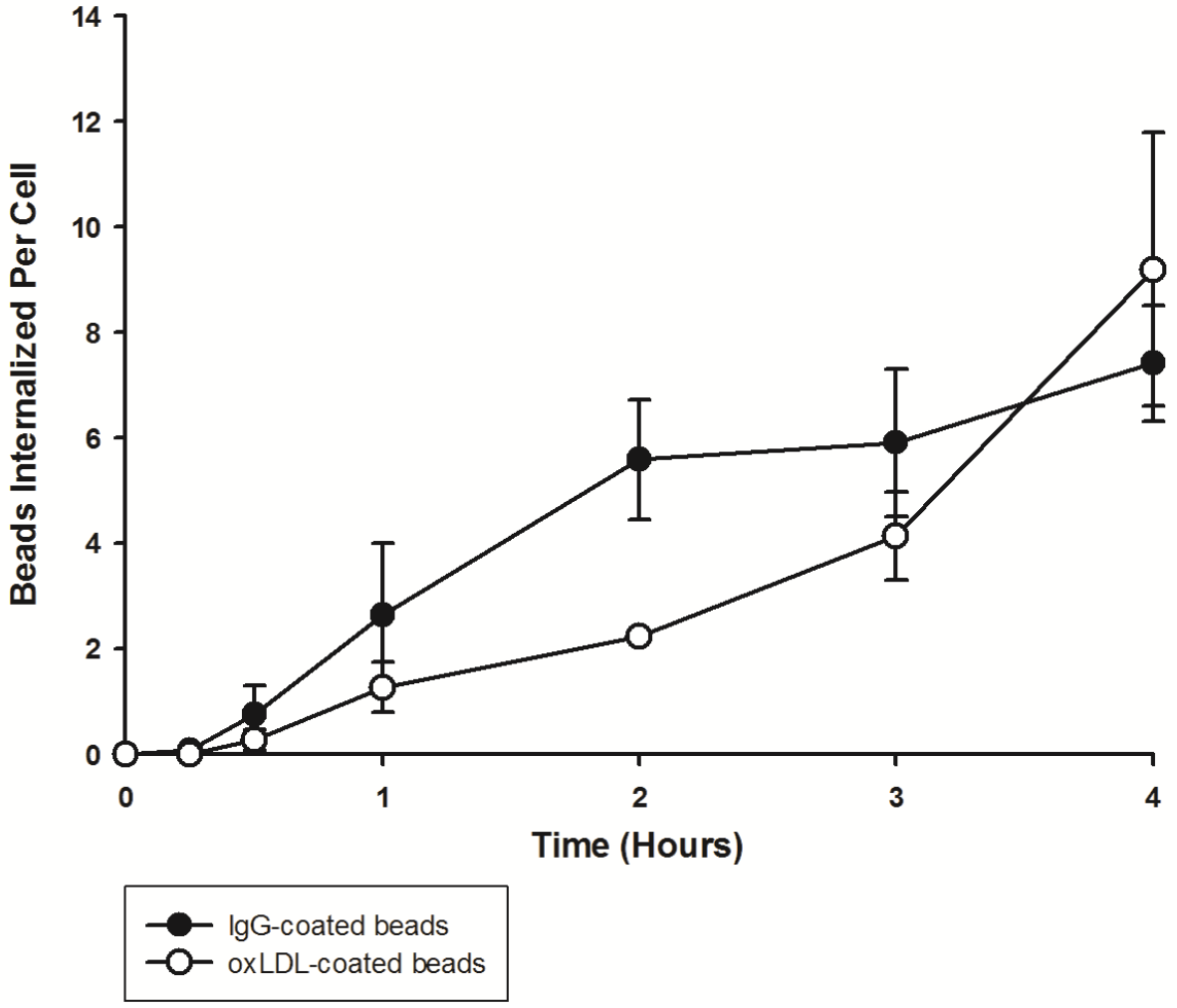

Figure 9: Number of IgG-coated and oxLDL-coated Beads internalized by U937 in RPMI with 10% fetal bovine serum over 4 hours.

Cells were differentiated for 3 days with 100 nM PMA and incubated with oxLDL-coated or IgG-coated beads. Cells were fixed in a 5% paraformaldehye solution at 15 min, 30 min, 1h, 2h, 3h or 4h. Beads were subsequently stained with Cy3-conjugated anti-IgG antibody or rabbit polyclonal anti-oxLDL antibody followed by Cy3-conjugated donkey anti-rabbit antibody to visualize non-internalized beads. Quantification of bead internalization of at least 3 replicates with an average of 3 images per treatment and 15 cells per image +/- standard error.

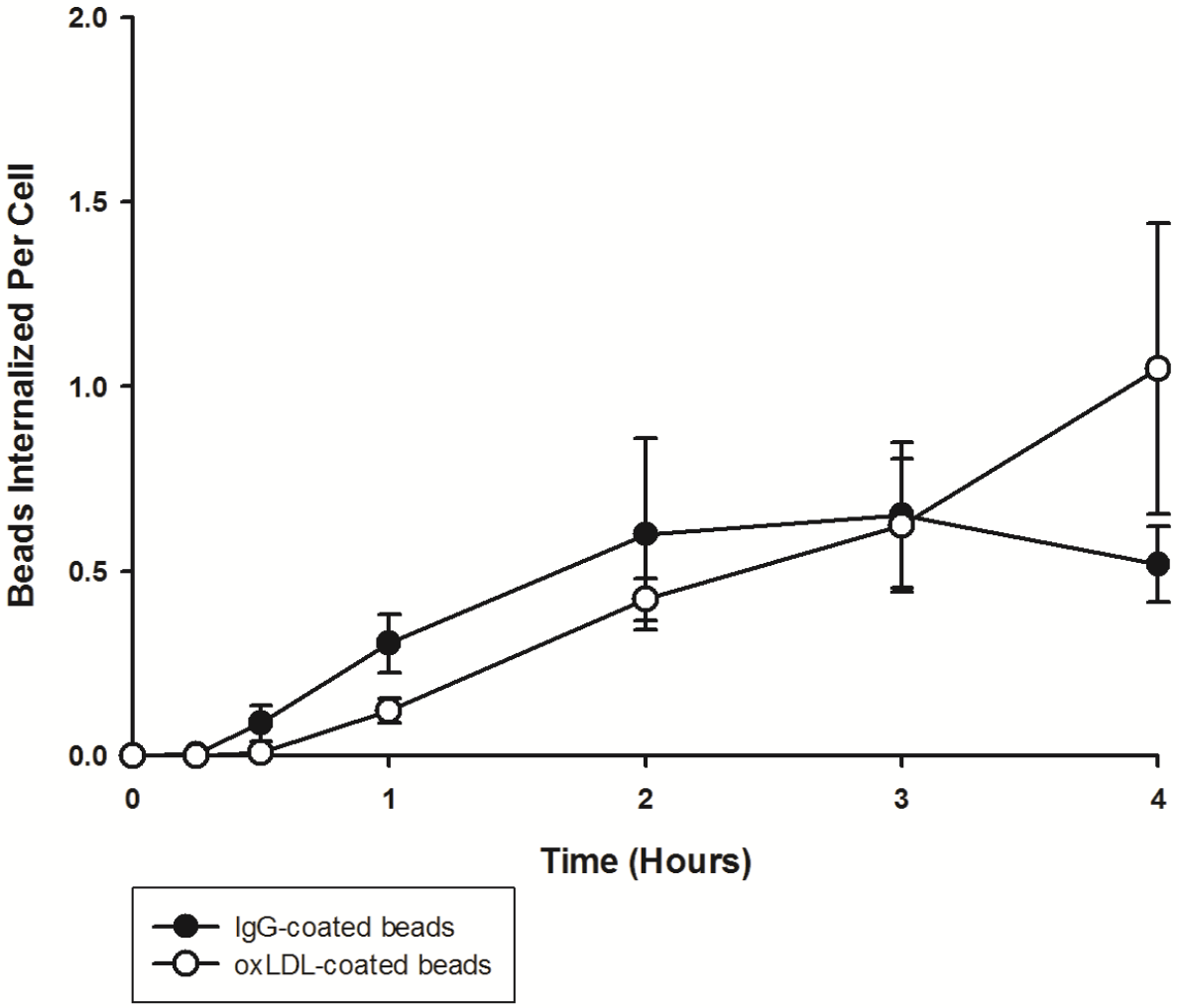

Figure 10: Number of IgG-coated and oxLDL-coated beads internalized by U937 after a limited 30 minute bead incubation in RPMI with 10% fetal bovine serum over 4 hours

Cells were differentiated for 3 days with 100 nM PMA washed 3 times with PBS and incubated with oxLDL-coated or IgG-coated beads for 30 min. Excess beads were washed off and replaced with fresh medium and cells were fixed in a 5% paraformaldehye solution at 15 min, 30 min, 1h, 2h, 3h or 4h. Beads were subsequently stained with Cy3-conjugated anti-IgG antibody or rabbit polyclonal anti-oxLDL antibody followed by Cy3-conjugated donkey anti-rabbit antibody to visualize non-internalized beads. Quantification of bead internalization of at least 3 replicates with an average of 3 images per treatment and 15 cells per image +/- standard error.

Bead Internalization Assay in the Presence of Pharmacological Inhibitors

Macrophages were incubated with oxLDL or IgG beads in isotonic experimental medium for 4 hours as above. Cells were incubated with a variety of pharmacological inhibitors (Table 2) for one hour prior to bead incubation and during bead incubation. The effect of the actin polymerization inhibitor Cytochalasin D is shown (Figure 11). Bead internalization for all inhibitors was assessed as above and quantified over 3 replicates (Figure 12). The actin polymerization inhibitors Cytochalasin D and Latrunculin B completely prevented bead internalization. Inhibition of Src and Syk by 3,4-methylenedioxy-betanitrostyrene prevent 99% of IgG and 94% of oxLDL bead internalization. Inhibition of Phospholipase C by U73122 prevented 90% of IgG and 75% of oxLDL bead internalization. Inhibition of Janus kinase by AG 490 prevented 84% of IgG and 77% of oxLDL bead internalization. Finally, General protein tyrosine kinase inhibiton by Genistein prevented 60% of IgG and 76% of oxLDL bead internalization. Wortmannin (PI3K), PP2 (Src tyrosine kinases), ethanol (PLD), LY 294 002 (PI3K), BAY 61 3606 (Syk tyrosine kinases), PF 573228 (FAK), Go6983 (PKC), propranolol (PAP-1) and lovastatin (HMGCR) had little effect on bead internalization. Results were analyzed by JMP statistical analysis software (Appendices G-J).

Live-cell Affinity Chromatography of oxLDL and IgG Phagocytic Receptor Complex

U937 cells were incubated on ice for 30 min with IgG-coated or oxLDL coated beads. Excess beads were then washed off and cells were incubated at 37°C to allow for bead internalization for 0 min, 30 min, 1h, 2h or 4h. Cells were then scraped and all time points were pooled and lysed. A control sample was created by adding beads just prior to lysis. Beads were

isolated via sucrose density gradient centrifugation and associated proteins were sequentially dissociated by a series of NaCl concentrations. Elutes were analyzed by nano LC-ESI-MS/MS.

The base peak trace results of the 500 mM NaCl LARC elution (Figure 13) were selected arbitrarily to ascertain the ability of the IgG/oxLDL-bead LARC system to distinguish IgG/FcR receptor complex associated proteins from oxLDL/CD36 receptor complex associated proteins. Qualitative differences between the patterns were observed.

AG490, U73122, MNS, Latrunculin B and Cytochalain D inhibited bead phagocytosis. Accordingly, the mass spectra of various isoforms of the Src-family, Syk-family, JAK, PLC, and actin protein groups detected via LC-ESI-MS/MS in IgG, oxLDL, anti-CD36 IgA and anti-CD36 IgG coated bead LARC treatments were compiled (Appendix I). The mass spectra of additional proteins investigated in this study are also shown.

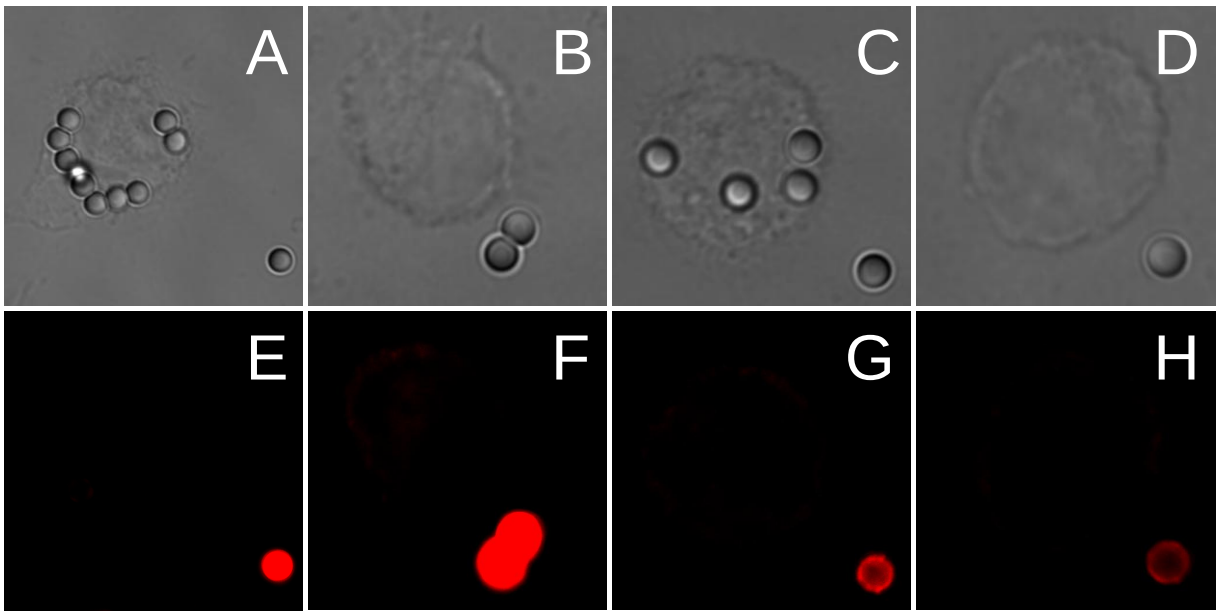

Figure 11: Effect of Cytochalasin D on the internalization of oxLDL-coated and IgG-coated beads. Cells were differentiated for 3 days with 100 nM PMA then incubated with 10 µM Cytochalasin D or a 0.1% DMSO vehicle control for 1 hour.

Cells were subsequently washed 5 times with PBS and incubated for 4 hours with oxLDL-coated or IgG-coated beads in isotonic experimental medium with or without 10 µM Cytochalasin D. Beads were stained with Cy3-conjugated anti-IgG antibody or rabbit polyclonal anti-oxLDL antibody followed by Cy3-conjugated donkey anti-rabbit antibody to visualize non-internalized beads. (A) oxLDL beads without Cytochalasin D DIC. (B) Staining of external oxLDL beads without Cytochalasin D. (C) oxLDL beads with Cytochalasin D DIC. (D) Staining of external oxLDL beads with Cytochalasin D. (E) IgG beads without Cytochalasin D DIC. (F) Staining of external IgG beads without Cytochalasin D. (G) IgG beads with Cytochalasin D DIC. (H) Staining of external IgG beads with Cytochalasin D. (Scale bar: 5 µm)

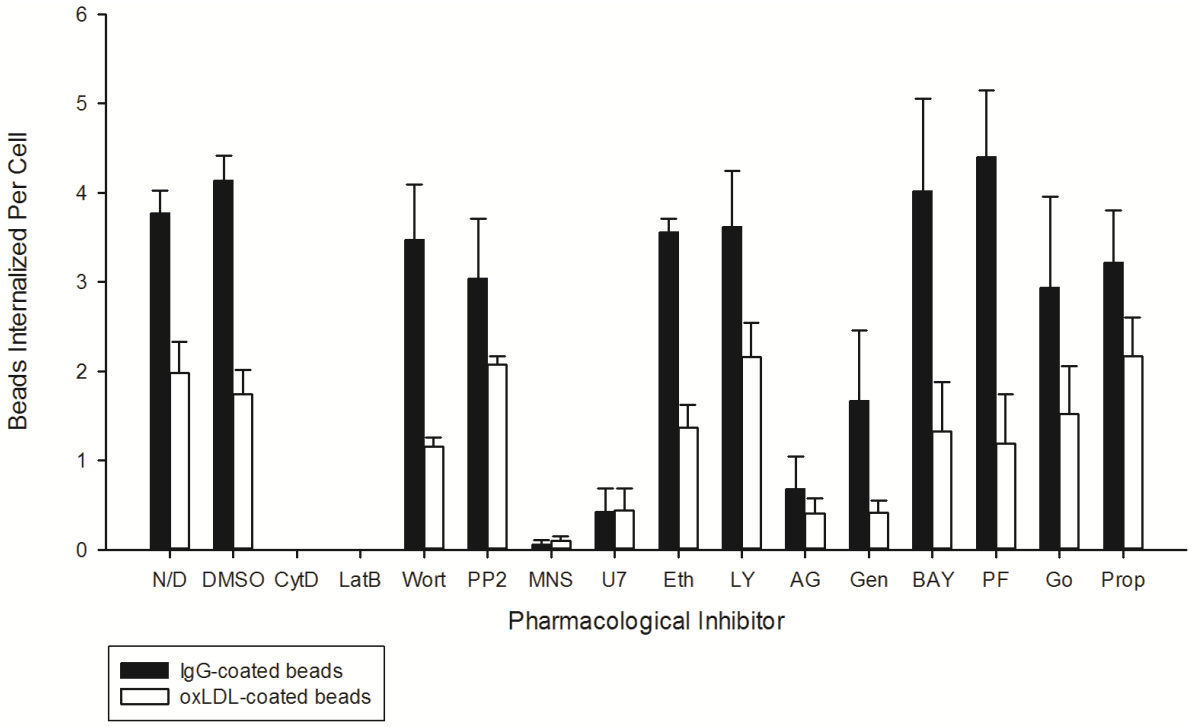

Figure 12: Pharmacological inhibition of oxLDL-coated and IgG-coated bead internalization.

Cells were differentiated for 3 days with 100 nM PMA then incubated with one of 13 pharmacological inhibitors at indicated concentrations (Table 1) or 0.1% DMSO for 1 hour. Cells were subsequently washed 5-times with PBS and incubated with oxLDL-coated or IgG-coated beads in isotonic experimental medium with their respective inhibitors. Cells were fixed in a 5% paraformaldehye solution and external beads were subsequently stained with Cy3-conjugated anti-IgG antibody or rabbit polyclonal anti-oxLDL antibody followed by Cy3-conjugated donkey anti-rabbit antibody to visualize non-internalized beads. At least 3 replicates were conducted with an average of 3 images per treatment and 15 cells per image. Error bars indicate standard error. Abbreviations with drug target in parenthesis as follows: N/D – No drug; DMSO – Dimethyl sulphoxide; CytD – Cytochalasin D (actin); LatB – Latrunculin B (actin); Wort – Wortmannin (PI3K); PP2 – AG 1879 (Src); MNS – 3,4-Methylenedioxy-beta-nitrostyrene (Src and Syk); U7 – U73122 (PLC); Eth – Ethanol (PLD); LY – LY 294 002 (PI3K); AG – AG 490 (JAK); Gen – Genistein (protein tyrosine kinases); BAY – BAY 61 3606 (Syk); PF – PF 573228 (FAK); Go – Gö6983 (PKC); Prop – Propranolol hydrochloride (PAP-1).

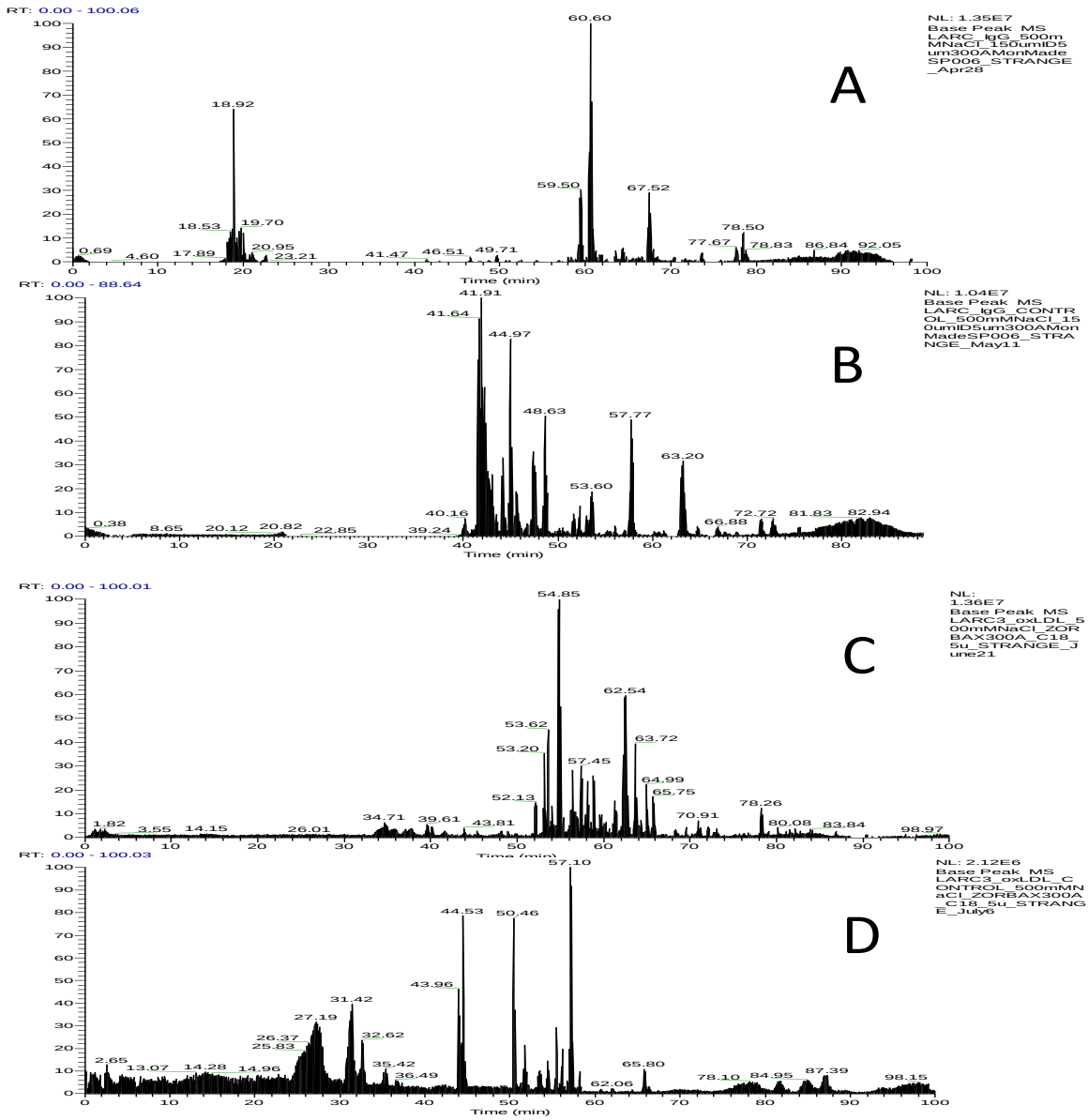

Figure 13: Live-cell affinity receptor chromatography of oxLDL and IgG receptor complex 500 mM NaCl elution base peak mass spectrometric traces. U937 cells were differentiated for 3 days in PMA washed three times with PBS and incubated on ice for 30 minutes with IgG-coated or oxLDL coated beads. Excess beads were then washed off with three washes of PBS and cells were incubated at 37°C to allow for bead internalization for 30 min, 1h, 2h or 4h. Cells were then scraped and all time points were pooled and lysed in a French pressure cell press. A control sample was created by adding beads just prior to lysis. Beads were isolated via sucrose density gradient centrifugation and associated proteins were sequentially dissociated by a series of NaCl concentrations. Elutes were analyzed by nano LC-ESI-MS/MS with an LTQ ion trap. (A) 500 mM NaCl elution of IgG-coated bead associated proteins. (B) 500 mM NaCl elution of IgG-coated bead control. (C) 500 mM NaCl elution of oxLDL-coated bead associated proteins. (D) 500 mM NaCl elution of IgG-coated bead control.

DISCUSSION

The successful Western blotting and immunofluorescent cell-staining of CD36 confirms the presence of the scavenger receptor for oxLDL at the plasmalemma (Figures 4 & 5). The differential immunofluorescent staining of intracellular and extracellular oxLDL and IgG beads demonstrates the ability of the experimental system to quantify bead internalization. Moreover, only extracellular 2µm beads need to be stained in order to be quantified.

The differences between IgG and oxLDL bead internalization (figures 8, 9 and 10) imply that IgG and oxLDL mediated phagocytosis utilize different internalization pathways.

Src and Syk

The dual selective Src/Syk inhibitor MNS significantly inhibited both IgG and oxLDL bead internalization.

CD36 is known to associate with Src and Syk and the Src kinases Fyn Lyn and Yes co-precipitate with CD36 from monocytic cell lysate (Medeiros et al., 2004). Additionally, Fyn and Lyn are phosphorylated and activated by CD36-mediated oxLDL internalization in mouse peritoneal macrophages and the internalization of oxLDL from the fluid phase in macrophages has been shown to require Src kinases (Collins et al., 2009; Rahaman et al., 2006). Correspondingly previous studies have found that pharmacological inhibition of Src blocks foam-cell formation in vitro and in vivo (Rahaman et al., 2006). Furthermore, Lyn-deficient mice display a lower rate of atherosclerosis than wildtype specimens (Miki et al., 2001).

It should also be noted that the use of Src as a CD36 signalling molecule is not exclusive to macrophages. Fyn Lyn and Yes co-precipitate with CD36 from platelets and endothelial cell

lysate (Huang et al., 1991; Bull et al., 1994). Upon interaction with thrombospodin-1, CD36 activates Fyn in microvascular endothelial cells leading to a proapoptotic antiangiogenic effect.(Jimenez et al., 2000) Src is also integral to oxLDL-mediated CD36 signalling in platelet avtivation (Chen et al., 2008). oxLDL/CD36 mediated platelet activation involves the activation and phosphorylation of Fyn and Lyn and is stopped by Src inhibition (Chen et al., 2008). Syk present in human umbilical vein endothelial cells is known to associate with CD36 (Kazerounian et al., 2011). Upon binding fibrillar amyloid-β, CD36, $\alpha_6\beta_1$-integrin and integrin-associated protein (CD47) form a receptor complex in microglial cells that activates Syk (Wilkinson et al., 2006; Bamberger et al., 2003).

The FcR is also known to signal through Src and Syk. It has previously been established that binding of IgG to the FcR allows Src family kinases to phosphorylate tyrosine pairs on ITAMs thus allowing the binding of the SH2 domains of Syk which, in turn, activates downstream phagocytic signalling components (Underhill and Goodridge, 2007). However, the selective Src inhibitor PP2 and the highly selective Syk inhibitor BAY 61 3606 on their own did not produce a large effect.

Actin

There is considerable evidence that actin is required for phagocytosis (Aderem and Underhill, 1999; Etienne-Manneville and Hall, 2002). A phosphorylation chain following Src and Syk FcγR-ITAM-mediated phosphorylation precipitates the polymerization of actin, in addition to other events required for phagosome formation such as myosin activation, membrane

fusion and ROS production (Aderem and Underhill, 1999; Etienne-Manneville and Hall, 2002; Underhill and Goodridge, 2007).

Fluid phase CD36-mediated oxLDL uptake in macrophages also requires actin (Collins et al., 2009). There is some evidence that CD36 initiates this actin polymerization using the scaffold protein p130Cas, Pyk2, paxillin and Fyn via a phosphorylation cascade (Stuart et al., 2007)

Accordingly, inhibition of actin by Cytochalasin D or Latrunculin B completely inhibited bead phagocytosis.

FAK

Inhibition of FAK by PF 573228 did not produce a large effect on oxLDL or IgG bead phagocytosis.

Previous research postulated that fluid-phase oxLDL induced CD36 activation initiated NADPH oxidase ROS production leading to oxidative SHP-1 inactivation which would, in turn, constitutively activate FAK, leading to actin polymerization and that this reforming of the cytoskeleton would cause macrophages to become trapped in the arterial intima leading to foam cell formation (Park et al., 2009).

When examining Fcγ signalling, one study found that by cross-linking Fcγ receptors they could precipitate a rapid transient Fak phosphorylation in human macrophages (Pan et al., 1999). However, another study found no increased tyrosine phosphorylation of p125Fak during mAb-

mediated FcγII & III receptor aggregation in murine macrophages (Greenberg et al., 1994). The lack of IgG bead internalization inhibiton under Fak inhibition seems to support the latter.

PI3K

PI3K has previously been shown to be involved in several key IgG-mediated phagocytic processes such as the depletion of $PI(4,5)P_2$, an actin assembly and remodelling molecule present at the phagosome (Scott et al., 2005), the regulation of the small g-proteins ADP-ribosylation factor 1 and 6 and pseudopod extension via Myosin X (Groves et al., 2008).

The present study found that inhibition of PI3K by LY 294 002 or Wortmannin did not produce a large reduction in oxLDL or IgG bead internalization. This is consistent with previous findings that phagocytosis of IgG-coated beads smaller than 3µm were not affected by PI3K inhibition by either Wortmannin or LY294002 (Groves et al., 2008). It is also consistent with earlier research that found no correlation between PI3K and CD36-mediated fluid phase oxLDL internalization or foam-cell formation (Rahaman et al., 2006; Collins et al., 2009).

PLC

There is little prior evidence directly linking PLC and CD36 however CD36-mediated platelet activation tyrosine kinase phosphorylation is associated with PLC activation and both PLC and CD36 are localized to platelet lipid rafts (Gousset et al., 2004).

With regards to the FcγR, PLC was implicated in both the depletion of the actin assembly and remodelling molecule $PI(4,5)P_2$ at the phagosome and the depolymerization of actin around the nascent phagosome (Scott et al., 2005).

Accordingly, inhibition of PLC by U73122 significantly inhibits IgG bead internalization by approximately 90% (Figure 12). The internalization of oxLDL beads was also significantly reduced suggesting that PLC may play a more general role in phagocytosis.

Jak

Inhibition of Jak by AG 490 significantly inhibited both oxLDL and IgG bead internalization.

Earlier research found no correlation between foam-cell formation and Jak when murine macrophages were exposed to fluid-phase oxLDL (Rahaman et al., 2006).

There has been some evidence of cross-regulation between ITAM motifs and the cytokine receptor Jak-STAT pathway (Ivashkiv, 2009; Hu et al., 2007). The Jak/Stat pathway is inhibited by the binding of immune complexes to the FcγR leading to the suppression of Interferon-gamma activation while this does not imply a requirement for phagocytosis it does establish a signalling association (Boekhoudt et al., 2007; Feldman et al., 1995).

PKC

Inhibition of PKC by Gö6983 did not produce a large effect on oxLDL or IgG bead internalization.

Earlier research found no correlation between foam-cell formation and PKC when macrophages were exposed to fluid-phase oxLDL (Rahaman et al., 2006). However, the overexpression of PKC-ε (which is not inhibited by Gö 6983) increases the rate of FcR-mediated phagocytosis in RAW 264.7 macrophages (Larsen et al., 2002). During phagoytosis PKC-α, δ and ε, but not necissaily PKC-β or ζ, localize to the plasma membrane in murine RAW 264.7 macrophages (Larsen et al., 2000).

A study by Zheleznyak et. al. found that IgG-coated 3μm bead internalization by human monocytes was inhibited by the PKC inhibitors H7, staurosporine and calphostin C (Zheleznyak and Brown, 1992). While another study found that IgG-opsonized red-blood cell phagocytosis by murine macrophages was insensitive to the same PKC inhibitors (Greenberg et al., 1993). Furthermore, a later study found staurosporine and calphostin C (general PKC inhibitors) but not Gö6976 and CGP 41251(classic/selective inhibitors) inhibit the phagocytosis of IgG-opsonized erythrocytes by RAW 264.7 (Larsen et al., 2000). Accordingly, it is possible that an isoform of PKC not effectively inhibited by Gö 6983 is required for IgG-coated and/or oxLDL-coated bead phagocytosis.

PLD

Ethanol, a phospholipase D inhibitor, did not have a large effect on oxLDL or IgG bead internalization.

There has been no prior direct evidence for interaction between CD36 and PLD however a strong association was found between PLD activation and the phagocytosis of *Mycobacterium*

tuberculosis in monocyte-derived macrophages, a process that has been shown to involve CD36 (Kusner et al., 1996).

3 µm IgG-coated latex bead uptake has been reported to have been impaired upon the inactivation of PLD isoforms 1 and 2 in murine macrophages (Corrotte et al., 2006). Also, in response to FcγR ligation phosphatidic acid, a product of PLD, localizes to the inner leaflet of the plasma membrane (Groves et al., 2008). Additionally, mechanical cell membrane processes such as membrane ruffling and cell migration have been shown to require PLD (O'Luanaigh et al., 2002; Santy and Casanova, 2001).

PAP

The PAP-1 inhibitor Propranolol did not have a large effect on oxLDL or IgG bead internalization.

Propranolol has been successfully used to treat atherosclerosis-related conditions (Olakowska and Olakowski, 2006). Additionally, PAP and CD36 both participate in phospholipid recruitment (Engelmann and Wiedmann, 2010). However, there has been no direct evidence of PAP activity regulation by CD36.

To date, phosphatidate phosphatase has not been directly implicated in IgG-mediated phagocytosis either. However, some speculate that the NADPH oxidase catalyzed ROS production concomitant with phagocytosis is reliant, in part, on PAP-mediated production of diacylglycerol (Lennartz, 1999). Thus it remains possible that PAP-1 still plays an important role in the response to oxLDL.

HMGCR

A significant reduction in IgG or oxLDL bead phagocytosis was not observed in response to HMGCR inhibition by Lovastatin (Appendix F).

Excess serum LDL can be controlled by inhibiting the rate-limiting LDL biosynthesis enzyme HMGCR via Lovastatin and CD36 expression has been shown to be upregulated in some cases by Lovastatin (Endo, 1979; Ruiz-Velasco et al., 2004). It is not known, however whether CD36 has a direct effect on HMGCR levels or activity.

Partial inhibition of the phagocytosis of IgG-opsonized sheep red blood cells by human monocytes has been reported in response to 10 μM lovastatin (Loike et al., 2004). Additionally, Fcγ signal transduction tyrosine kinase activation was inhibited by Fluvastatin, a related inhibitor of HMGCR, although this was hypothesized to be due to disruption of lipid rafts in monocytes (Hillyard et al., 2004).

LARC Determination of oxLDL/CD36 Receptor Complex Binding Partners

The selectivity of the base peak trace patterns of the 500 mM NaCl IgG, oxLDL and control elutions (Figure 13) demonstrate the ability of the aforementioned LARC system to distinguish IgG/FcR receptor complex associated proteins from oxLDL/CD36 receptor complex associated proteins.

A variety of Src-family, Syk-family, JAK, PLC, actin, FAK, PI3K, PLD, PKC, HMGCR and phosphatidate phosphatase isoforms were identified in IgG, oxLDL, anti-CD36 IgA and anti-CD36 IgG coated bead LARC thus supporting the validity of the central hypothesis. Many of

these protein groups were also identified in control treatments therefore further analysis must be conducted to eliminate irrelevant isoforms.

CONCLUSION

Pharmacological inhibition assays confirmed the validity of the system for quantifying phagocytic rates and demonstrated that actin, Janus kinase, PLC, Src and Syk are involved in oxLDL and IgG phagocytosis. Bead assays did not demonstrate a relationship between PI3K, HMGCR, Phosphatidate phosphatase, PKC, Fak, or PLD and oxLDL or IgG phagocytosis. Differential inhibition of oxLDL phagocytosis over IgG phagocytosis was not observed with the selected inhibitors under the tested conditions. However, further pharmacological testing may yet reveal an inhibitor that differentially inhibits oxLDL uptake thus elucidating the biochemical pathway involved in oxLDL phagocytosis and presenting a target for potential atherosclerosis treatment.

Bead internalization assays were successful in accurately assaying the number of beads internalized per cell and establishing statistically distinct uptake results. It seems that oxLDL-mediated phagocytosis can be quantified and differentiated from other types of phagocytosis using bead based assays and that the presence of specific types of enzymes potentially involved in oxLDL internalization such as SRC, SYK, Janus and PLC can be determined via nano LC-ESI-MS/MS.

LC-ESI-MS/MS of the U937 cell may be used to reveal the isoforms of the drug target proteins expressed in human macrophages.

FUTURE OBJECTIVES

Live-cell affinity receptor chromatography appears to be a useful technique in understanding the workings of oxLDL phagocytic signalling.

Now that a group of potential oxLDL receptor complex proteins has been identified via mass spectrometry, isoforms that are associated with the complex to a statistically relevant degree can be identified and the task of confirming their complicity in the pathogenic signalling pathways of oxLDL phagocytosis that lead to foam cell formation can be approached using dominant-negative transfection or siRNA. Additionally their presence at the site of internalization could be confirmed by GFP-fusion constructs or immunofluorescent staining.

APPENDIX A-BEADS INTERNALIZED IN RPMI WITH 10% FETAL BOVINE SERUM

DIC and Cy3 fluorescent images of IgG and oxLDL-coated beads internalized by U937 in RPMI with 10% fetal bovine serum for different periods of time. IgG-coated beads incubated for 15 min (A,B), 1h (C,D), 2h (E,F), 3h (G,H), 4(I,J). OxLDL-coated beads incubated for 15 min (K,L), 1h (M,N), 3h (O,P), 4h (Q,R). 3 replicates with an average of 3 images per treatment and 15 cells per image were collected.

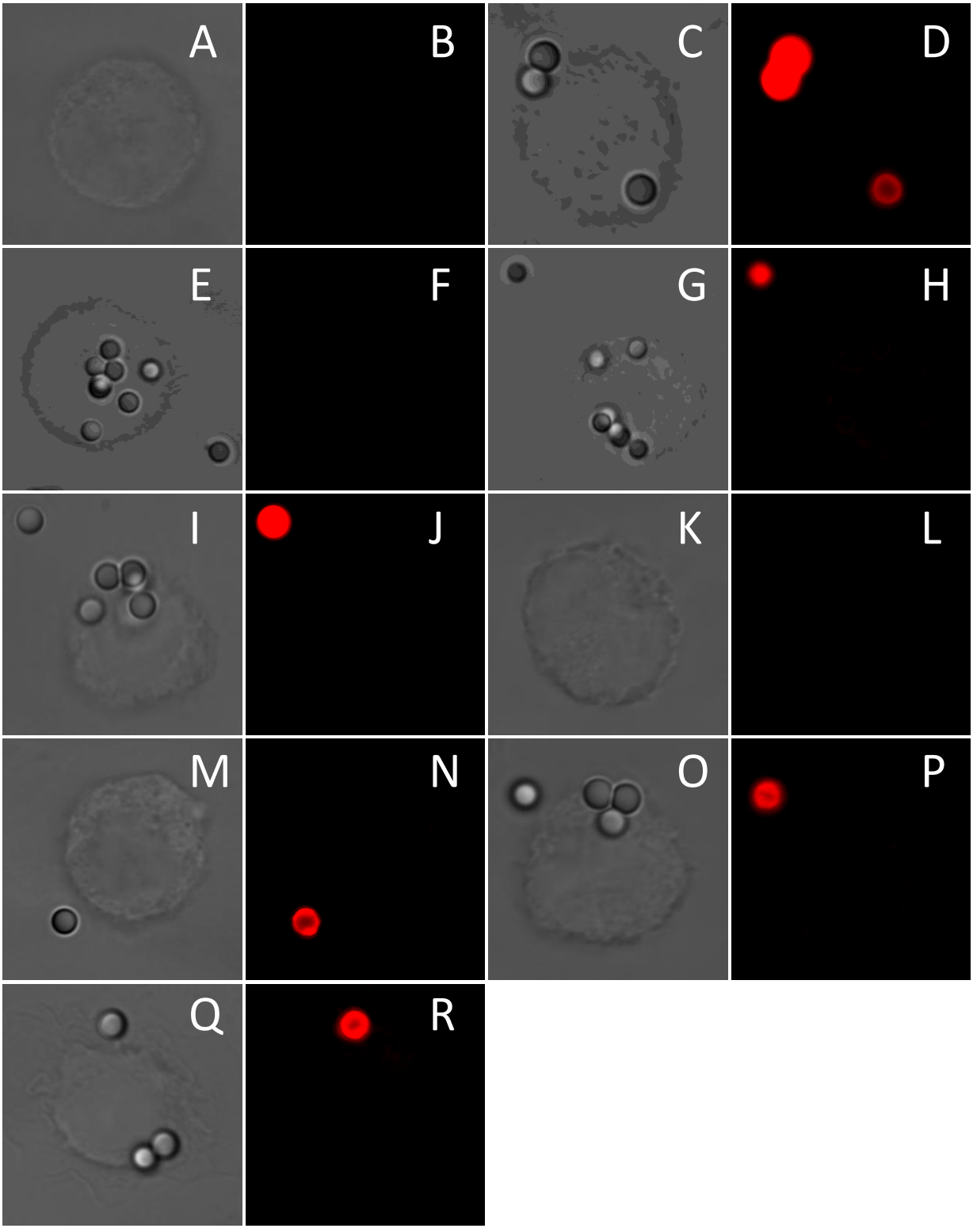

APPENDIX B - BEADS INTERNALIZED AFTER LIMITED BEAD PREINCUBATION

DIC and Cy3 fluorescent images of IgG-coated beads internalized by U937 after a limited 30 minute bead incubation in RPMI with 10% fetal bovine serum for different periods of time. 0h on ice (A,B), 15 min (C,D), 30min (E,F), 1h (G,H), 2h (I,J), 3h (K,L), 4h (M,N), 4h on ice (O,P), no bead (Q,R). 3 replicates with an average of 3 images per treatment and 15 cells per image were collected.

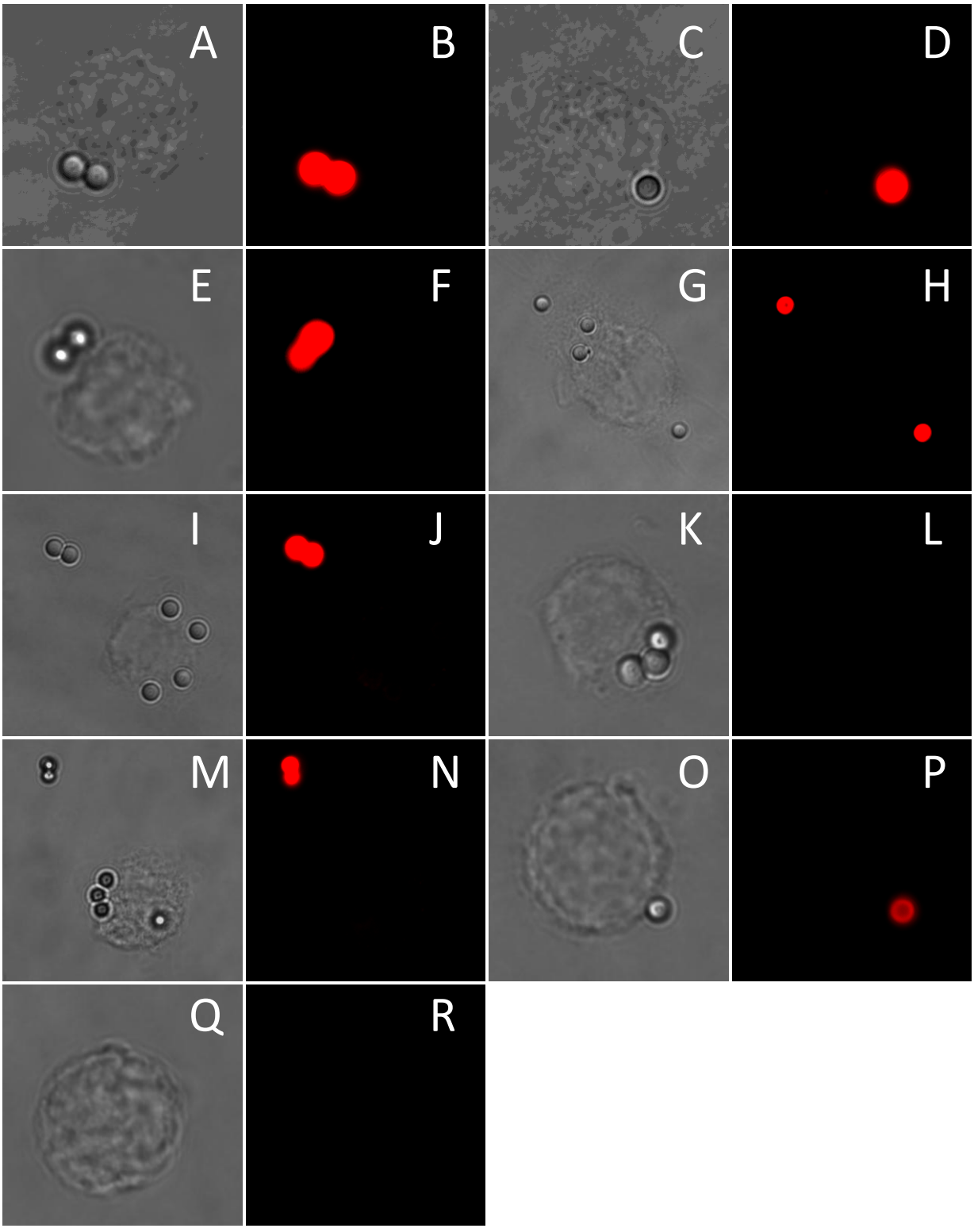

DIC and Cy3 fluorescent images of oxLDL-coated beads internalized by U937 after a limited 30 minute bead incubation in RPMI with 10% fetal bovine serum for different periods of time. 0h on ice (A,B), 15 min (C,D), 30min (E,F), 1h (G,H), 2h (I,J), 3h (K,L), 4h (M,N), 4h on ice (O,P), 2° antibody alone (Q,R). 3 replicates with an average of 3 images per treatment and 15 cells per image were collected.

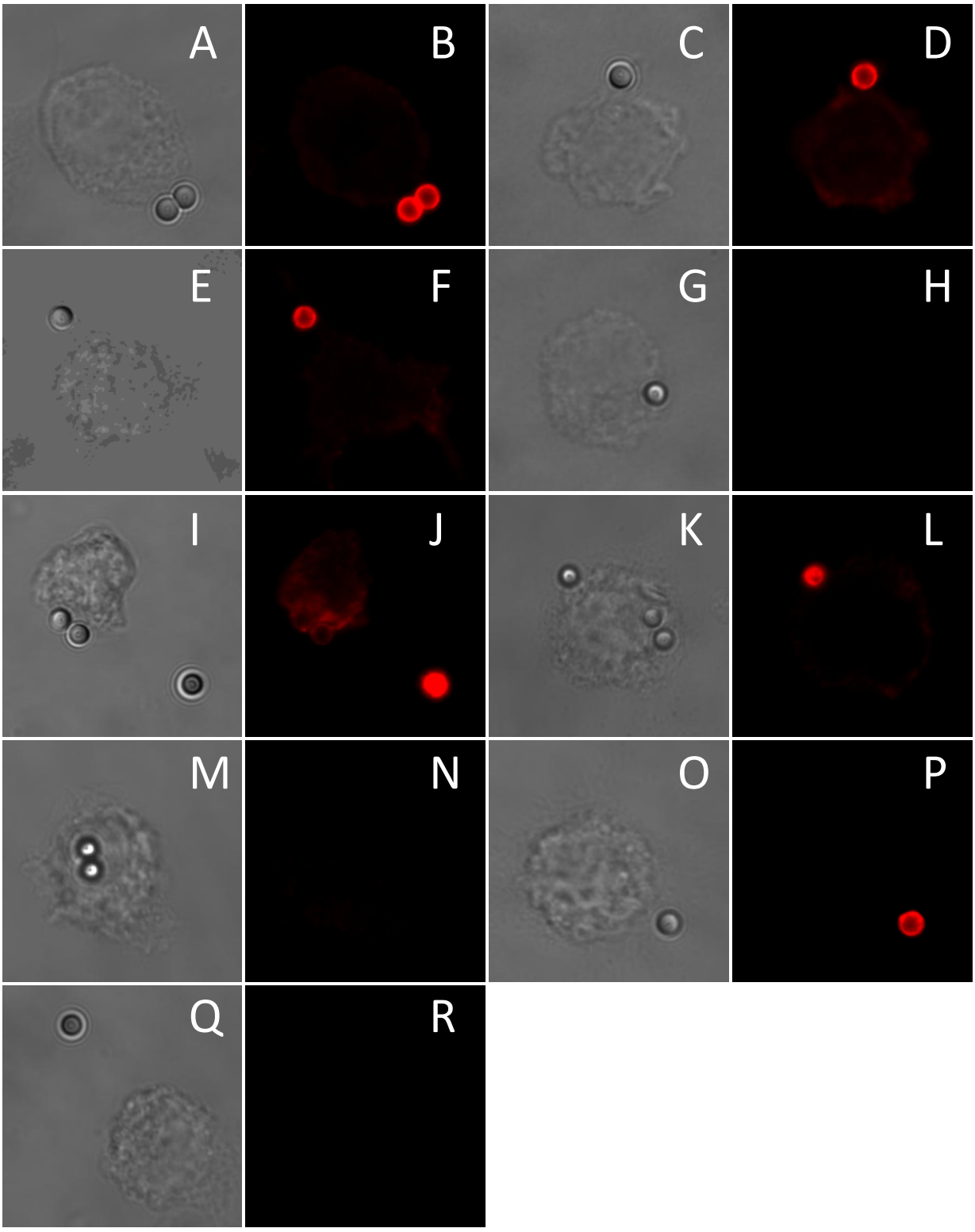

APPENDIX C – UNCOATED BEADS INTERNALIZED IN SALINE EXPERIMENTAL MEDIUM

DIC images of uncoated polystyrene bead internalization by U937 in Saline Experimental Medium at different time points. Cells were differentiated for 3 days with 100 nM PMA, washed 5-times with PBS and incubated with uncoated beads in isotonic experimental medium. Cells were fixed in a 5% paraformaldehye solution at 15min (A), 30min (B), 1h (C), 2h (D), 3h (E), 4h (F).

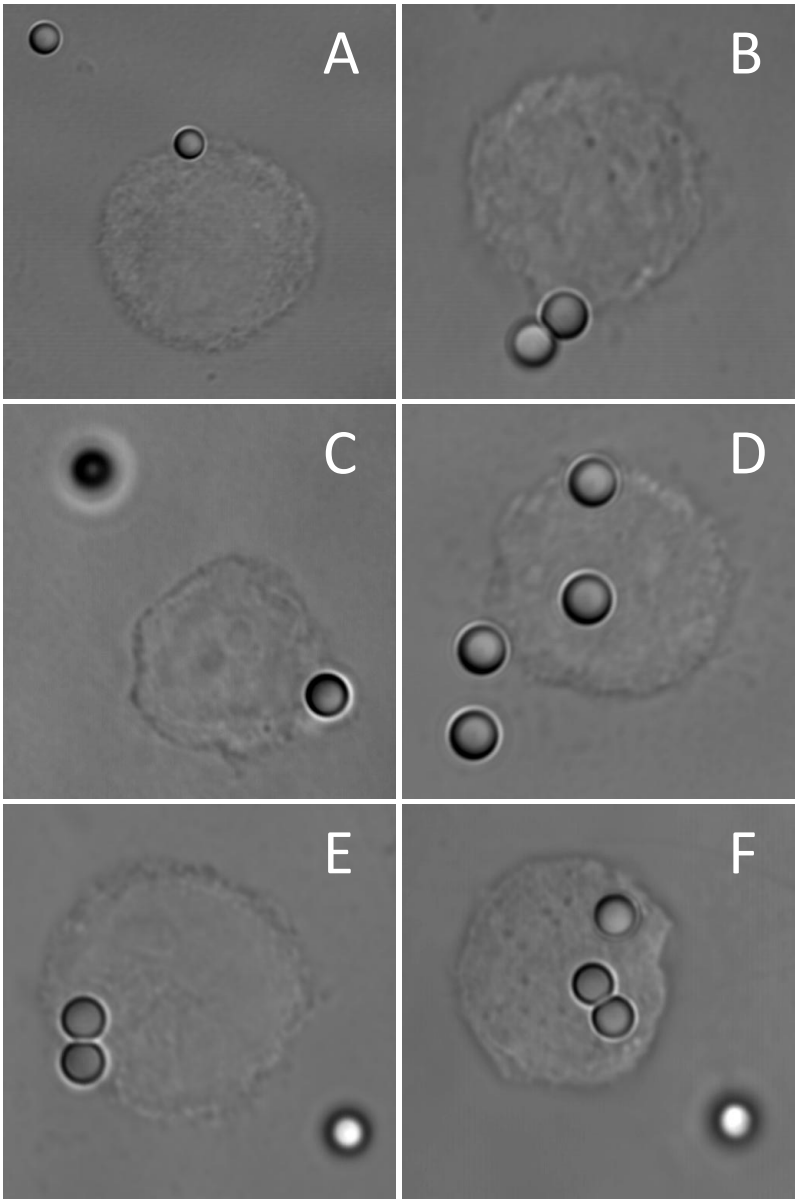

APPENDIX D – INTERNALIZATION OF UNCOATED, IGG-COATED AND OXLDL-COATED BEADS IN SALINE EXPERIMENTAL MEDIUM OVER 4 HOURS

Number of IgG-coated, oxLDL-coated and uncoated beads internalized by U937 in Saline Experimental Medium over 4 hours. Cells were differentiated for 3 days with 100 nM PMA, washed 5-times with PBS and incubated with oxLDL-coated or IgG-coated beads in isotonic experimental medium. Cells were fixed in a 5% paraformaldehye solution at 15 min, 30 min, 1h, 2h, 3h or 4h. Beads were subsequently stained with Cy3-conjugated anti-IgG antibody or rabbit polyclonal anti-oxLDL antibody followed by Cy3-conjugated donkey anti-rabbit antibody to visualize non-internalized beads. Quantification of bead internalization of at least 3 replicates +/- standard error.

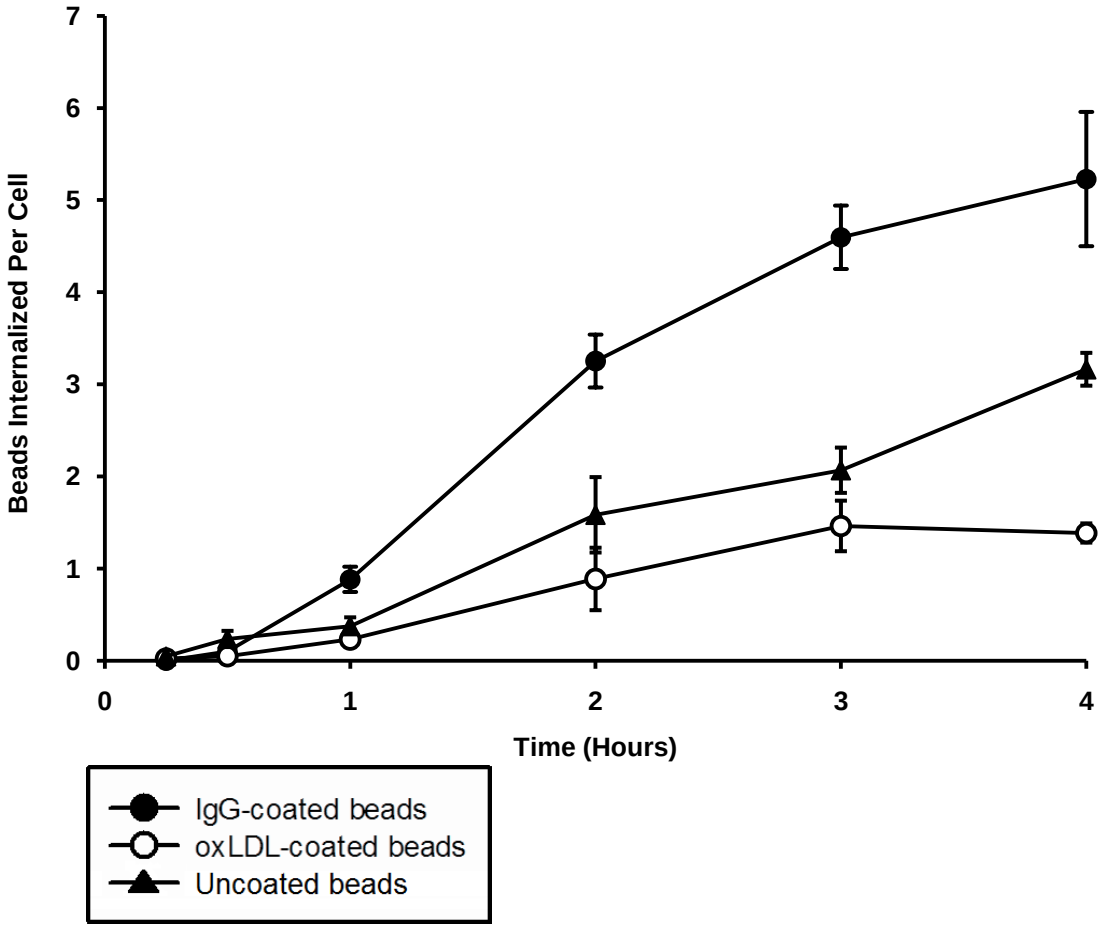

APPENDIX E: STATISTICAL ANALYSIS OF BEAD INTERNALIZATION IN SALINE EXPERIMENTAL MEDIUM ASSAY

The following model compares the average number of internalized beads per cell for oxLDL-coated IgG-coated and uncoated treatments at different time points. Significant differences between treatments and time points were observed.

Response in
Whole Model
Actual by Predicted Plot

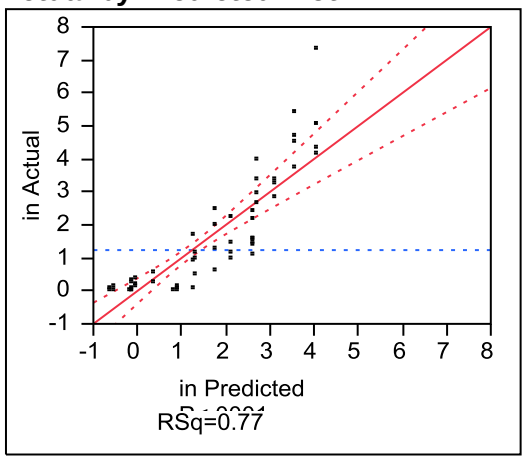

Summary of Fit

RSquare	0.765307
RSquare Adj	0.738096
Root Mean Square Error	0.839874
Mean of Response	1.235984
Observations (or Sum Wgts)	78

Analysis of Variance

Source	DF	Sum of Squares	Mean Square	F Ratio
Model	8	158.71342	19.8392	28.1252
Error	69	48.67182	0.7054	**Prob > F**
C. Total	77	207.38524		<.0001*

Lack Of Fit

Source	DF	Sum of Squares	Mean Square	F Ratio
Lack Of Fit	12	34.502011	2.87517	11.5658
Pure Error	57	14.169813	0.24859	**Prob > F**
Total Error	69	48.671825		<.0001*
				Max RSq
				0.9317

Effect Tests

Source	Nparm	DF	Sum of Squares	F Ratio	Prob > F
treatment	2	2	29.52328	20.9270	<.0001*
time	6	6	129.40448	30.5752	<.0001*

Residual by Predicted Plot

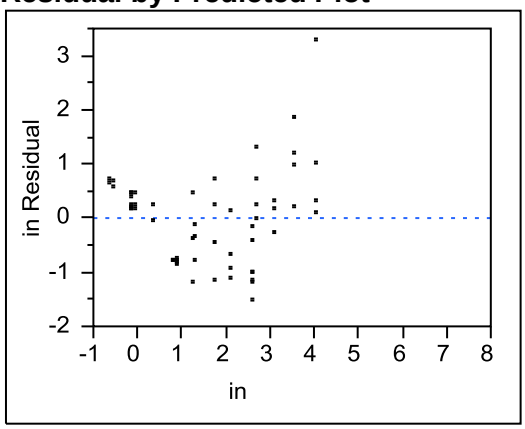

APPENDIX F – PHARMACOLOGICAL INHIBITION OF PHAGOCYTOSIS

DIC and Cy3 fluorescent images of IgG-coated bead internalization over 4 hours with pharmacological inhibitors. No drug (A, B), DMSO (C, D), BAY 61 3606 (E, F), Cytochalasin D (G, H), Latrunculin B (I, J), MNS (K, L), Wortmannin (M, N), Ethanol (O, P), PP2 (Q, R), U73122 (S, T).

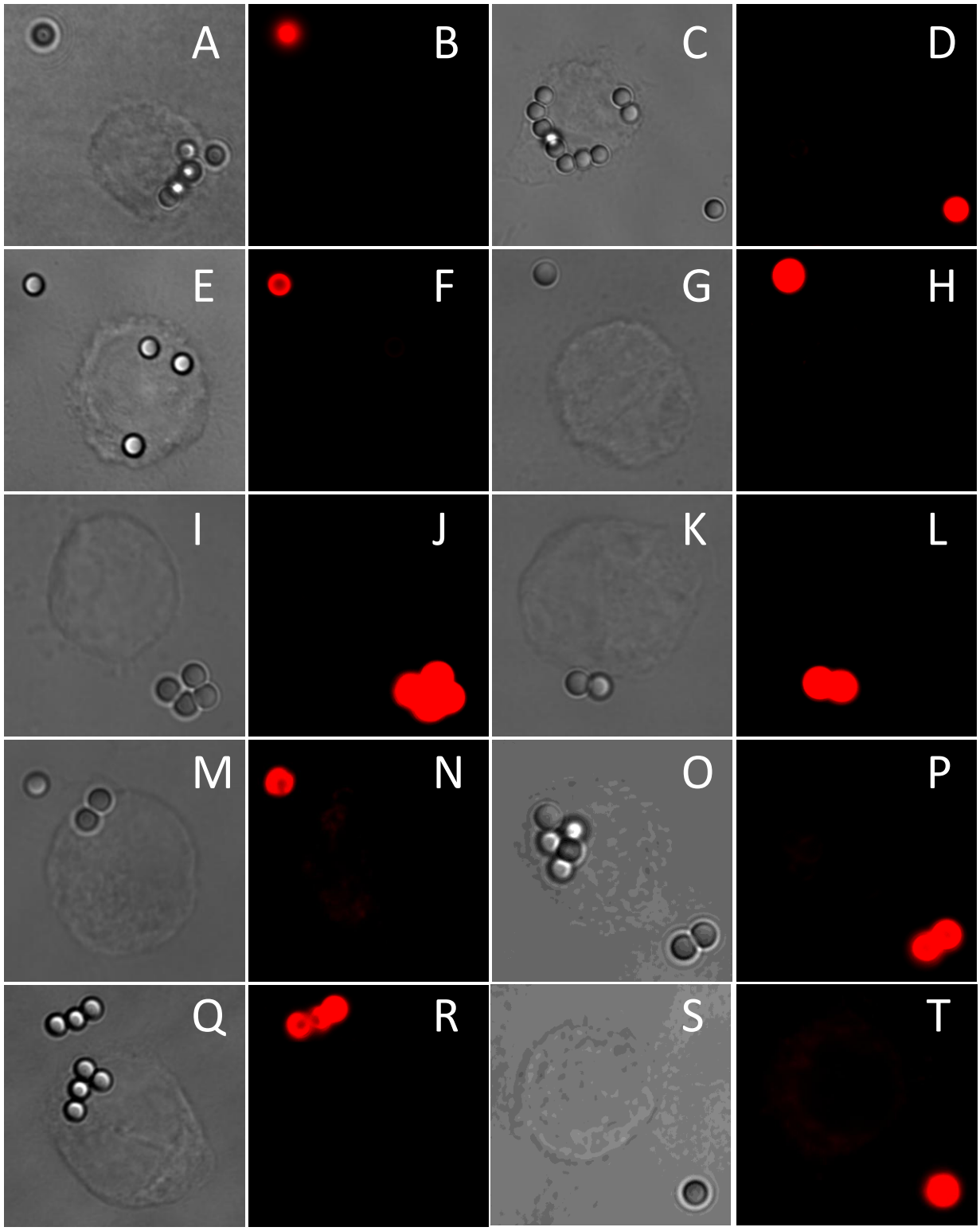

DIC and Cy3 fluorescent images of IgG-coated bead internalization over 4 hours when exposed to various pharmacological inhibitors. AG490 (A, B), Genistein (C, D), Go6983 (E, F), LY 294 002 (G, H), PF 573228 (I, J), Propranolol (K, L), Lovastatin (M, N). 3 replicates with an average of 3 images per treatment and 15 cells per image were collected.

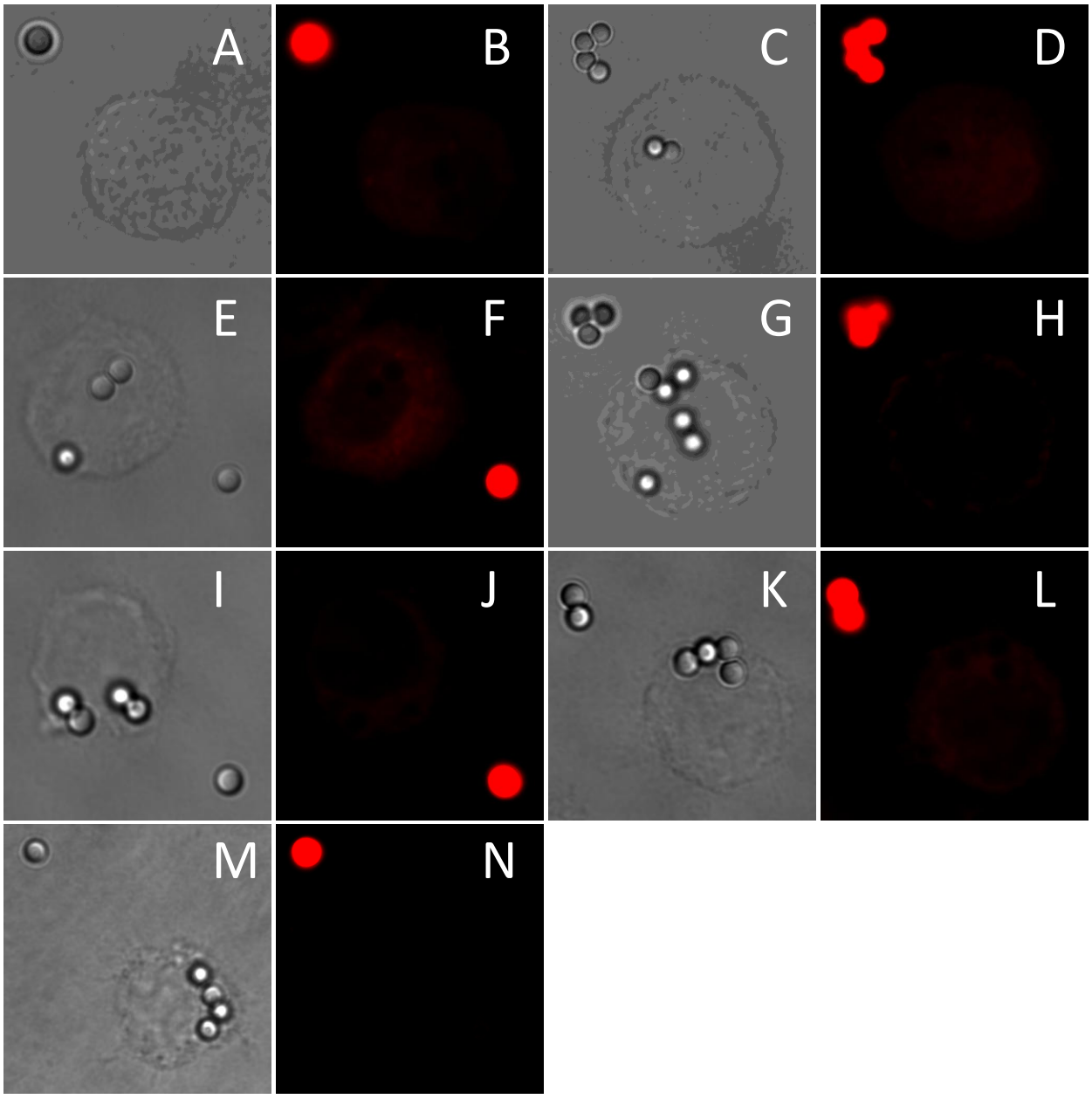

DIC and Cy3 fluorescent images of oxLDL-coated bead internalization over 4 hours when exposed to various pharmacological inhibitors. No drug (A, B), DMSO (C, D), BAY 61 3606 (E, F), Cytochalasin D (G, H), Latrunculin B (I, J), MNS (K, L), Wortmannin (M, N), Ethanol (O, P), PP2 (Q, R), U73122 (S, T).

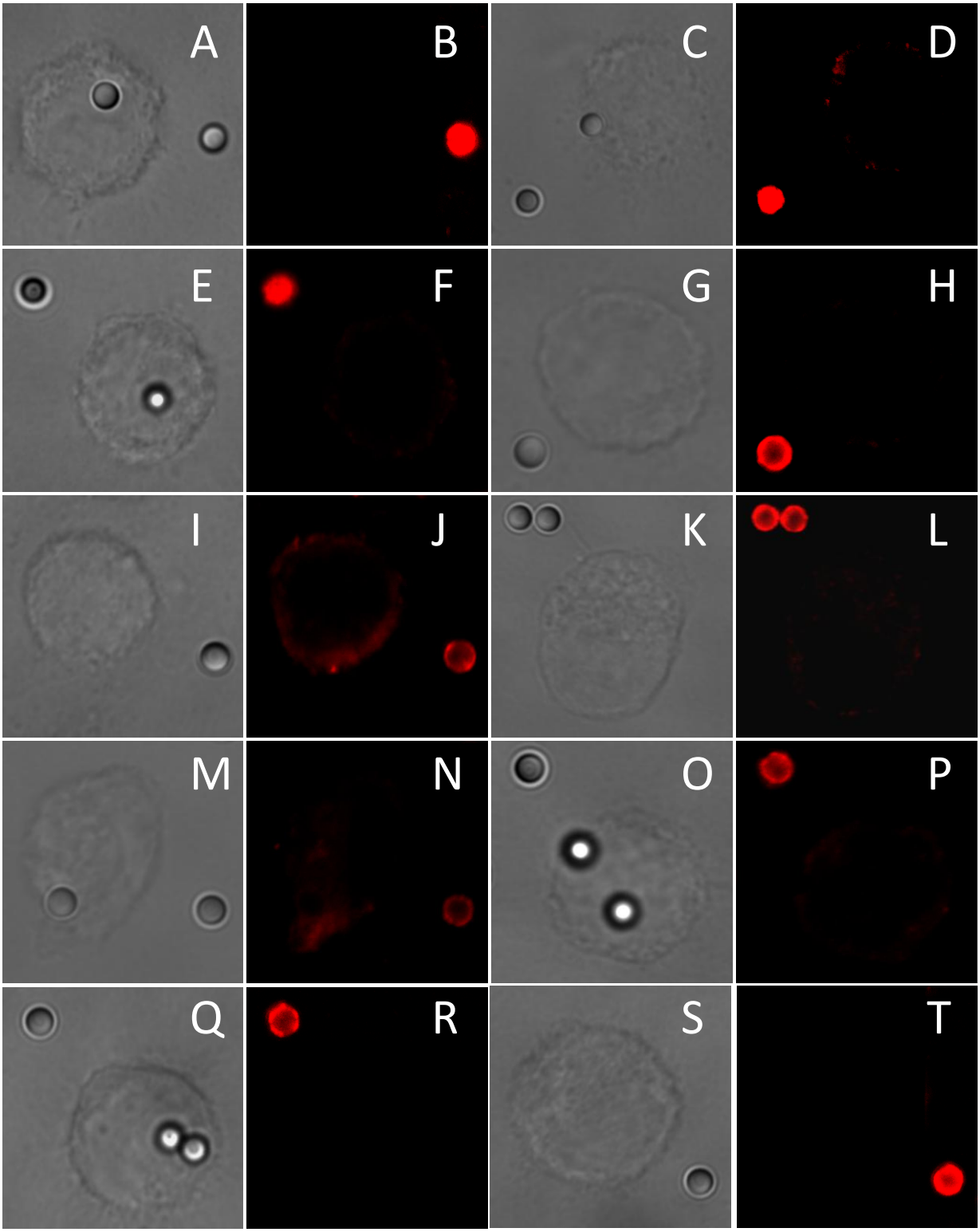

DIC and Cy3 fluorescent images of oxLDL-coated bead internalization over 4 hours when exposed to various pharmacological inhibitors. AG490 (A, B), Genistein (C, D), Go6983 (E, F), LY 294 002 (G, H), PF 573228 (I, J), Propranolol (K, L), Lovastatin (M, N). 3 replicates with an average of 3 images per treatment and 15 cells per image were collected.

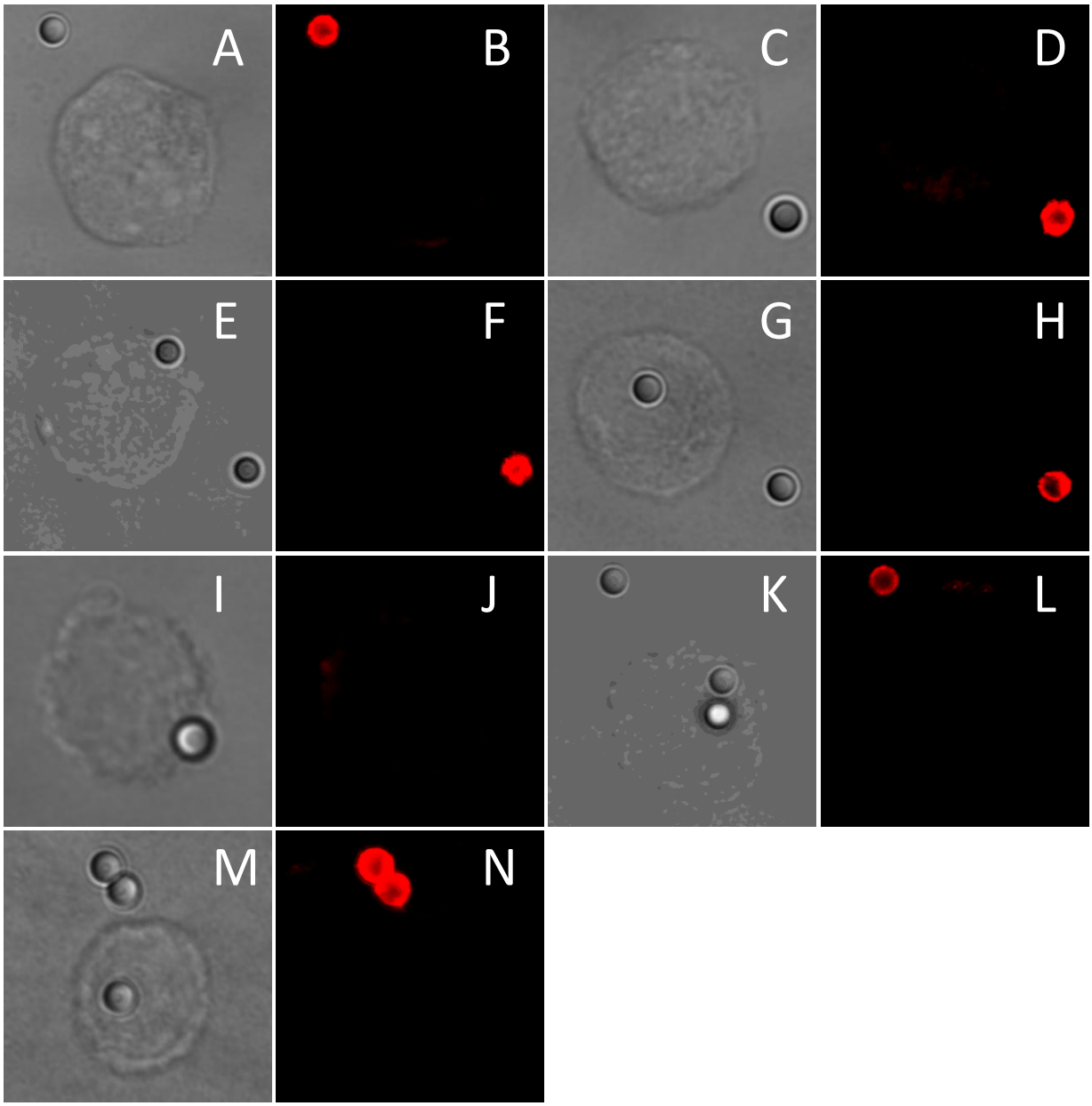

APPENDIX G: POOLED IGG AND OXLDL ONE-WAY ANOVA OF PHARMACOLOGICAL INHIBITION ASSAY

The following analysis compares the average number of internalized beads per cell for oxLDL-coated and IgG-coated bead treatments for different pharmacological inhibitors. Analysis by Tukey-Cramer HSD reveals significant bead internalization inhibition under AG 490, U73122, MNS, Cytochalasin D and Latrunculin B treatments.

Oneway Analysis of in By drug

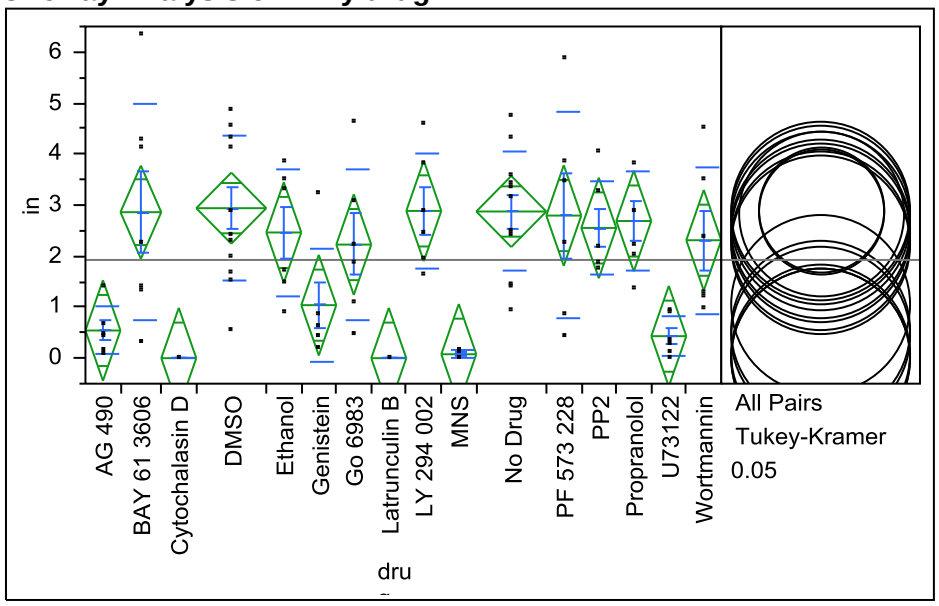

Missing Rows
35

Oneway Anova
Summary of Fit

Rsquare	0.509734
Adj Rsquare	0.430659
Root Mean Square Error	1.215823
Mean of Response	1.925164
Observations (or Sum Wgts)	109

Analysis of Variance

Source	DF	Sum of Squares	Mean Square	F Ratio	Prob > F
drug	15	142.93425	9.52895	6.4462	<.0001*
Error	93	137.47498	1.47823		
C. Total	108	280.40923			

Means for Oneway Anova

Level	Number	Mean	Std Error	Lower 95%	Upper 95%
AG 490	6	0.54205	0.49636	-0.444	1.5277
BAY 61 3606	7	2.86090	0.45954	1.948	3.7734
Cytochalasin D	6	0.00000	0.49636	-0.986	0.9857
DMSO	12	2.93935	0.35098	2.242	3.6363
Ethanol	6	2.46321	0.49636	1.478	3.4489
Genistein	6	1.03862	0.49636	0.053	2.0243

Level	Number	Mean	Std Error	Lower 95%	Upper 95%
Go 6983	6	2.22586	0.49636	1.240	3.2115
Latrunculin B	6	0.00000	0.49636	-0.986	0.9857
LY 294 002	6	2.88587	0.49636	1.900	3.8715
MNS	6	0.07667	0.49636	-0.909	1.0623
No Drug	12	2.87422	0.35098	2.177	3.5712
PF 573 228	6	2.79447	0.49636	1.809	3.7801
PP2	6	2.55202	0.49636	1.566	3.5377
Propranolol	6	2.68771	0.49636	1.702	3.6734
U73122	6	0.43123	0.49636	-0.554	1.4169
Wortmannin	6	2.31125	0.49636	1.326	3.2969

Std Error uses a pooled estimate of error variance

Means and Std Deviations

Level	Number	Mean	Std Dev	Std Err Mean	Lower 95%	Upper 95%
AG 490	6	0.54205	0.46572	0.19013	0.053	1.0308
BAY 61 3606	7	2.86090	2.12851	0.80450	0.892	4.8294
Cytochalasin D	6	0.00000	0.00000	0.00000	0.000	0.0000
DMSO	12	2.93935	1.40979	0.40697	2.044	3.8351
Ethanol	6	2.46321	1.24168	0.50691	1.160	3.7663
Genistein	6	1.03862	1.11479	0.45511	-0.131	2.2085
Go 6983	6	2.22586	1.48060	0.60445	0.672	3.7797
Latrunculin B	6	0.00000	0.00000	0.00000	0.000	0.0000
LY 294 002	6	2.88587	1.13302	0.46255	1.697	4.0749
MNS	6	0.07667	0.08472	0.03459	-0.012	0.1656
No Drug	12	2.87422	1.17225	0.33840	2.129	3.6190
PF 573 228	6	2.79447	2.03025	0.82885	0.664	4.9251
PP2	6	2.55202	0.91621	0.37404	1.591	3.5135
Propranolol	6	2.68771	0.98937	0.40391	1.649	3.7260
U73122	6	0.43123	0.39593	0.16164	0.016	0.8467
Wortmannin	6	2.31125	1.44263	0.58895	0.797	3.8252

Means Comparisons

Comparisons for all pairs using Tukey-Kramer HSD

Level					Mean
DMSO	A				2.9393535
LY 294 002	A	B	C		2.8858696
No Drug	A				2.8742167
BAY 61 3606	A	B			2.8608962
PF 573 228	A	B	C		2.7944682
Propranolol	A	B	C		2.6877135
PP2	A	B	C		2.5520207
Ethanol	A	B	C	D	2.4632132
Wortmannin	A	B	C	D	2.3112475
Go 6983	A	B	C	D	2.2258598
Genistein	A	B	C	D	1.0386202
AG 490		B	C	D	0.5420536
U73122			C	D	0.4312350
MNS				D	0.0766667
Cytochalasin D				D	0.0000000
Latrunculin B				D	0.0000000

Levels not connected by same letter are significantly different.

APPENDIX H: TWO-WAY ANOVA OF PHARMACOLOGICAL INHIBITION ASSAY

The following analyzes the average number of internalized oxLDL-coated beads, IgG-coated beads and the effect of different pharmacological inhibitors.

Response normal in Whole Model
Actual by Predicted Plot

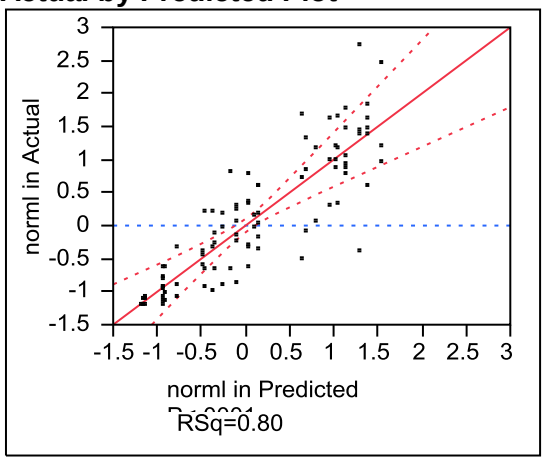

Summary of Fit

RSquare	0.800895
RSquare Adj	0.720736
Root Mean Square Error	0.528454
Mean of Response	-3.7e-16
Observations (or Sum Wgts)	109

Analysis of Variance

Source	DF	Sum of Squares	Mean Square	F Ratio
Model	31	86.49667	2.79022	9.9913
Error	77	21.50333	0.27926	**Prob > F**
C. Total	108	108.00000		<.0001*

Parameter Estimates

Term	Estimate	Std Error	t Ratio	Prob>|t|
Intercept	-0.089672	0.052004	-1.72	0.0887
treatment[IgG]	0.4062062	0.052004	7.81	<.0001*
drug[AG 490]	-0.768694	0.2084	-3.69	0.0004*
drug[BAY 61 3606]	0.5508209	0.195805	2.81	0.0062*
drug[Cytochalasin D]	-1.105096	0.2084	-5.30	<.0001*
drug[DMSO]	0.7190838	0.15188	4.73	<.0001*
drug[Ethanol]	0.4235885	0.2084	2.03	0.0455*
drug[Genistein]	-0.460522	0.2084	-2.21	0.0301*
drug[Go 6983]	0.2762856	0.2084	1.33	0.1888
drug[Latrunculin B]	-1.105096	0.2084	-5.30	<.0001*
drug[LY 294 002]	0.6858914	0.2084	3.29	0.0015*
drug[MNS]	-1.057516	0.2084	-5.07	<.0001*
drug[No Drug]	0.6786595	0.15188	4.47	<.0001*
drug[PF 573 228]	0.6291672	0.2084	3.02	0.0034*
drug[PP2]	0.4787029	0.2084	2.30	0.0243*
drug[Propranolol]	0.5629146	0.2084	2.70	0.0085*
drug[U73122]	-0.837469	0.2084	-4.02	0.0001*

Term	Estimate	Std Error	t Ratio	Prob>|t|
treatment[IgG]*drug[AG 490]	-0.321811	0.2084	-1.54	0.1266
treatment[IgG]*drug[BAY 61 3606]	0.430797	0.195805	2.20	0.0308*
treatment[IgG]*drug[Cytochalasin D]	-0.406206	0.2084	-1.95	0.0549
treatment[IgG]*drug[DMSO]	0.3376171	0.15188	2.22	0.0292*
treatment[IgG]*drug[Ethanol]	0.2733703	0.2084	1.31	0.1935
treatment[IgG]*drug[Genistein]	-0.020131	0.2084	-0.10	0.9233
treatment[IgG]*drug[Go 6983]	0.0344156	0.2084	0.17	0.8693
treatment[IgG]*drug[Latrunculin B]	-0.406206	0.2084	-1.95	0.0549
treatment[IgG]*drug[LY 294 002]	0.0472874	0.2084	0.23	0.8211
treatment[IgG]*drug[MNS]	-0.420687	0.2084	-2.02	0.0470*
treatment[IgG]*drug[No Drug]	0.1470031	0.15188	0.97	0.3361
treatment[IgG]*drug[PF 573 228]	0.5890716	0.2084	2.83	0.0060*
treatment[IgG]*drug[PP2]	-0.107233	0.2084	-0.51	0.6083
treatment[IgG]*drug[Propranolol]	-0.080322	0.2084	-0.39	0.7010
treatment[IgG]*drug[U73122]	-0.410076	0.2084	-1.97	0.0527

Effect Tests

Source	Nparm	DF	Sum of Squares	F Ratio	Prob > F
treatment	1	1	17.038341	61.0116	<.0001*
drug	15	15	54.141406	12.9248	<.0001*
treatment*drug	15	15	10.722640	2.5597	0.0038*

Residual by Predicted Plot

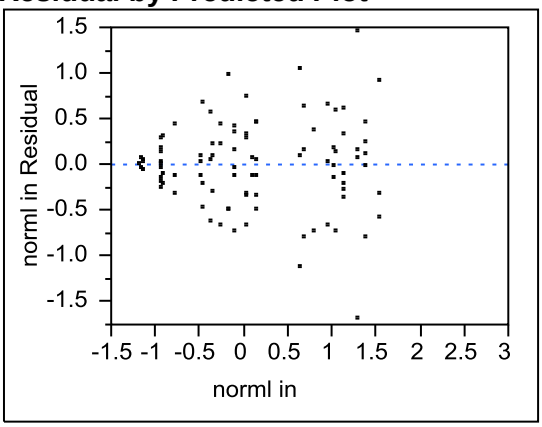

treatment
Leverage Plot

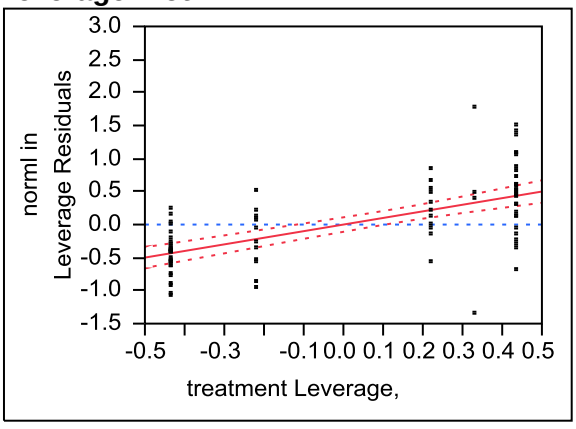

Least Squares Means Table

Level	Least Sq Mean	Std Error	Mean
IgG	0.3165339	0.07323571	0.43706
oxLDL	-0.4958785	0.07385374	-0.44515

drug
Leverage Plot

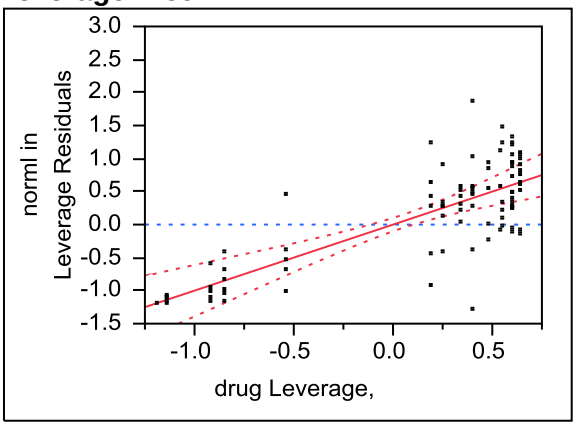

treatment*drug
Leverage Plot

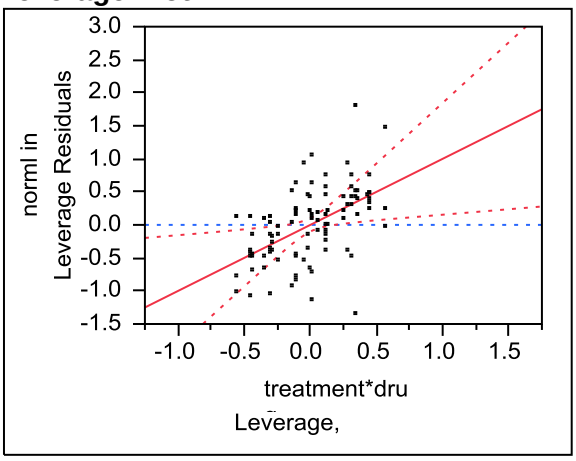

APPENDIX I: ONE-WAY ANOVA OF NORMALIZED IGG-BEAD INTERNALIZATION DURING PHARMACOLOGICAL INHIBITION ASSAY

The following analysis compares the average number of internalized beads per cell for IgG-coated bead treatments for different pharmacological inhibitors. Analysis by Tukey-Cramer HSD reveals significant bead internalization inhibition under Genistein, AG 490, U73122, MNS, Cytochalasin D and Latrunculin B treatments.

Oneway Analysis of normal in By drug

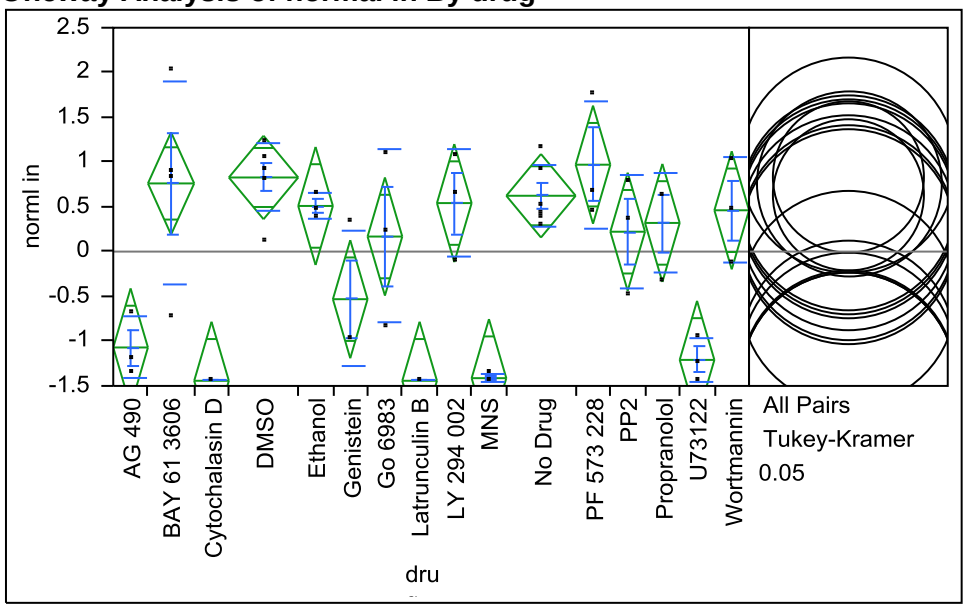

Missing Rows
17

Oneway Anova
Summary of Fit

Rsquare	0.769876
Adj Rsquare	0.681367
Root Mean Square Error	0.564476
Mean of Response	-7.7e-17
Observations (or Sum Wgts)	55

Analysis of Variance

Source	DF	Sum of Squares	Mean Square	F Ratio	Prob > F
drug	15	41.573311	2.77155	8.6983	<.0001*
Error	39	12.426689	0.31863		
C. Total	54	54.000000			

Means for Oneway Anova

Level	Number	Mean	Std Error	Lower 95%	Upper 95%
AG 490	3	-1.0706	0.32590	-1.730	-0.411
BAY 61 3606	4	0.7612	0.28224	0.190	1.332
Cytochalasin D	3	-1.4426	0.32590	-2.102	-0.783

Level	Number	Mean	Std Error	Lower 95%	Upper 95%
DMSO	6	0.8276	0.23045	0.361	1.294
Ethanol	3	0.5096	0.32590	-0.150	1.169
Genistein	3	-0.5315	0.32590	-1.191	0.128
Go 6983	3	0.1681	0.32590	-0.491	0.827
Latrunculin B	3	-1.4426	0.32590	-2.102	-0.783
LY 294 002	3	0.5416	0.32590	-0.118	1.201
MNS	3	-1.4133	0.32590	-2.073	-0.754
No Drug	6	0.6234	0.23045	0.157	1.089
PF 573 228	3	0.9704	0.32590	0.311	1.630
PP2	3	0.2218	0.32590	-0.437	0.881
Propranolol	3	0.3201	0.32590	-0.339	0.979
U73122	3	-1.2094	0.32590	-1.869	-0.550
Wortmannin	3	0.4613	0.32590	-0.198	1.121

Std Error uses a pooled estimate of error variance

Means and Std Deviations

Level	Number	Mean	Std Dev	Std Err Mean	Lower 95%	Upper 95%
AG 490	3	-1.0706	0.34687	0.20026	-1.932	-0.209
BAY 61 3606	4	0.7612	1.13503	0.56751	-1.045	2.567
Cytochalasin D	3	-1.4426	0.00000	0.00000	-1.443	-1.443
DMSO	6	0.8276	0.37448	0.15288	0.435	1.221
Ethanol	3	0.5096	0.14288	0.08249	0.155	0.865
Genistein	3	-0.5315	0.75513	0.43597	-2.407	1.344
Go 6983	3	0.1681	0.96606	0.55776	-2.232	2.568
Latrunculin B	3	-1.4426	0.00000	0.00000	-1.443	-1.443
LY 294 002	3	0.5416	0.59346	0.34263	-0.933	2.016
MNS	3	-1.4133	0.05068	0.02926	-1.539	-1.287
No Drug	6	0.6234	0.34602	0.14126	0.260	0.986
PF 573 228	3	0.9704	0.70875	0.40919	-0.790	2.731
PP2	3	0.2218	0.64274	0.37108	-1.375	1.818
Propranolol	3	0.3201	0.55797	0.32214	-1.066	1.706
U73122	3	-1.2094	0.24802	0.14320	-1.826	-0.593
Wortmannin	3	0.4613	0.58630	0.33850	-0.995	1.918

Means Comparisons

Comparisons for all pairs using Tukey-Kramer HSD

q*	Alpha
3.65655	0.05

Abs(Dif)-HSD	PF	DMSO	BAY	N/D	LY	Eth.	Wort.	Prop.	PP2	Go	Gen.	AG	U7.	MNS	Cyto. D	Lat. B
PF	-1.6853	-1.3167	-1.3673	-1.1124	-1.2565	-1.2245	-1.1762	-1.0349	-0.9367	-0.8830	-0.1834	0.3557	0.4945	0.6984	0.7277	0.7277
DMSO	-1.3167	-1.1917	-1.2660	-0.9874	-1.1735	-1.1415	-1.0932	-0.9520	-0.8537	-0.8000	-0.1004	0.4387	0.5775	0.7814	0.8107	0.8107
BAY	-1.3673	-1.2660	-1.4595	-1.1945	-1.3568	-1.3248	-1.2765	-1.1353	-1.0370	-0.9833	-0.2838	0.2554	0.3942	0.5981	0.6274	0.6274
N/D	-1.1124	-0.9874	-1.1945	-1.1917	-1.3777	-1.3457	-1.2975	-1.1562	-1.0580	-1.0043	-0.3047	0.2344	0.3733	0.5772	0.6064	0.6064
LY	-1.2565	-1.1735	-1.3568	-1.3777	-1.6853	-1.6533	-1.6050	-1.4638	-1.3655	-1.3118	-0.6122	-0.0731	0.0657	0.2696	0.2989	0.2989
Eth.	-1.2245	-1.1415	-1.3248	-1.3457	-1.6533	-1.6853	-1.6370	-1.4958	-1.3975	-1.3438	-0.6442	-0.1051	0.0337	0.2376	0.2669	0.2669
Wort	-1.1762	-1.0932	-1.2765	-1.2975	-1.6050	-1.6370	-1.6853	-1.5440	-1.4458	-1.3921	-0.6925	-0.1534	-0.0145	0.1894	0.2186	0.2186
Prop.	-1.0349	-0.9520	-1.1353	-1.1562	-1.4638	-1.4958	-1.5440	-1.6853	-1.5870	-1.5333	-0.8337	-0.2946	-0.1558	0.0481	0.0774	0.0774
PP2	-0.9367	-0.8537	-1.0370	-1.0580	-1.3655	-1.3975	-1.4458	-1.5870	-1.6853	-1.6316	-0.9320	-0.3929	-0.2540	-0.0501	-0.0209	-0.0209
Gö	-0.8830	-0.8000	-0.9833	-1.0043	-1.3118	-1.3438	-1.3921	-1.5333	-1.6316	-1.6853	-0.9857	-0.4466	-0.3078	-0.1038	-0.0746	-0.0746
Gen.	-0.1834	-0.1004	-0.2838	-0.3047	-0.6122	-0.6442	-0.6925	-0.8337	-0.9320	-0.9857	-1.6853	-1.1462	-1.0073	-0.8034	-0.7742	-0.7742
AG	0.3557	0.4387	0.2554	0.2344	-0.0731	-0.1051	-0.1534	-0.2946	-0.3929	-0.4466	-1.1462	-1.6853	-1.5465	-1.3425	-1.3133	-1.3133
U7.	0.4945	0.5775	0.3942	0.3733	0.0657	0.0337	-0.0145	-0.1558	-0.2540	-0.3078	-1.0073	-1.5465	-1.6853	-1.4814	-1.4521	-1.4521
MNS	0.6984	0.7814	0.5981	0.5772	0.2696	0.2376	0.1894	0.0481	-0.0501	-0.1038	-0.8034	-1.3425	-1.4814	-1.6853	-1.6560	-1.6560
Cyto. D	0.7277	0.8107	0.6274	0.6064	0.2989	0.2669	0.2186	0.0774	-0.0209	-0.0746	-0.7742	-1.3133	-1.4521	-1.6560	-1.6853	-1.6853
Lat. B	0.7277	0.8107	0.6274	0.6064	0.2989	0.2669	0.2186	0.0774	-0.0209	-0.0746	-0.7742	-1.3133	-1.4521	-1.6560	-1.6853	-1.6853

Positive values show pairs of means that are significantly different.

Level					Mean
PF 573 228	A				0.970406
DMSO	A				0.827603
BAY 61 3606	A				0.761228
No Drug	A				0.623360
LY 294 002	A	B			0.541602
Ethanol	A	B			0.509583
Wortmannin	A	B	C		0.461341
Propranolol	A	B	C		0.320079
PP2	A	B	C	D	0.221844
Go 6983	A	B	C	D	0.168123
Genistein	A	B	C	D	-0.531452
AG 490		B	C	D	-1.070575
U73122			C	D	-1.209401
MNS				D	-1.413309
Cytochalasin D				D	-1.442569
Latrunculin B				D	-1.442569

Levels not connected by same letter are significantly different.

Level	- Level	Difference	Std Err Dif	Lower CL	Upper CL	p-Value	Difference
PF 573 228	Cytochalasin D	2.412975	0.4608927	0.72770	4.098252	0.0006*	
PF 573 228	Latrunculin B	2.412975	0.4608927	0.72770	4.098252	0.0006*	
PF 573 228	MNS	2.383715	0.4608927	0.69844	4.068992	0.0007*	
DMSO	Cytochalasin D	2.270172	0.3991447	0.81068	3.729665	0.0001*	
DMSO	Latrunculin B	2.270172	0.3991447	0.81068	3.729665	0.0001*	
DMSO	MNS	2.240912	0.3991447	0.78142	3.700405	0.0002*	
BAY 61 3606	Cytochalasin D	2.203797	0.4311256	0.62736	3.780229	0.0008*	
BAY 61 3606	Latrunculin B	2.203797	0.4311256	0.62736	3.780229	0.0008*	
PF 573 228	U73122	2.179808	0.4608927	0.49453	3.865085	0.0026*	
BAY 61 3606	MNS	2.174537	0.4311256	0.59810	3.750969	0.0010*	
No Drug	Cytochalasin D	2.065929	0.3991447	0.60644	3.525422	0.0007*	
No Drug	Latrunculin B	2.065929	0.3991447	0.60644	3.525422	0.0007*	
PF 573 228	AG 490	2.040981	0.4608927	0.35570	3.726258	0.0063*	
DMSO	U73122	2.037004	0.3991447	0.57751	3.496497	0.0009*	
No Drug	MNS	2.036669	0.3991447	0.57718	3.496162	0.0009*	
LY 294 002	Cytochalasin D	1.984171	0.4608927	0.29889	3.669448	0.0089*	
LY 294 002	Latrunculin B	1.984171	0.4608927	0.29889	3.669448	0.0089*	
BAY 61 3606	U73122	1.970629	0.4311256	0.39420	3.547062	0.0042*	
LY 294 002	MNS	1.954911	0.4608927	0.26963	3.640188	0.0107*	
Ethanol	Cytochalasin D	1.952152	0.4608927	0.26687	3.637429	0.0108*	
Ethanol	Latrunculin B	1.952152	0.4608927	0.26687	3.637429	0.0108*	
Ethanol	MNS	1.922892	0.4608927	0.23761	3.608169	0.0129*	
Wortmannin	Cytochalasin D	1.903909	0.4608927	0.21863	3.589187	0.0145*	
Wortmannin	Latrunculin B	1.903909	0.4608927	0.21863	3.589187	0.0145*	
DMSO	AG 490	1.898178	0.3991447	0.43869	3.357671	0.0024*	
Wortmannin	MNS	1.874649	0.4608927	0.18937	3.559927	0.0172*	
No Drug	U73122	1.832762	0.3991447	0.37327	3.292254	0.0039*	
BAY 61 3606	AG 490	1.831803	0.4311256	0.25537	3.408236	0.0104*	
Propranolol	Cytochalasin D	1.762648	0.4608927	0.07737	3.447925	0.0327*	
Propranolol	Latrunculin B	1.762648	0.4608927	0.07737	3.447925	0.0327*	
LY 294 002	U73122	1.751004	0.4608927	0.06573	3.436281	0.0349*	
Propranolol	MNS	1.733387	0.4608927	0.04811	3.418665	0.0385*	
Ethanol	U73122	1.718984	0.4608927	0.03371	3.404262	0.0416*	
No Drug	AG 490	1.693935	0.3991447	0.23444	3.153428	0.0106*	
Wortmannin	U73122	1.670742	0.4608927	-0.01454	3.356019	0.0540	
PP2	Cytochalasin D	1.664412	0.4608927	-0.02086	3.349690	0.0559	
PP2	Latrunculin B	1.664412	0.4608927	-0.02086	3.349690	0.0559	
PP2	MNS	1.635152	0.4608927	-0.05013	3.320429	0.0652	
LY 294 002	AG 490	1.612177	0.4608927	-0.07310	3.297455	0.0734	
Go 6983	Cytochalasin D	1.610692	0.4608927	-0.07459	3.295969	0.0740	

Level	- Level	Difference	Std Err Dif	Lower CL	Upper CL	p-Value	Difference
Go 6983	Latrunculin B	1.610692	0.4608927	-0.07459	3.295969	0.0740	
Go 6983	MNS	1.581431	0.4608927	-0.10385	3.266709	0.0858	
Ethanol	AG 490	1.580158	0.4608927	-0.10512	3.265435	0.0864	
Wortmannin	AG 490	1.531916	0.4608927	-0.15336	3.217193	0.1096	
Propranolol	U73122	1.529480	0.4608927	-0.15580	3.214757	0.1109	
PF 573 228	Genistein	1.501859	0.4608927	-0.18342	3.187136	0.1266	
PP2	U73122	1.431245	0.4608927	-0.25403	3.116522	0.1748	
Propranolol	AG 490	1.390654	0.4608927	-0.29462	3.075931	0.2083	
Go 6983	U73122	1.377524	0.4608927	-0.30775	3.062801	0.2201	
DMSO	Genistein	1.359055	0.3991447	-0.10044	2.818548	0.0912	
BAY 61 3606	Genistein	1.292680	0.4311256	-0.28375	2.869113	0.2161	
PP2	AG 490	1.292418	0.4608927	-0.39286	2.977696	0.3082	
Go 6983	AG 490	1.238698	0.4608927	-0.44658	2.923975	0.3735	
No Drug	Genistein	1.154812	0.3991447	-0.30468	2.614305	0.2632	
LY 294 002	Genistein	1.073055	0.4608927	-0.61222	2.758332	0.6069	
Ethanol	Genistein	1.041035	0.4608927	-0.64424	2.726313	0.6534	
Wortmannin	Genistein	0.992793	0.4608927	-0.69248	2.678070	0.7210	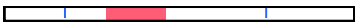
Genistein	Cytochalasin D	0.911117	0.4608927	-0.77416	2.596394	0.8230	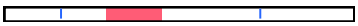
Genistein	Latrunculin B	0.911117	0.4608927	-0.77416	2.596394	0.8230	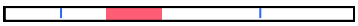
Genistein	MNS	0.881856	0.4608927	-0.80342	2.567134	0.8543	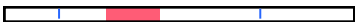
Propranolol	Genistein	0.851531	0.4608927	-0.83375	2.536808	0.8832	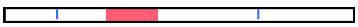
PF 573 228	Go 6983	0.802284	0.4608927	-0.88299	2.487561	0.9222	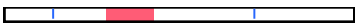
PP2	Genistein	0.753296	0.4608927	-0.93198	2.438573	0.9513	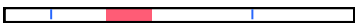
PF 573 228	PP2	0.748563	0.4608927	-0.93671	2.433840	0.9537	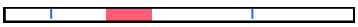
Go 6983	Genistein	0.699575	0.4608927	-0.98570	2.384852	0.9733	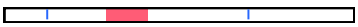
Genistein	U73122	0.677949	0.4608927	-1.00733	2.363226	0.9797	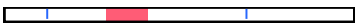
DMSO	Go 6983	0.659480	0.3991447	-0.80001	2.118973	0.9471	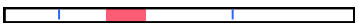
PF 573 228	Propranolol	0.650328	0.4608927	-1.03495	2.335605	0.9860	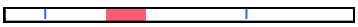
DMSO	PP2	0.605760	0.3991447	-0.85373	2.065253	0.9734	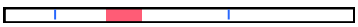
BAY 61 3606	Go 6983	0.593105	0.4311256	-0.98333	2.169538	0.9889	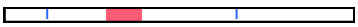
BAY 61 3606	PP2	0.539385	0.4311256	-1.03705	2.115817	0.9956	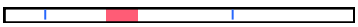
Genistein	AG 490	0.539123	0.4608927	-1.14615	2.224400	0.9978	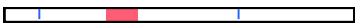
PF 573 228	Wortmannin	0.509066	0.4608927	-1.17621	2.194343	0.9988	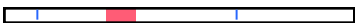
DMSO	Propranolol	0.507524	0.3991447	-0.95197	1.967017	0.9948	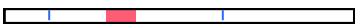
PF 573 228	Ethanol	0.460823	0.4608927	-1.22445	2.146100	0.9996	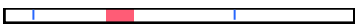
No Drug	Go 6983	0.455237	0.3991447	-1.00426	1.914730	0.9983	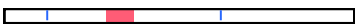
BAY 61 3606	Propranolol	0.441149	0.4311256	-1.13528	2.017582	0.9995	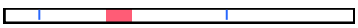
PF 573 228	LY 294 002	0.428804	0.4608927	-1.25647	2.114081	0.9998	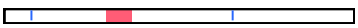
No Drug	PP2	0.401517	0.3991447	-1.05798	1.861010	0.9996	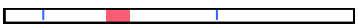
LY 294 002	Go 6983	0.373480	0.4608927	-1.31180	2.058757	1.0000	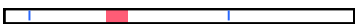
AG 490	Cytochalasin D	0.371994	0.4608927	-1.31328	2.057271	1.0000	
AG 490	Latrunculin B	0.371994	0.4608927	-1.31328	2.057271	1.0000	
DMSO	Wortmannin	0.366262	0.3991447	-1.09323	1.825755	0.9999	
PF 573 228	No Drug	0.347046	0.3991447	-1.11245	1.806539	0.9999	
AG 490	MNS	0.342734	0.4608927	-1.34254	2.028011	1.0000	
Ethanol	Go 6983	0.341460	0.4608927	-1.34382	2.026738	1.0000	
LY 294 002	PP2	0.319759	0.4608927	-1.36552	2.005036	1.0000	
DMSO	Ethanol	0.318020	0.3991447	-1.14147	1.777513	1.0000	
No Drug	Propranolol	0.303281	0.3991447	-1.15621	1.762774	1.0000	
BAY 61 3606	Wortmannin	0.299887	0.4311256	-1.27655	1.876320	1.0000	
Wortmannin	Go 6983	0.293218	0.4608927	-1.39206	1.978495	1.0000	
Ethanol	PP2	0.287740	0.4608927	-1.39754	1.973017	1.0000	
DMSO	LY 294 002	0.286001	0.3991447	-1.17349	1.745494	1.0000	
BAY 61 3606	Ethanol	0.251645	0.4311256	-1.32479	1.828078	1.0000	
Wortmannin	PP2	0.239497	0.4608927	-1.44578	1.924774	1.0000	
U73122	Cytochalasin D	0.233167	0.4608927	-1.45211	1.918445	1.0000	
U73122	Latrunculin B	0.233167	0.4608927	-1.45211	1.918445	1.0000	
LY 294 002	Propranolol	0.221524	0.4608927	-1.46375	1.906801	1.0000	
BAY 61 3606	LY 294 002	0.219626	0.4311256	-1.35681	1.796058	1.0000	
PF 573 228	BAY 61 3606	0.209178	0.4311256	-1.36725	1.785611	1.0000	
DMSO	No Drug	0.204243	0.3259003	-0.98743	1.395914	1.0000	

Level	- Level	Difference	Std Err Dif	Lower CL	Upper CL	p-Value	Difference
U73122	MNS	0.203907	0.4608927	-1.48137	1.889184	1.0000	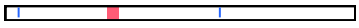
Ethanol	Propranolol	0.189504	0.4608927	-1.49577	1.874782	1.0000	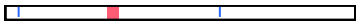
No Drug	Wortmannin	0.162019	0.3991447	-1.29747	1.621512	1.0000	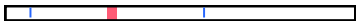
Propranolol	Go 6983	0.151956	0.4608927	-1.53332	1.837233	1.0000	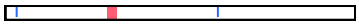
PF 573 228	DMSO	0.142803	0.3991447	-1.31669	1.602296	1.0000	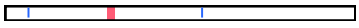
Wortmannin	Propranolol	0.141262	0.4608927	-1.54402	1.826539	.	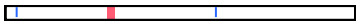
AG 490	U73122	0.138826	0.4608927	-1.54645	1.824104	.	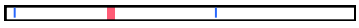
BAY 61 3606	No Drug	0.137868	0.3643676	-1.19446	1.470197	1.0000	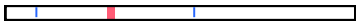
No Drug	Ethanol	0.113777	0.3991447	-1.34572	1.573270	.	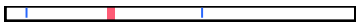
Propranolol	PP2	0.098235	0.4608927	-1.58704	1.783512	.	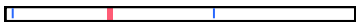
No Drug	LY 294 002	0.081758	0.3991447	-1.37774	1.541251	.	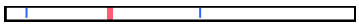
LY 294 002	Wortmannin	0.080262	0.4608927	-1.60502	1.765539	.	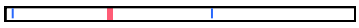
DMSO	BAY 61 3606	0.066375	0.3643676	-1.26595	1.398704	.	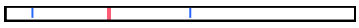
PP2	Go 6983	0.053721	0.4608927	-1.63156	1.738998	.	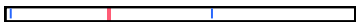
Ethanol	Wortmannin	0.048242	0.4608927	-1.63703	1.733520	.	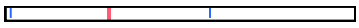
LY 294 002	Ethanol	0.032019	0.4608927	-1.65326	1.717297	.	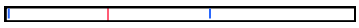
MNS	Cytochalasin D	0.029260	0.4608927	-1.65602	1.714537	.	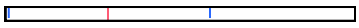
MNS	Latrunculin B	0.029260	0.4608927	-1.65602	1.714537	.	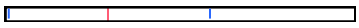
Latrunculin B	Cytochalasin D	0.000000	0.4608927	-1.68528	1.685277	1.0000	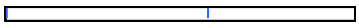

APPENDIX J: ONE-WAY ANOVA OF NORMALIZED OXLDL-BEAD INTERNALIZATION DURING PHARMACOLOGICAL INHIBITION ASSAY

The following analysis compares the average number of internalized beads per cell for oxLDL-coated bead treatments for different pharmacological inhibitors. Analysis by Tukey-Cramer HSD reveals significant bead internalization inhibition under MNS, Cytochalasin D and Latrunculin B treatments.

Oneway Analysis of normal in By drug

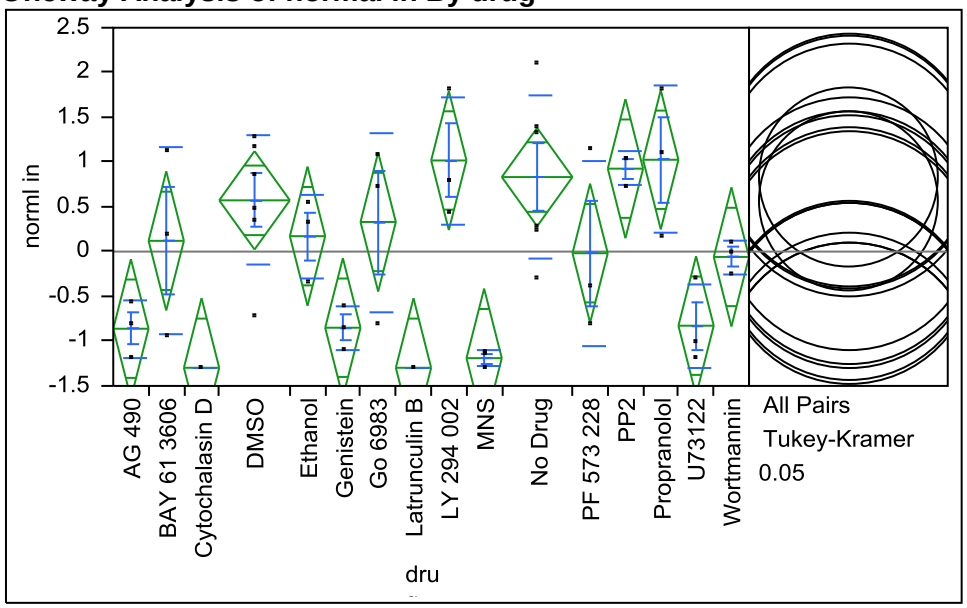

Missing Rows
18

Oneway Anova
Summary of Fit

Rsquare	0.683408
Adj Rsquare	0.558437
Root Mean Square Error	0.664502
Mean of Response	-3.1e-16
Observations (or Sum Wgts)	54

Analysis of Variance

Source	DF	Sum of Squares	Mean Square	F Ratio	Prob > F
drug	15	36.220618	2.41471	5.4686	<.0001*
Error	38	16.779382	0.44156		
C. Total	53	53.000000			

Means for Oneway Anova

Level	Number	Mean	Std Error	Lower 95%	Upper 95%
AG 490	3	-0.8612	0.38365	-1.638	-0.085
BAY 61 3606	3	0.1199	0.38365	-0.657	0.897
Cytochalasin D	3	-1.2973	0.38365	-2.074	-0.521

Level	Number	Mean	Std Error	Lower 95%	Upper 95%
DMSO	6	0.5724	0.27128	0.023	1.122
Ethanol	3	0.1722	0.38365	-0.604	0.949
Genistein	3	-0.8500	0.38365	-1.627	-0.073
Go 6983	3	0.3308	0.38365	-0.446	1.107
Latrunculin B	3	-1.2973	0.38365	-2.074	-0.521
LY 294 002	3	1.0174	0.38365	0.241	1.794
MNS	3	-1.1899	0.38365	-1.967	-0.413
No Drug	6	0.8323	0.27128	0.283	1.381
PF 573 228	3	-0.0184	0.38365	-0.795	0.758
PP2	3	0.9263	0.38365	0.150	1.703
Propranolol	3	1.0254	0.38365	0.249	1.802
U73122	3	-0.8275	0.38365	-1.604	-0.051
Wortmannin	3	-0.0598	0.38365	-0.836	0.717

Std Error uses a pooled estimate of error variance

Means and Std Deviations

Level	Number	Mean	Std Dev	Std Err Mean	Lower 95%	Upper 95%
AG 490	3	-0.8612	0.31685	0.18293	-1.648	-0.074
BAY 61 3606	3	0.1199	1.03861	0.59964	-2.460	2.700
Cytochalasin D	3	-1.2973	0.00000	0.00000	-1.297	-1.297
DMSO	6	0.5724	0.72764	0.29706	-0.191	1.336
Ethanol	3	0.1722	0.46740	0.26985	-0.989	1.333
Genistein	3	-0.8500	0.24359	0.14064	-1.455	-0.245
Go 6983	3	0.3308	1.00041	0.57759	-2.154	2.816
Latrunculin B	3	-1.2973	0.00000	0.00000	-1.297	-1.297
LY 294 002	3	1.0174	0.71031	0.41010	-0.747	2.782
MNS	3	-1.1899	0.09472	0.05469	-1.425	-0.955
No Drug	6	0.8323	0.91033	0.37164	-0.123	1.788
PF 573 228	3	-0.0184	1.03029	0.59484	-2.578	2.541
PP2	3	0.9263	0.18562	0.10717	0.465	1.387
Propranolol	3	1.0254	0.82189	0.47452	-1.016	3.067
U73122	3	-0.8275	0.46497	0.26845	-1.983	0.328
Wortmannin	3	-0.0598	0.18819	0.10865	-0.527	0.408

Means Comparisons

Comparisons for all pairs using Tukey-Kramer HSD

q*	Alpha
3.66273	0.05

Abs(Dif)-HSD	Prop.	LY	PP2	N/D	DMSO	Gö	Eth.	BAY	PF	Wort.	U7.	Gen.	AG	MNS	Cyto. D	Lat. B
Prop.	-1.9873	-1.9792	-1.8881	-1.5279	-1.2680	-1.2926	-1.1340	-1.0818	-0.9434	-0.9020	-0.1344	-0.1119	-0.1006	0.2281	0.3355	0.3355
LY	-1.9792	-1.9873	-1.8961	-1.5359	-1.2760	-1.3007	-1.1420	-1.0898	-0.9515	-0.9100	-0.1424	-0.1199	-0.1087	0.2201	0.3275	0.3275
PP2	-1.8881	-1.8961	-1.9873	-1.6271	-1.3672	-1.3918	-1.2332	-1.1809	-1.0426	-1.0012	-0.2335	-0.2110	-0.1998	0.1289	0.2363	0.2363
N/D	-1.5279	-1.5359	-1.6271	-1.4052	-1.1453	-1.2195	-1.0609	-1.0086	-0.8703	-0.8289	-0.0612	-0.0387	-0.0275	0.3012	0.4086	0.4086
DMSO	-1.2680	-1.2760	-1.3672	-1.1453	-1.4052	-1.4794	-1.3208	-1.2686	-1.1302	-1.0888	-0.3212	-0.2987	-0.2874	0.0413	0.1487	0.1487
Gö	-1.2926	-1.3007	-1.3918	-1.2195	-1.4794	-1.9873	-1.8286	-1.7764	-1.6381	-1.5967	-0.8290	-0.8065	-0.7953	-0.4665	-0.3591	-0.3591
Ethanol	-1.1340	-1.1420	-1.2332	-1.0609	-1.3208	-1.8286	-1.9873	-1.9350	-1.7967	-1.7553	-0.9876	-0.9651	-0.9539	-0.6252	-0.5178	-0.5178
BAY	-1.0818	-1.0898	-1.1809	-1.0086	-1.2686	-1.7764	-1.9350	-1.9873	-1.8489	-1.8075	-1.0399	-1.0174	-1.0061	-0.6774	-0.5700	-0.5700
PF	-0.9434	-0.9515	-1.0426	-0.8703	-1.1302	-1.6381	-1.7967	-1.8489	-1.9873	-1.9459	-1.1782	-1.1557	-1.1445	-0.8157	-0.7083	-0.7083
Wort.	-0.9020	-0.9100	-1.0012	-0.8289	-1.0888	-1.5967	-1.7553	-1.8075	-1.9459	-1.9873	-1.2196	-1.1971	-1.1859	-0.8572	-0.7497	-0.7497
U7.	-0.1344	-0.1424	-0.2335	-0.0612	-0.3212	-0.8290	-0.9876	-1.0399	-1.1782	-1.2196	-1.9873	-1.9648	-1.9535	-1.6248	-1.5174	-1.5174
Gen.	-0.1119	-0.1199	-0.2110	-0.0387	-0.2987	-0.8065	-0.9651	-1.0174	-1.1557	-1.1971	-1.9648	-1.9873	-1.9760	-1.6473	-1.5399	-1.5399
AG	-0.1006	-0.1087	-0.1998	-0.0275	-0.2874	-0.7953	-0.9539	-1.0061	-1.1445	-1.1859	-1.9535	-1.9760	-1.9873	-1.6585	-1.5511	-1.5511
MNS	0.2281	0.2201	0.1289	0.3012	0.0413	-0.4665	-0.6252	-0.6774	-0.8157	-0.8572	-1.6248	-1.6473	-1.6585	-1.9873	-1.8799	-1.8799
Cyto. D	0.3355	0.3275	0.2363	0.4086	0.1487	-0.3591	-0.5178	-0.5700	-0.7083	-0.7497	-1.5174	-1.5399	-1.5511	-1.8799	-1.9873	-1.9873
Lat. B	0.3355	0.3275	0.2363	0.4086	0.1487	-0.3591	-0.5178	-0.5700	-0.7083	-0.7497	-1.5174	-1.5399	-1.5511	-1.8799	-1.9873	-1.9873

Positive values show pairs of means that are significantly different.

Level			Mean
Propranolol	A		1.025425
LY 294 002	A		1.017408
PP2	A		0.926257
No Drug	A		0.832318
DMSO	A		0.572392
Go 6983	A	B	0.330799
Ethanol	A	B	0.172181
BAY 61 3606	A	B	0.119925
PF 573 228	A	B	-0.018403
Wortmannin	A	B	-0.059813
U73122	A	B	-0.827464
Genistein	A	B	-0.849958
AG 490	A	B	-0.861194
MNS		B	-1.189924
Cytochalasin D		B	-1.297329
Latrunculin B		B	-1.297329

Levels not connected by same letter are significantly different.

Level	- Level	Difference	Std Err Dif	Lower CL	Upper CL	p-Value	Difference
Propranolol	Cytochalasin D	2.322754	0.5425635	0.33549	4.310017	0.0098*	
Propranolol	Latrunculin B	2.322754	0.5425635	0.33549	4.310017	0.0098*	
LY 294 002	Cytochalasin D	2.314737	0.5425635	0.32747	4.302000	0.0102*	
LY 294 002	Latrunculin B	2.314737	0.5425635	0.32747	4.302000	0.0102*	
PP2	Cytochalasin D	2.223587	0.5425635	0.23632	4.210849	0.0162*	
PP2	Latrunculin B	2.223587	0.5425635	0.23632	4.210849	0.0162*	
Propranolol	MNS	2.215349	0.5425635	0.22809	4.202611	0.0169*	
LY 294 002	MNS	2.207332	0.5425635	0.22007	4.194594	0.0176*	
No Drug	Cytochalasin D	2.129648	0.4698738	0.40863	3.850668	0.0048*	
No Drug	Latrunculin B	2.129648	0.4698738	0.40863	3.850668	0.0048*	
PP2	MNS	2.116181	0.5425635	0.12892	4.103444	0.0274*	
No Drug	MNS	2.022243	0.4698738	0.30122	3.743262	0.0092*	
Propranolol	AG 490	1.886619	0.5425635	-0.10064	3.873882	0.0780	
LY 294 002	AG 490	1.878602	0.5425635	-0.10866	3.865865	0.0808	
Propranolol	Genistein	1.875383	0.5425635	-0.11188	3.862646	0.0819	
DMSO	Cytochalasin D	1.869722	0.4698738	0.14870	3.590742	0.0223*	
DMSO	Latrunculin B	1.869722	0.4698738	0.14870	3.590742	0.0223*	
LY 294 002	Genistein	1.867366	0.5425635	-0.11990	3.854629	0.0847	
Propranolol	U73122	1.852888	0.5425635	-0.13437	3.840151	0.0901	
LY 294 002	U73122	1.844871	0.5425635	-0.14239	3.832134	0.0932	
PP2	AG 490	1.787452	0.5425635	-0.19981	3.774714	0.1180	
PP2	Genistein	1.776216	0.5425635	-0.21105	3.763478	0.1235	
DMSO	MNS	1.762316	0.4698738	0.04130	3.483336	0.0402*	
PP2	U73122	1.753721	0.5425635	-0.23354	3.740984	0.1350	
No Drug	AG 490	1.693513	0.4698738	-0.02751	3.414533	0.0577	
No Drug	Genistein	1.682277	0.4698738	-0.03874	3.403297	0.0611	
No Drug	U73122	1.659782	0.4698738	-0.06124	3.380802	0.0685	
Go 6983	Cytochalasin D	1.628128	0.5425635	-0.35913	3.615391	0.2162	
Go 6983	Latrunculin B	1.628128	0.5425635	-0.35913	3.615391	0.2162	
Go 6983	MNS	1.520723	0.5425635	-0.46654	3.507985	0.3098	
Ethanol	Cytochalasin D	1.469510	0.5425635	-0.51775	3.456773	0.3621	
Ethanol	Latrunculin B	1.469510	0.5425635	-0.51775	3.456773	0.3621	
DMSO	AG 490	1.433586	0.4698738	-0.28743	3.154606	0.1961	
DMSO	Genistein	1.422350	0.4698738	-0.29867	3.143370	0.2055	
BAY 61 3606	Cytochalasin D	1.417255	0.5425635	-0.57001	3.404517	0.4201	
BAY 61 3606	Latrunculin B	1.417255	0.5425635	-0.57001	3.404517	0.4201	
DMSO	U73122	1.399856	0.4698738	-0.32116	3.120876	0.2253	
Ethanol	MNS	1.362105	0.5425635	-0.62516	3.349368	0.4851	
BAY 61 3606	MNS	1.309849	0.5425635	-0.67741	3.297112	0.5491	
PF 573 228	Cytochalasin D	1.278927	0.5425635	-0.70834	3.266189	0.5875	

Level	- Level	Difference	Std Err Dif	Lower CL	Upper CL	p-Value	Difference
PF 573 228	Latrunculin B	1.278927	0.5425635	-0.70834	3.266189	0.5875	
Wortmannin	Cytochalasin D	1.237516	0.5425635	-0.74975	3.224779	0.6387	
Wortmannin	Latrunculin B	1.237516	0.5425635	-0.74975	3.224779	0.6387	
Go 6983	AG 490	1.191993	0.5425635	-0.79527	3.179256	0.6936	
Go 6983	Genistein	1.180757	0.5425635	-0.80651	3.168020	0.7068	
PF 573 228	MNS	1.171521	0.5425635	-0.81574	3.158784	0.7176	
Go 6983	U73122	1.158262	0.5425635	-0.82900	3.145525	0.7328	
Wortmannin	MNS	1.130111	0.5425635	-0.85715	3.117374	0.7640	
Propranolol	Wortmannin	1.085238	0.5425635	-0.90202	3.072500	0.8104	
LY 294 002	Wortmannin	1.077221	0.5425635	-0.91004	3.064483	0.8182	
Propranolol	PF 573 228	1.043827	0.5425635	-0.94344	3.031090	0.8489	
LY 294 002	PF 573 228	1.035810	0.5425635	-0.95145	3.023073	0.8559	
Ethanol	AG 490	1.033375	0.5425635	-0.95389	3.020638	0.8579	
Ethanol	Genistein	1.022139	0.5425635	-0.96512	3.009402	0.8673	
Ethanol	U73122	0.999645	0.5425635	-0.98762	2.986907	0.8849	
PP2	Wortmannin	0.986070	0.5425635	-1.00119	2.973333	0.8948	
BAY 61 3606	AG 490	0.981120	0.5425635	-1.00614	2.968382	0.8983	
BAY 61 3606	Genistein	0.969884	0.5425635	-1.01738	2.957146	0.9059	
BAY 61 3606	U73122	0.947389	0.5425635	-1.03987	2.934652	0.9201	
PP2	PF 573 228	0.944660	0.5425635	-1.04260	2.931923	0.9217	
Propranolol	BAY 61 3606	0.905499	0.5425635	-1.08176	2.892762	0.9426	
LY 294 002	BAY 61 3606	0.897482	0.5425635	-1.08978	2.884745	0.9463	
No Drug	Wortmannin	0.892132	0.4698738	-0.82889	2.613152	0.8607	
Propranolol	Ethanol	0.853244	0.5425635	-1.13402	2.840506	0.9640	
No Drug	PF 573 228	0.850721	0.4698738	-0.87030	2.571741	0.8974	
LY 294 002	Ethanol	0.845227	0.5425635	-1.14204	2.832489	0.9666	
PF 573 228	AG 490	0.842791	0.5425635	-1.14447	2.830054	0.9674	
PF 573 228	Genistein	0.831555	0.5425635	-1.15571	2.818818	0.9709	
PF 573 228	U73122	0.809061	0.5425635	-1.17820	2.796323	0.9769	
PP2	BAY 61 3606	0.806332	0.5425635	-1.18093	2.793595	0.9776	
Wortmannin	AG 490	0.801381	0.5425635	-1.18588	2.788644	0.9788	
Wortmannin	Genistein	0.790145	0.5425635	-1.19712	2.777408	0.9812	
Wortmannin	U73122	0.767650	0.5425635	-1.21961	2.754913	0.9855	
PP2	Ethanol	0.754076	0.5425635	-1.23319	2.741339	0.9877	
No Drug	BAY 61 3606	0.712393	0.4698738	-1.00863	2.433413	0.9734	
Propranolol	Go 6983	0.694626	0.5425635	-1.29264	2.681889	0.9944	
LY 294 002	Go 6983	0.686609	0.5425635	-1.30065	2.673872	0.9950	
No Drug	Ethanol	0.660137	0.4698738	-1.06088	2.381157	0.9864	
DMSO	Wortmannin	0.632205	0.4698738	-1.08881	2.353225	0.9909	
PP2	Go 6983	0.595459	0.5425635	-1.39180	2.582721	0.9989	
DMSO	PF 573 228	0.590795	0.4698738	-1.13022	2.311815	0.9953	
No Drug	Go 6983	0.501520	0.4698738	-1.21950	2.222540	0.9992	
U73122	Cytochalasin D	0.469866	0.5425635	-1.51740	2.457129	0.9999	
U73122	Latrunculin B	0.469866	0.5425635	-1.51740	2.457129	0.9999	
Propranolol	DMSO	0.453032	0.4698738	-1.26799	2.174052	0.9997	
DMSO	BAY 61 3606	0.452467	0.4698738	-1.26855	2.173487	0.9998	
Genistein	Cytochalasin D	0.447371	0.5425635	-1.53989	2.434634	1.0000	
Genistein	Latrunculin B	0.447371	0.5425635	-1.53989	2.434634	1.0000	
LY 294 002	DMSO	0.445015	0.4698738	-1.27600	2.166035	0.9998	
AG 490	Cytochalasin D	0.436135	0.5425635	-1.55113	2.423398	1.0000	
AG 490	Latrunculin B	0.436135	0.5425635	-1.55113	2.423398	1.0000	
DMSO	Ethanol	0.400211	0.4698738	-1.32081	2.121231	0.9999	
Go 6983	Wortmannin	0.390612	0.5425635	-1.59665	2.377874	1.0000	
U73122	MNS	0.362461	0.5425635	-1.62480	2.349723	1.0000	
PP2	DMSO	0.353865	0.4698738	-1.36715	2.074885	1.0000	
Go 6983	PF 573 228	0.349201	0.5425635	-1.63806	2.336464	1.0000	
Genistein	MNS	0.339966	0.5425635	-1.64730	2.327228	1.0000	
AG 490	MNS	0.328730	0.5425635	-1.65853	2.315993	1.0000	
No Drug	DMSO	0.259926	0.3836503	-1.14528	1.665133	1.0000	
DMSO	Go 6983	0.241594	0.4698738	-1.47943	1.962614	1.0000	
Ethanol	Wortmannin	0.231994	0.5425635	-1.75527	2.219257	1.0000	

Level	- Level	Difference	Std Err Dif	Lower CL	Upper CL	p-Value	Difference
Go 6983	BAY 61 3606	0.210873	0.5425635	-1.77639	2.198136	1.0000	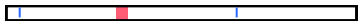
Propranolol	No Drug	0.193106	0.4698738	-1.52791	1.914126	1.0000	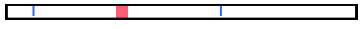
Ethanol	PF 573 228	0.190584	0.5425635	-1.79668	2.177847	1.0000	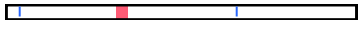
LY 294 002	No Drug	0.185089	0.4698738	-1.53593	1.906109	1.0000	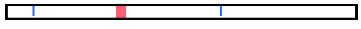
BAY 61 3606	Wortmannin	0.179739	0.5425635	-1.80752	2.167001	1.0000	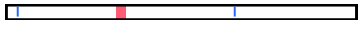
Go 6983	Ethanol	0.158618	0.5425635	-1.82865	2.145880	.	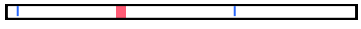
BAY 61 3606	PF 573 228	0.138328	0.5425635	-1.84893	2.125591	.	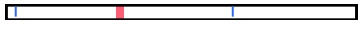
MNS	Cytochalasin D	0.107405	0.5425635	-1.87986	2.094668	.	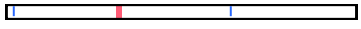
MNS	Latrunculin B	0.107405	0.5425635	-1.87986	2.094668	.	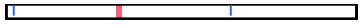
Propranolol	PP2	0.099167	0.5425635	-1.88810	2.086430	.	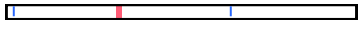
PP2	No Drug	0.093939	0.4698738	-1.62708	1.814959	.	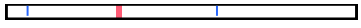
LY 294 002	PP2	0.091150	0.5425635	-1.89611	2.078413	.	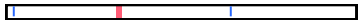
Ethanol	BAY 61 3606	0.052256	0.5425635	-1.93501	2.039518	.	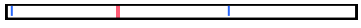
PF 573 228	Wortmannin	0.041410	0.5425635	-1.94585	2.028673	.	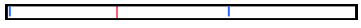
U73122	AG 490	0.033731	0.5425635	-1.95353	2.020993	.	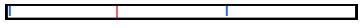
U73122	Genistein	0.022495	0.5425635	-1.96477	2.009757	.	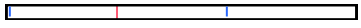
Genistein	AG 490	0.011236	0.5425635	-1.97603	1.998499	.	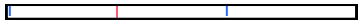
Propranolol	LY 294 002	0.008017	0.5425635	-1.97925	1.995280	.	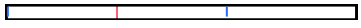
Latrunculin B	Cytochalasin D	0.000000	0.5425635	-1.98726	1.987263	1.0000	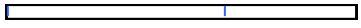

APPENDIX K - LARC BASE PEAK TRACES

IgG Bead LARC Base Peak Traces of the following bead elutions NaCl concentrations in mM: (A) 50; (B) 100; (C) 150; (D) 200; (E) 250; (F) 300; (G) 350; (H) 400; (I) 450; (J) 500; (K) 550; (L) 600; (M) 700; (N) 800; (O) 900; (P) 1000. The following additional elution conditions: (Q) Acetonitrile; (R) Trypsin; (S) Chloroform; (T) PBS; (U) First Wash

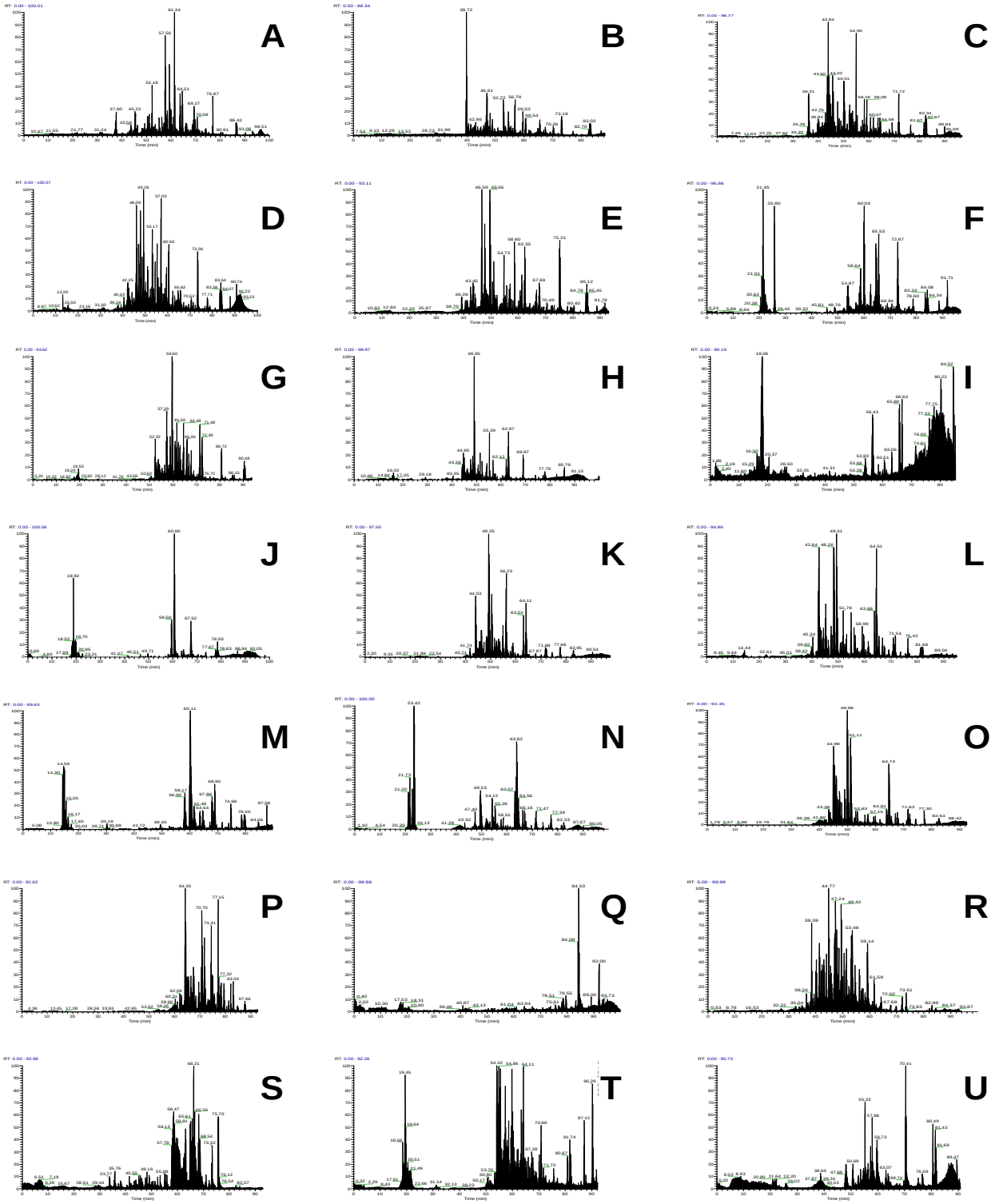

IgG Bead Control LARC Base Peak Traces of the following bead elutions NaCl concentrations in mM: (A) 50; (B) 100; (C) 150; (D) 200; (E) 250; (F) 300; (G) 350; (H) 400; (I) 450; (J) 500; (K) 550; (L) 600; (M) 700; (N) 800; (O) 900; (P) 1000. The following additional elution conditions: (Q) Acetonitrile; (R) Trypsin; (S) Chloroform; (T) PBS; (U) First Wash

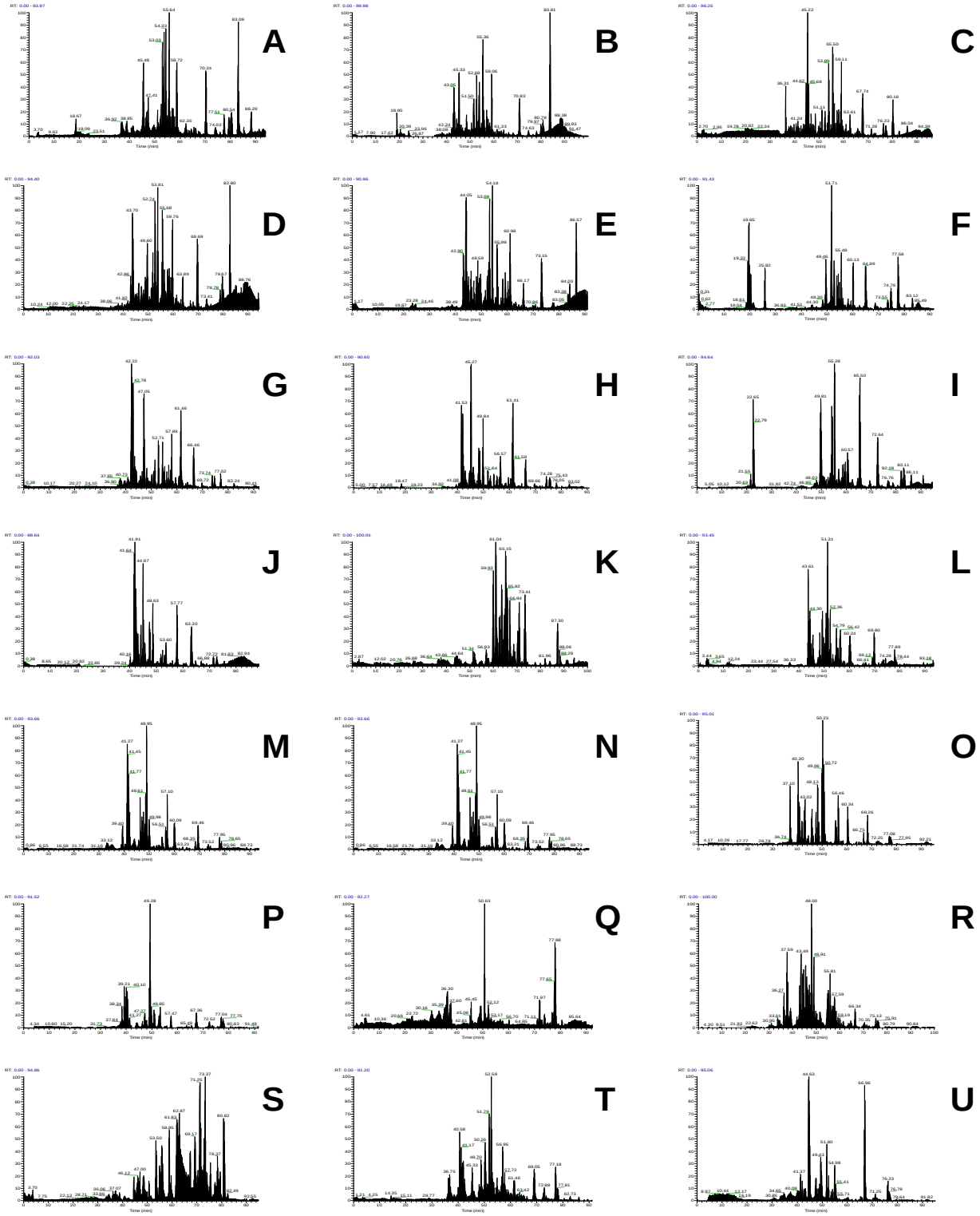

oxLDL Bead LARC Base Peak Traces of the following bead elutions NaCl concentrations in mM: (A) 50; (B) 100; (C) 150; (D) 200; (E) 250; (F) 300; (G) 350; (H) 400; (I) 450; (J) 500; (K) 550; (L) 600; (M) 700; (N) 800; (O) 900; (P) 1000. The following additional elution conditions: (Q) Acetonitrile; (R) Trypsin; (S) Chloroform; (T) PBS; (U) First Wash

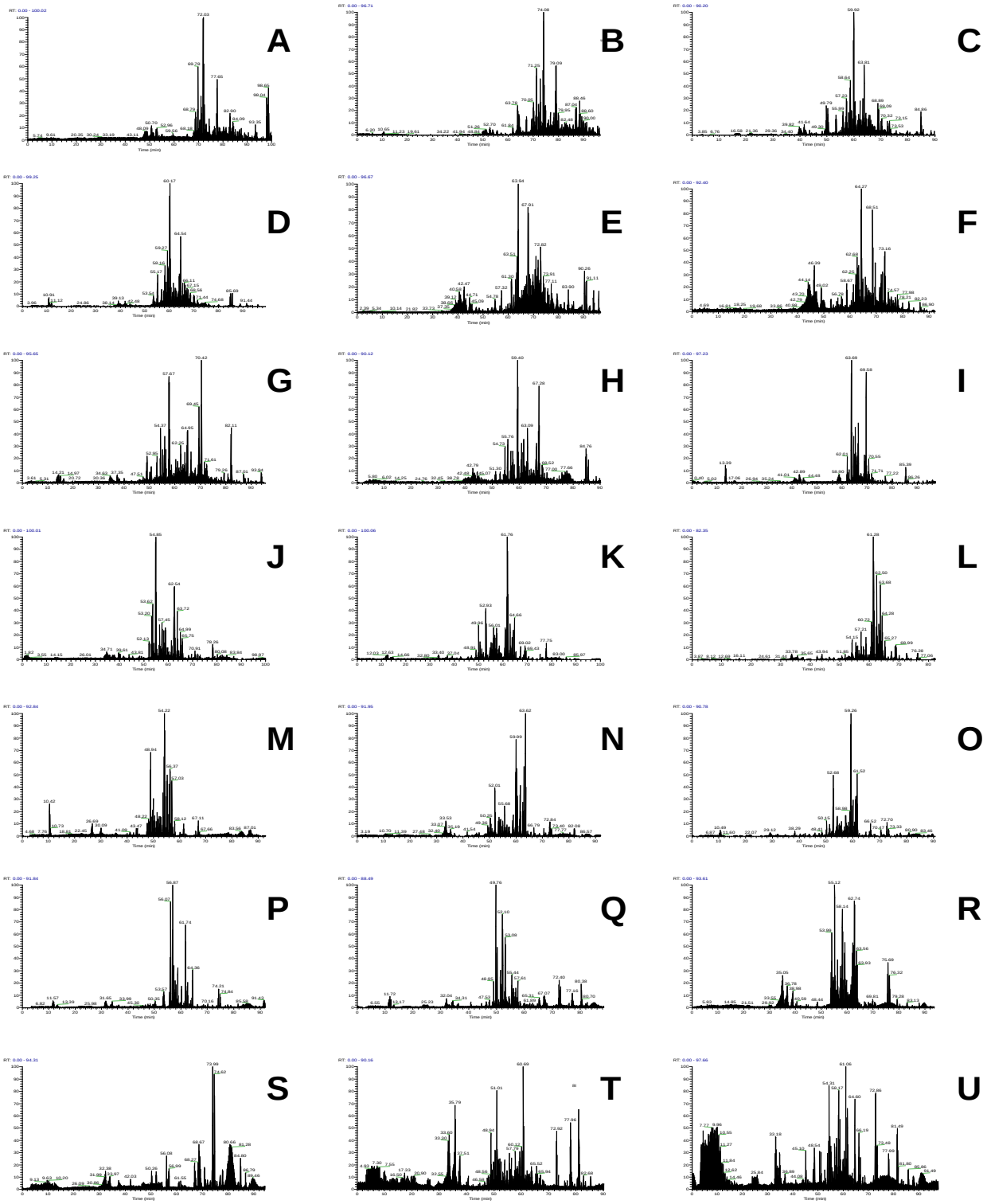

oxLDL Bead Control LARC Base Peak Traces of the following bead elutions NaCl concentrations in mM: (A) 50; (B) 100; (C) 150; (D) 200; (E) 250; (F) 300; (G) 350; (H) 400; (I) 450; (J) 500; (K) 550; (L) 600; (M) 700; (N) 800; (O) 900; (P) 1000. The following additional elution conditions: (Q) Acetonitrile; (R) Trypsin; (S) Chloroform; (T) PBS; (U) First Wash

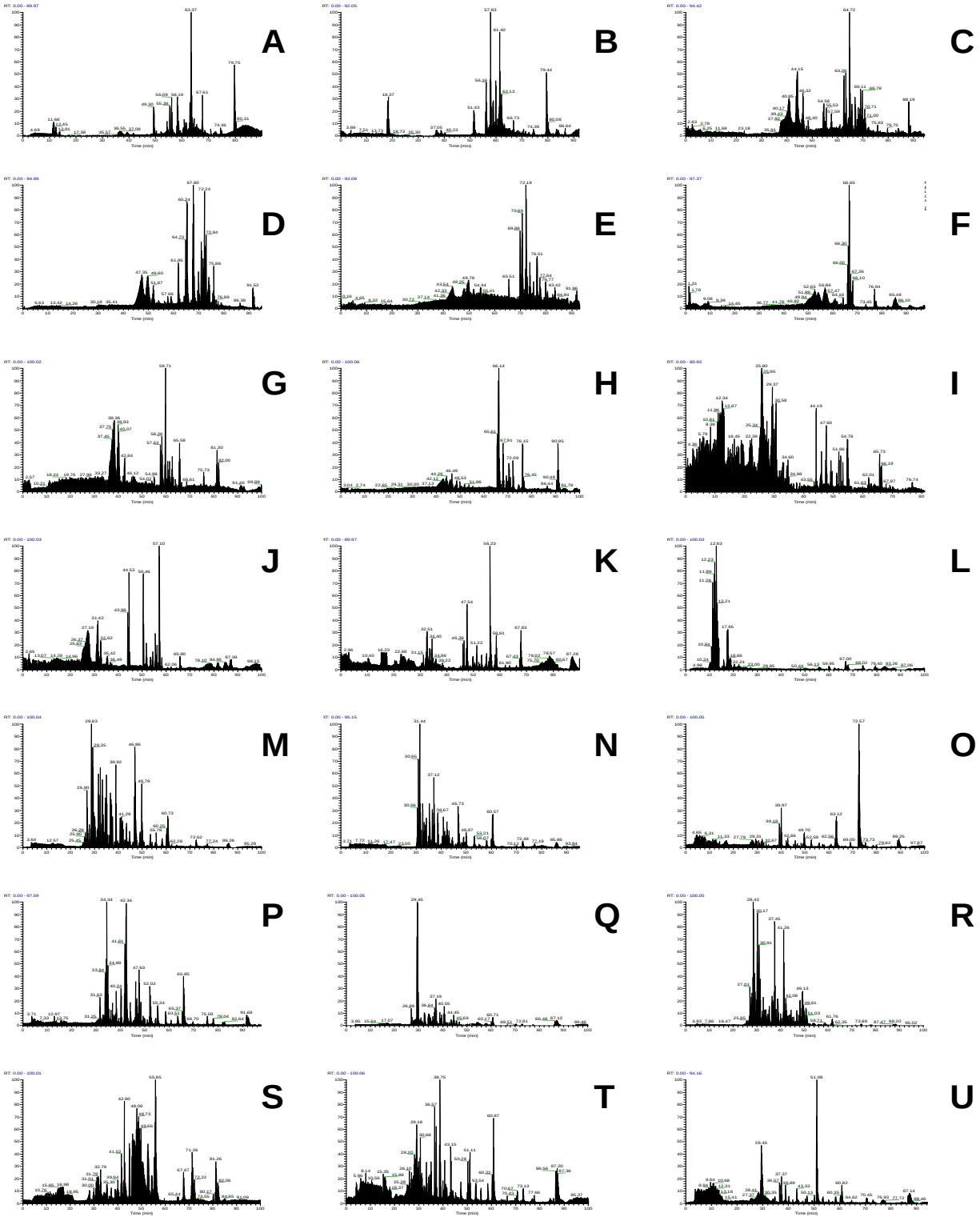

APPENDIX L – OXLDL, IGG, CD36 IGG AND CD36 IGA LARC MASS SPECTRA

The following spectra were collected from IgG, oxLDL, CD36 IgG and CD36 IgA-coated beads incubated with U937 for 0 min, 30 min, 1h, 2h or 4h (pooled) and subjected to two PBS washes, a series of increasing NaCl concentrations, Acetonitrile, direct bead trypsinization, detergent, and chloroform. Two mass spectrometers were used. Corresponding total ion current (TIC) and base peak chromatograms are also shown.

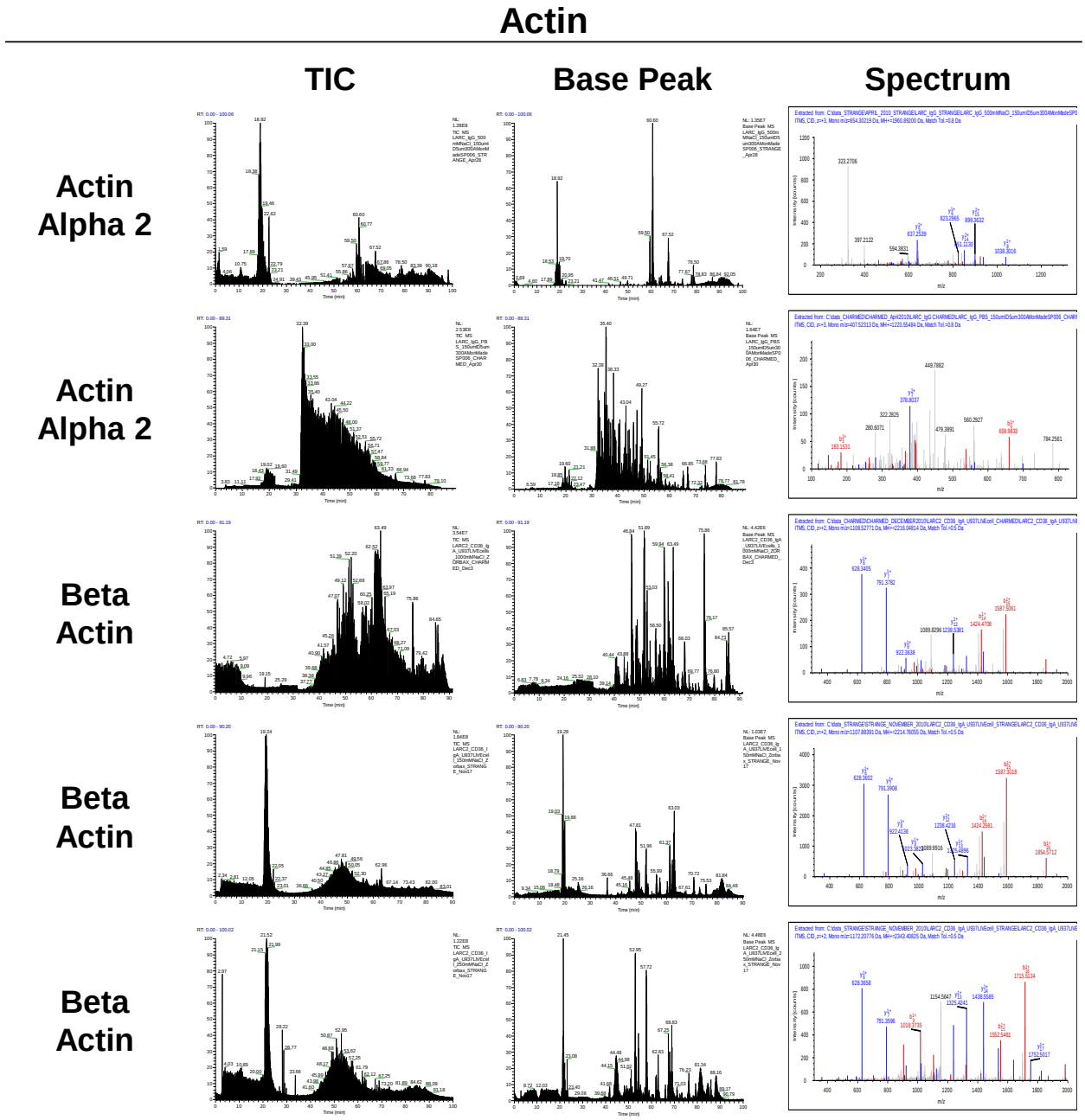

SRC-Family Kinases

	TIC	Base Peak	Spectrum
Src	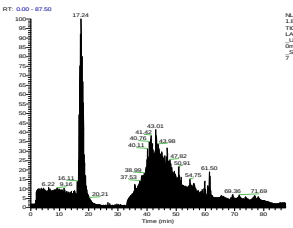	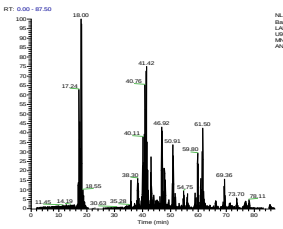	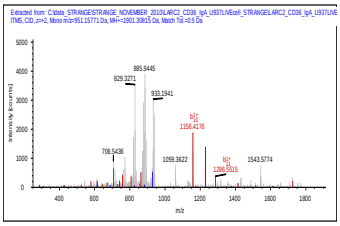
Src	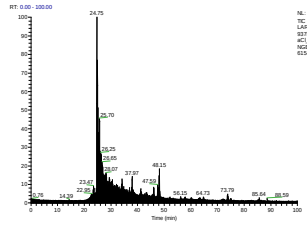	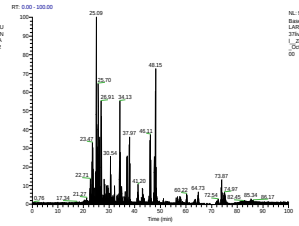	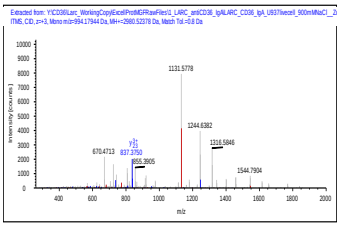
Src	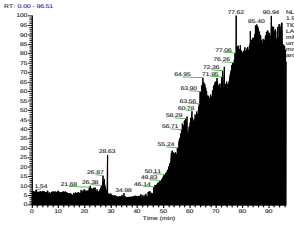	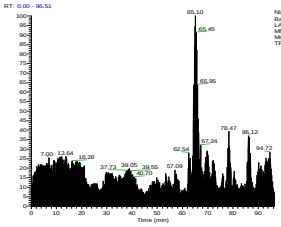	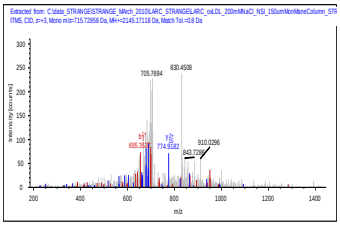
Src	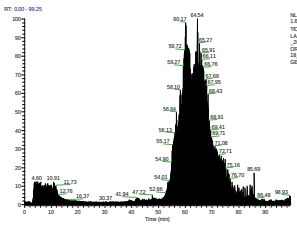	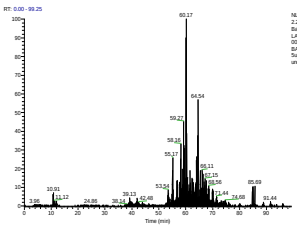	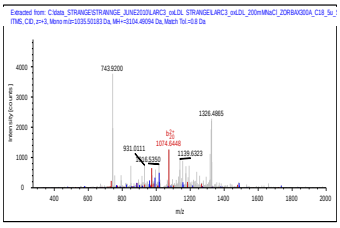
Fyn, Isoform A	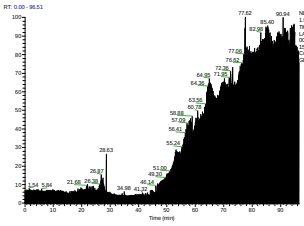	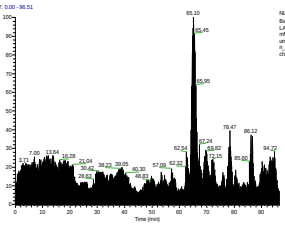	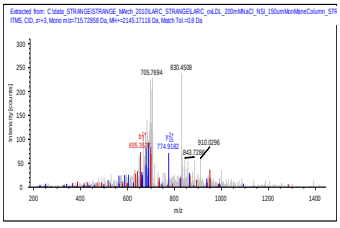
Yes-1	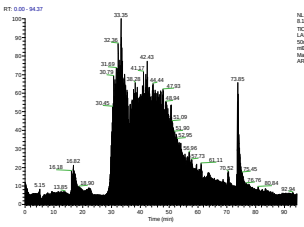	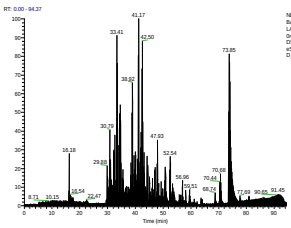	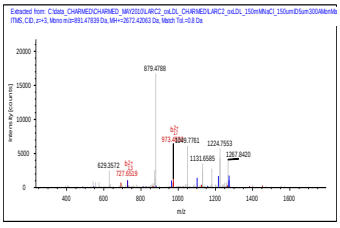

SRC-Family Kinases

	TIC	Base Peak	Spectrum
Lyn Isoform A	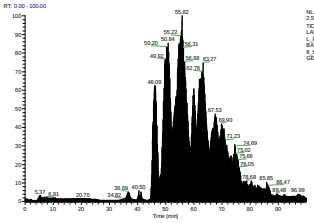	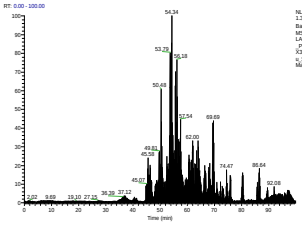	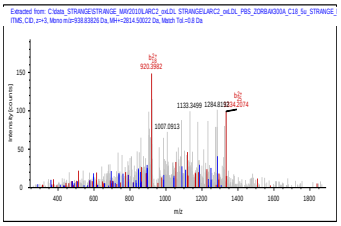
Lyn	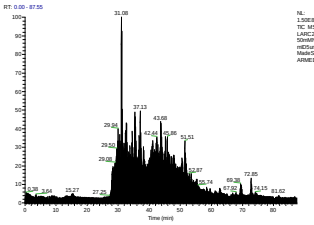	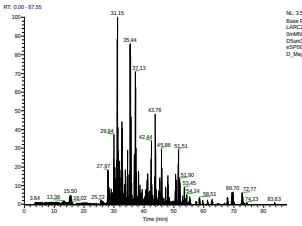	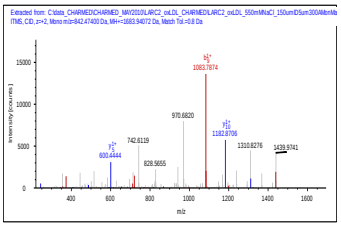
Lyn	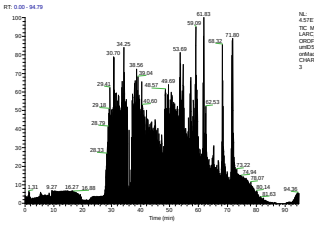	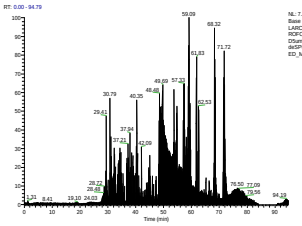	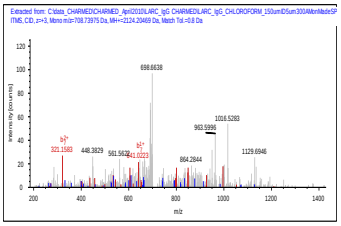
Lck	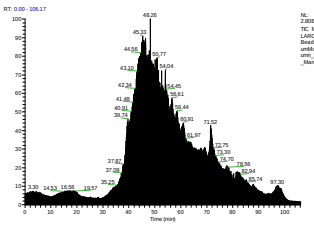	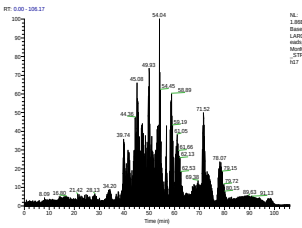	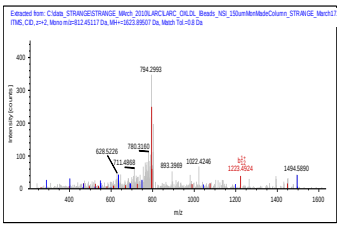
Lck	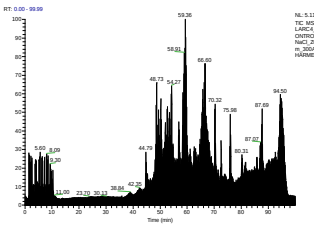	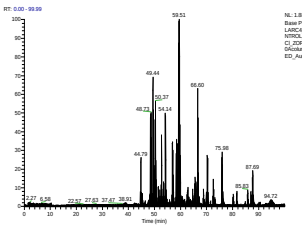	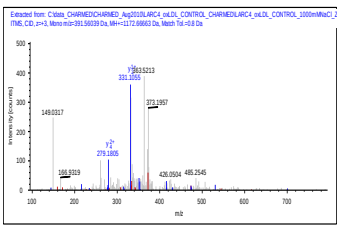
Hck	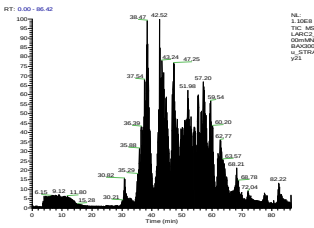	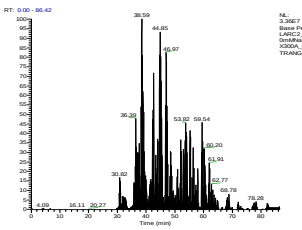	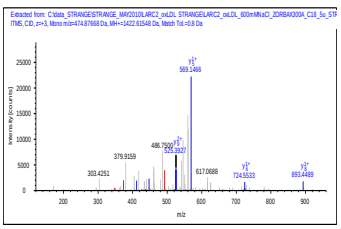

SRC-Family Kinases

	TIC	Base Peak	Spectrum
Blk	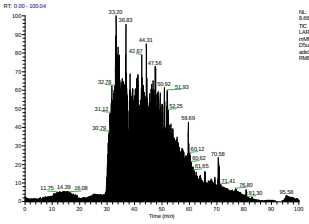	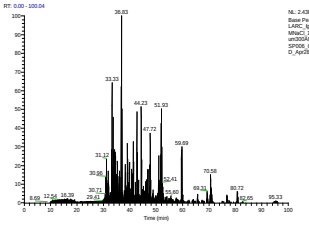	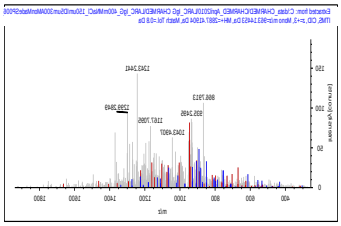
Csk	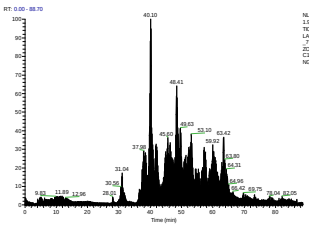	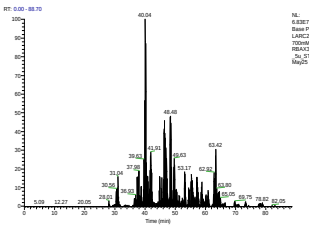	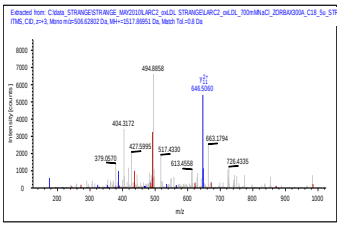
Fgr	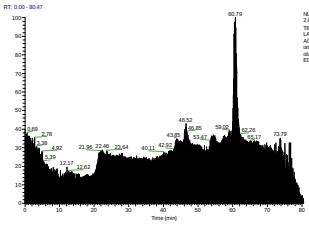	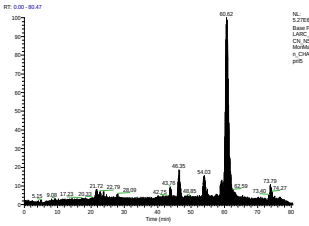	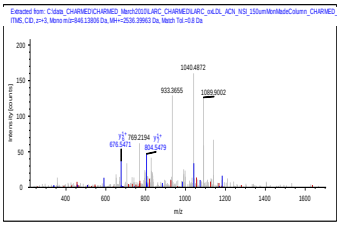
Frk	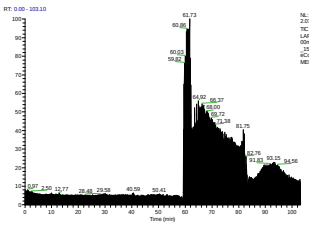	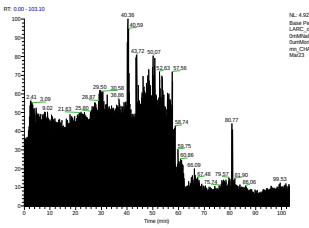	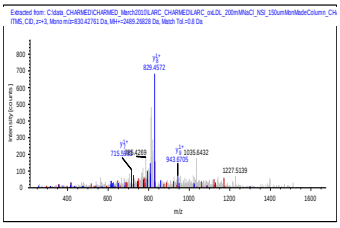

Syk Family Kinases

	TIC	Base Peak	Spectrum
ZAP-70 Isoform 1	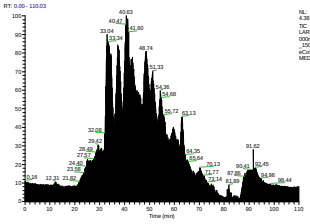	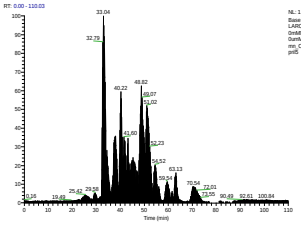	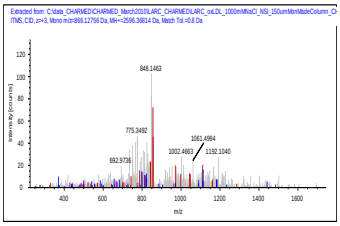
ZAP-70 Isoform 1	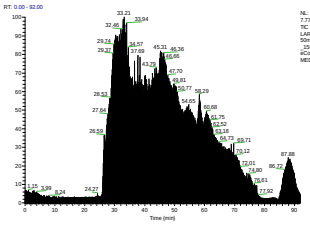	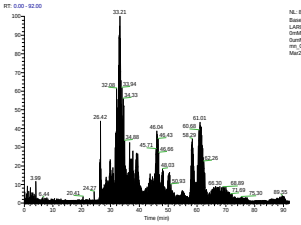	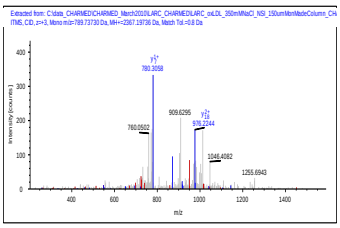
Syk	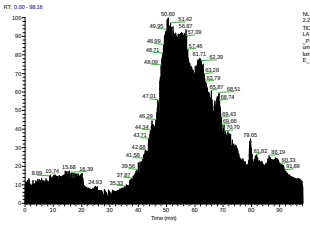	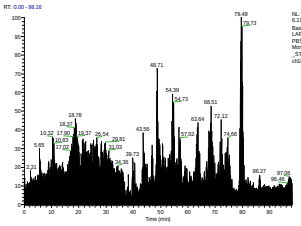	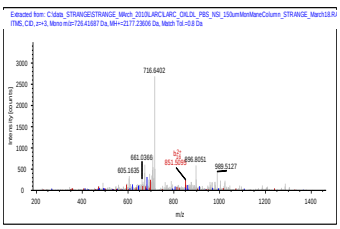
Syk	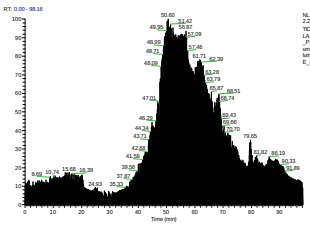	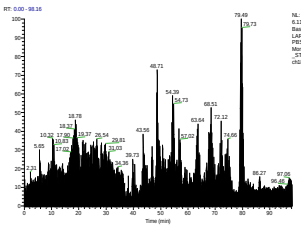	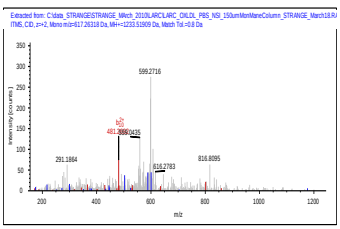

Focal Adhesion Kinases

	TIC	Base Peak	Spectrum

PTK2 Isoform B

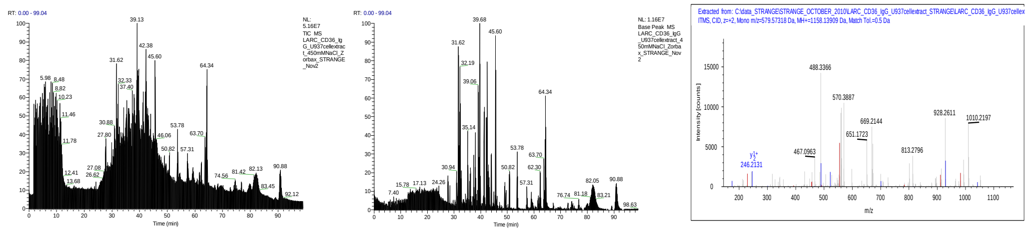

PTK2 Isoform B

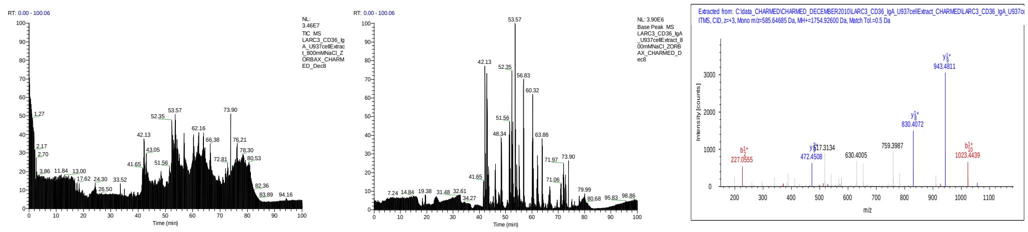

PTK2 Isoform B

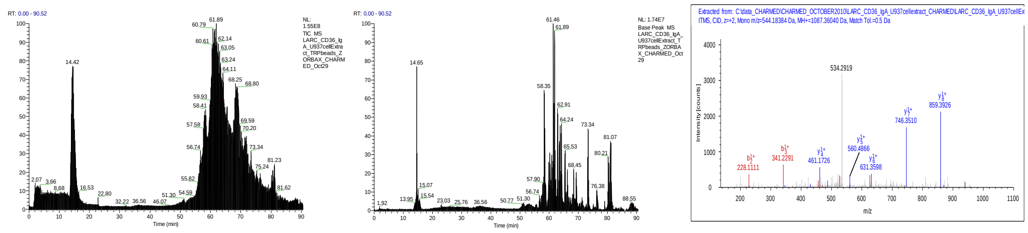

PTK2 Isoform B

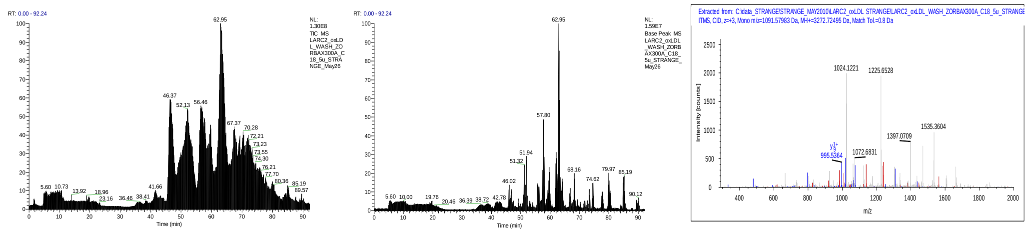

PTK2 Isoform B

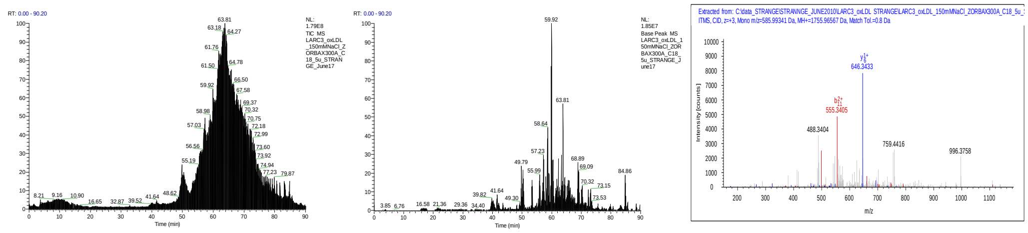

PTK2 Isoform B

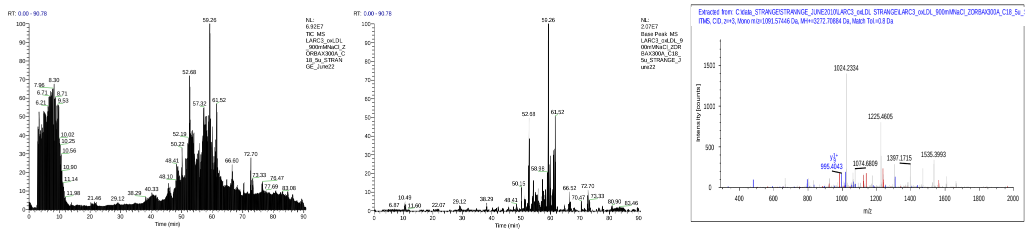

Focal Adhesion Kinases

	TIC	Base Peak	Spectrum
PTK2 Isoform B	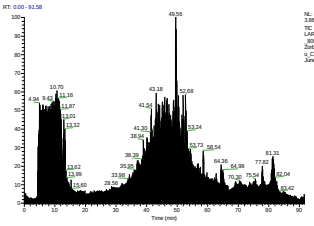	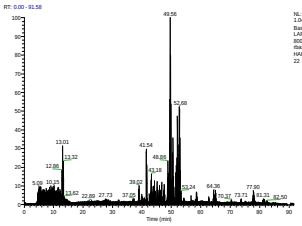	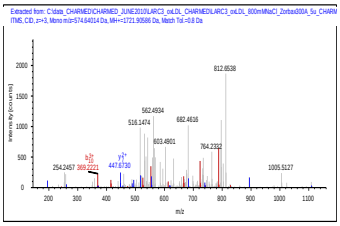

Phospholipase C

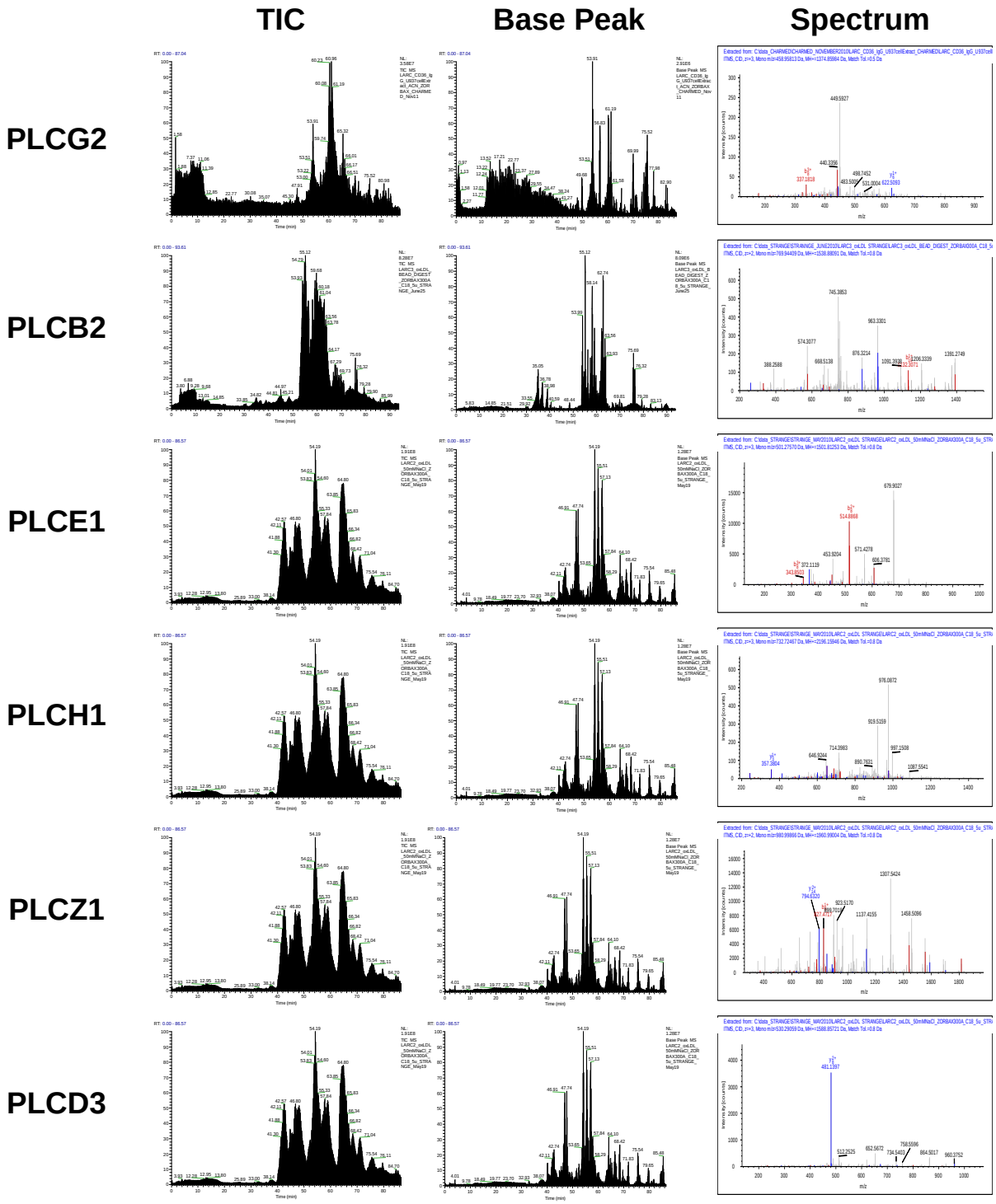

Protein Kinase C

TIC	Base Peak	Spectrum

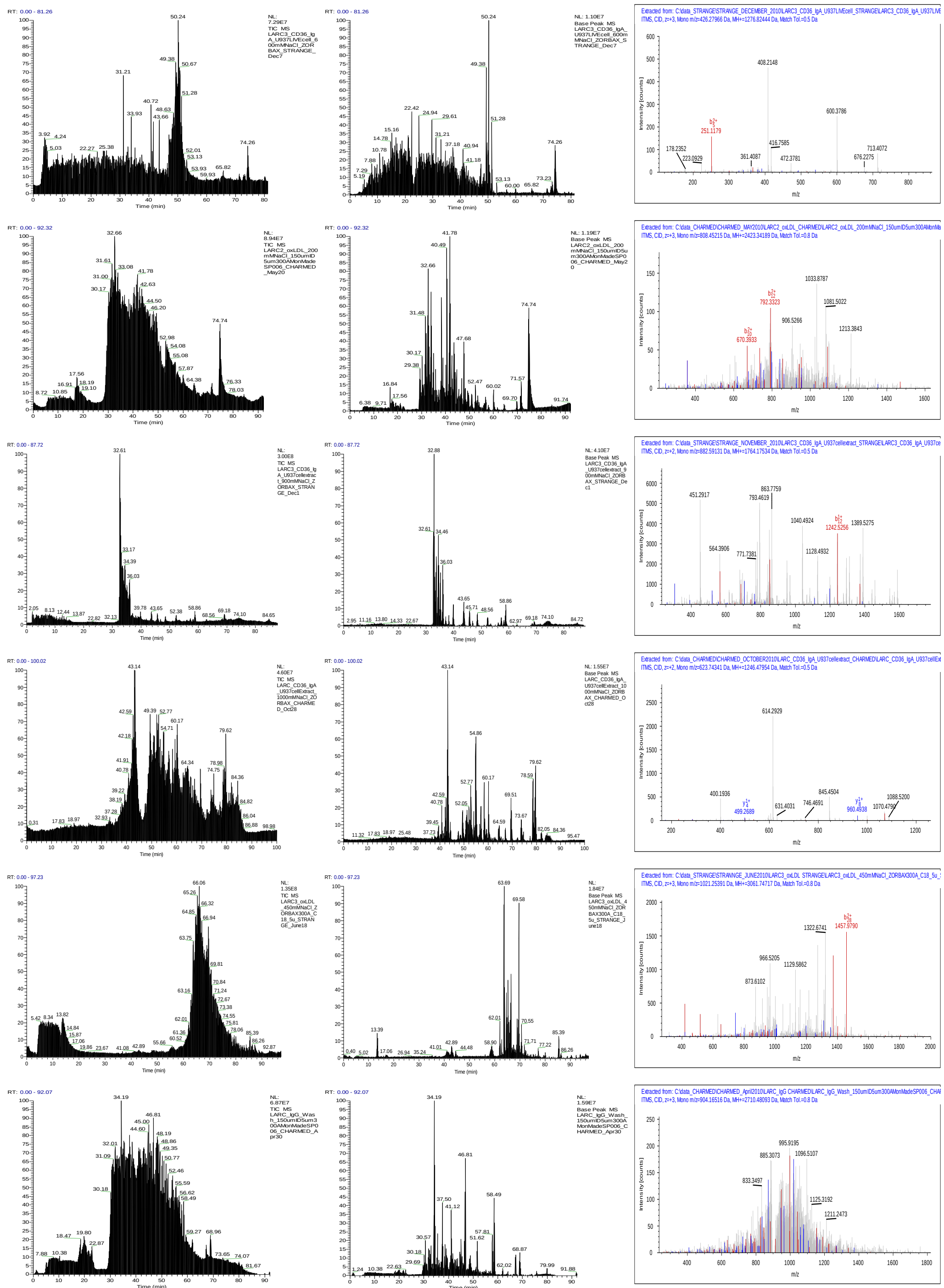

PKC Alpha

PKC Alpha

PKC Alpha

PKC Alpha

PKC Alpha

PKC Alpha

Protein Kinase C

	TIC	Base Peak	Spectrum
PKC Beta	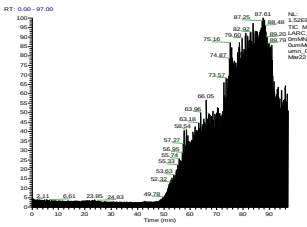	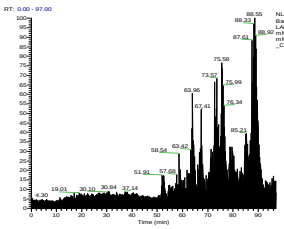	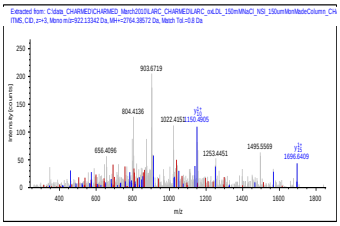
PKC Delta VIII	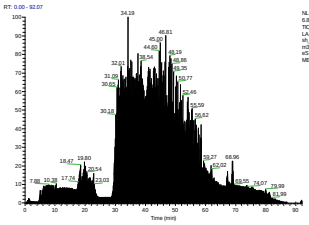	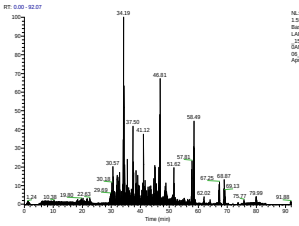	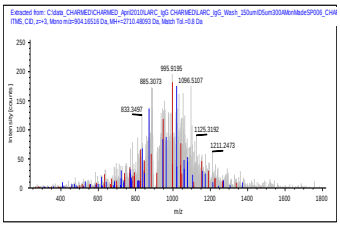
PKC Epsilon	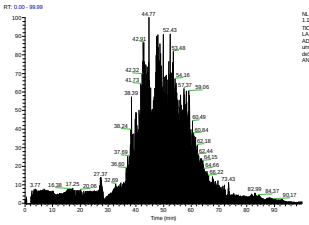	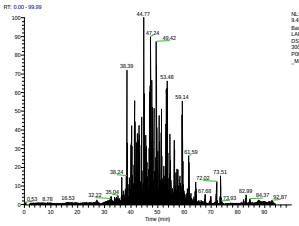	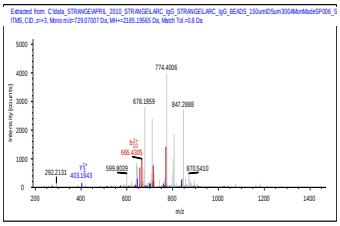
PKC Epsilon	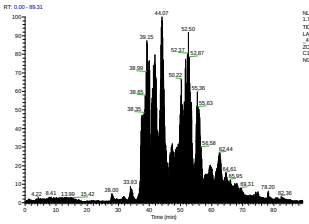	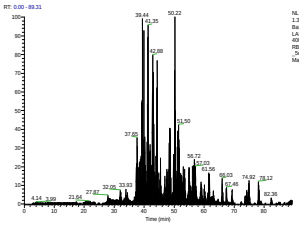	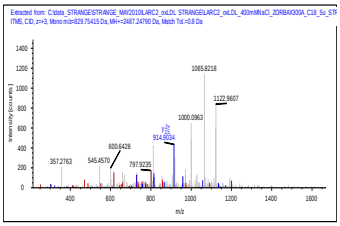
PKC Epsilon	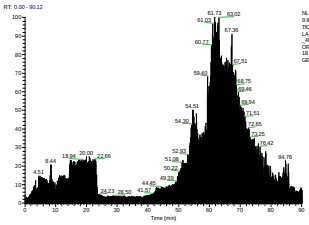	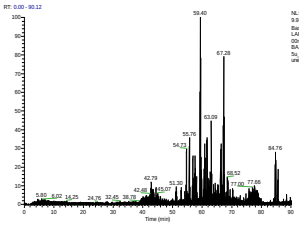	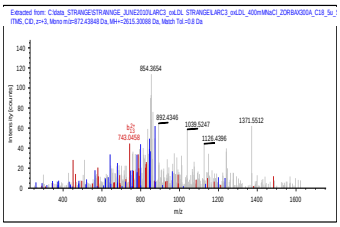
PKC Epsilon	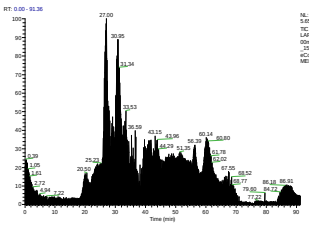	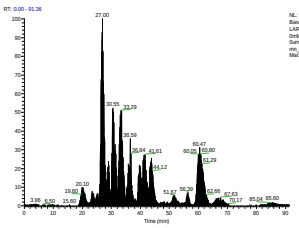	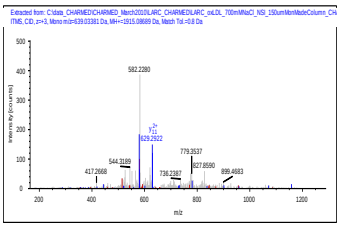

Protein Kinase C

	TIC	Base Peak	Spectrum
PKC Zeta Isoform 1	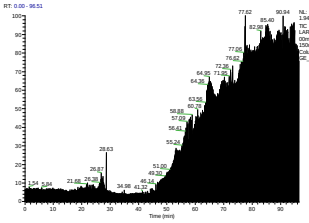	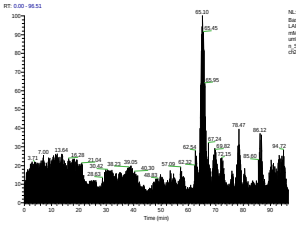	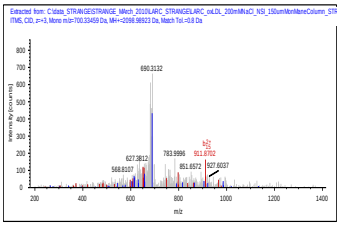
PKC Zeta Isoform 1	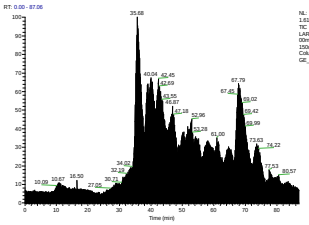	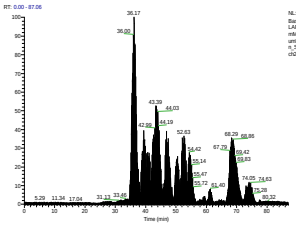	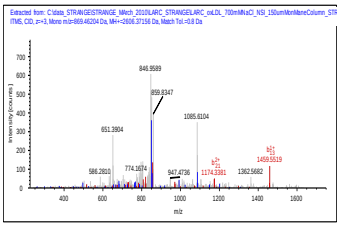
PKC Eta	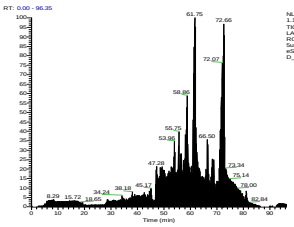	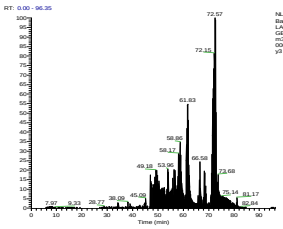	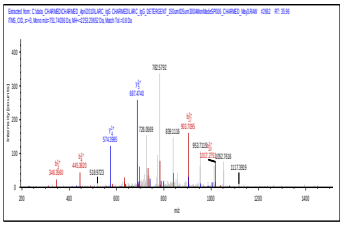
PKC Iota	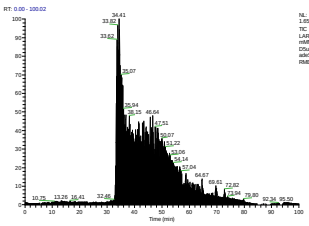	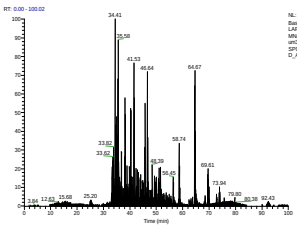	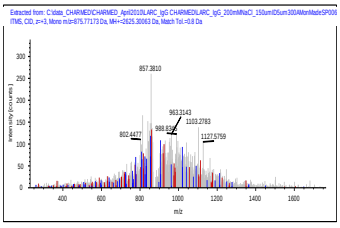

Phosphoinositide 3-kinase

	TIC	Base Peak	Spectrum
PI3KCA	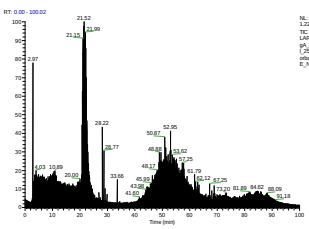	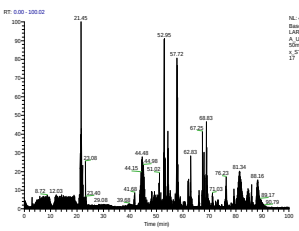	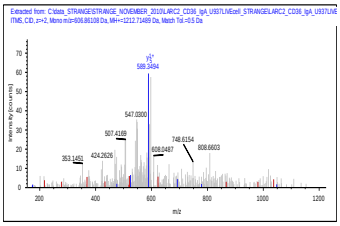
PIK3CB	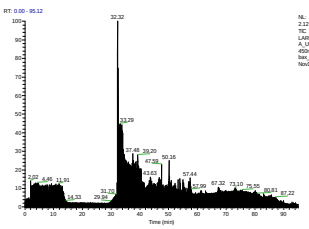	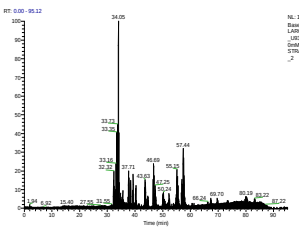	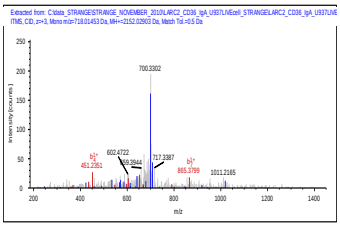
PIK3CB	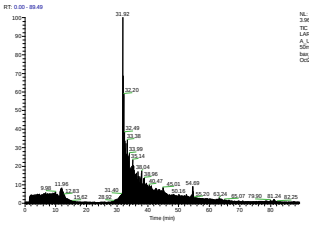	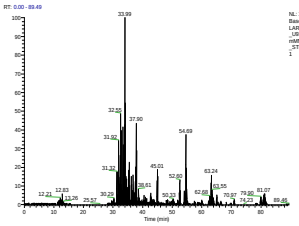	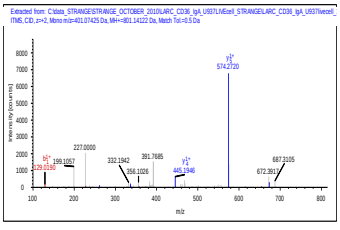
PIK3CB	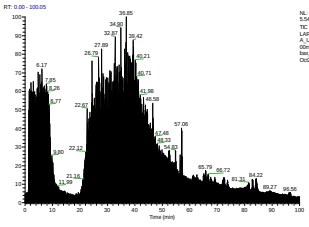	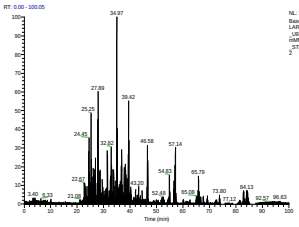	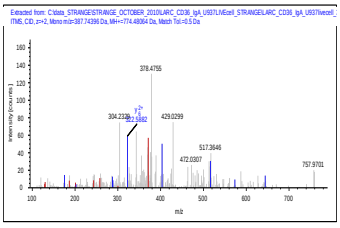
PIK3CB	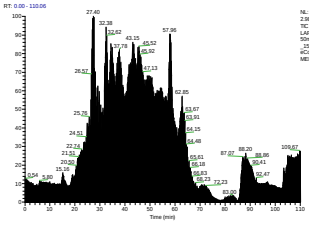	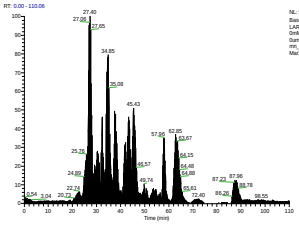	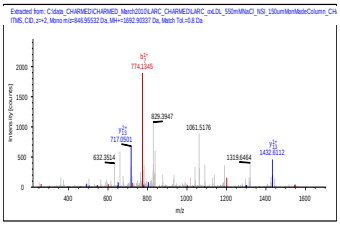
PIK3CB	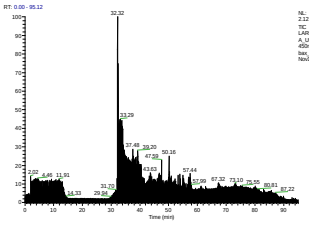	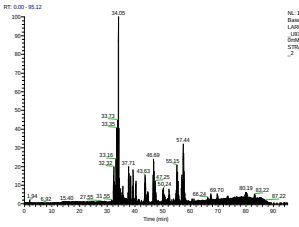	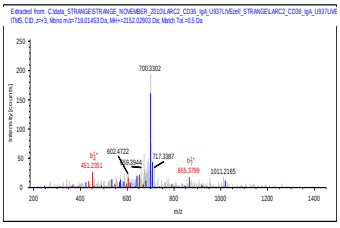

Phosphoinositide 3-kinase

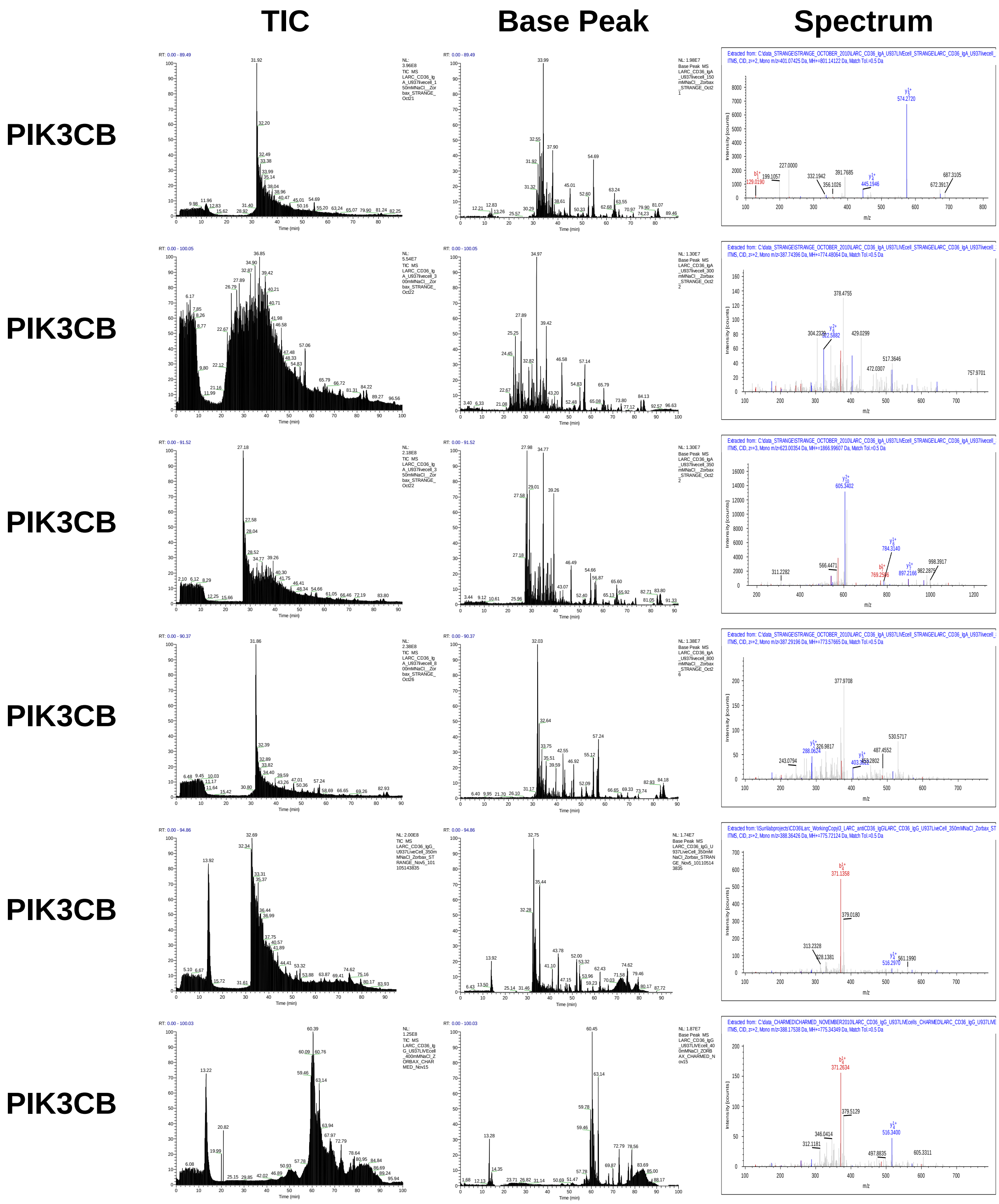

Phosphoinositide 3-kinase

	TIC	Base Peak	Spectrum
PIK3CB	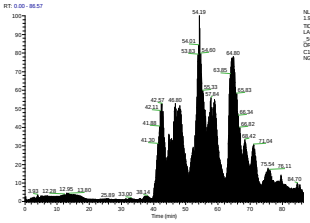	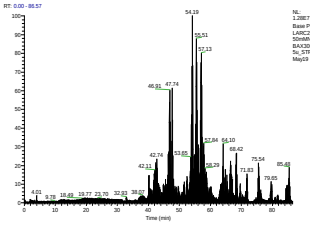	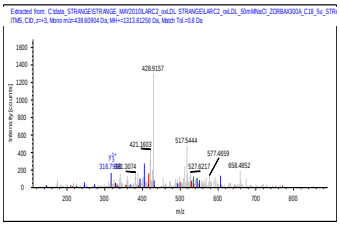
PIK3CB	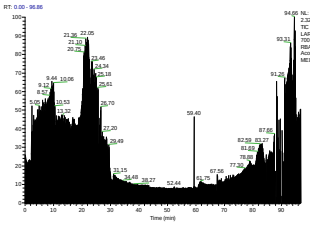	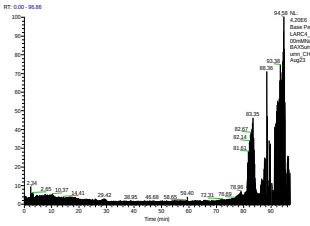	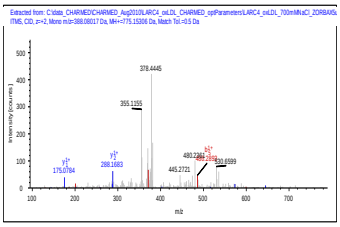

HMGCR

	TIC	Base Peak	Spectrum
HMGCR	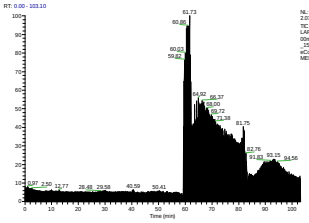	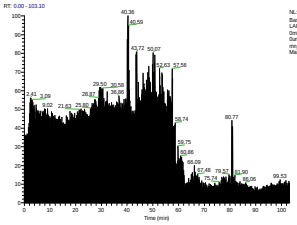	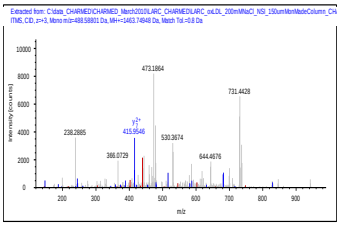
HMGCR	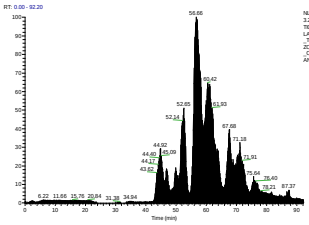	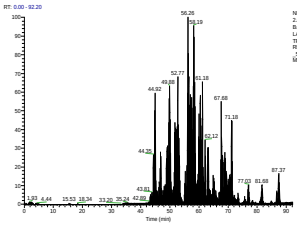	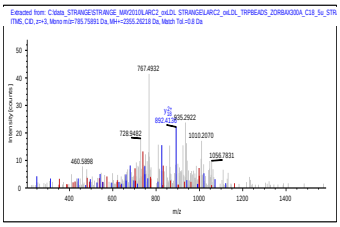
HMGCR	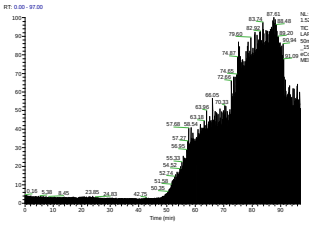	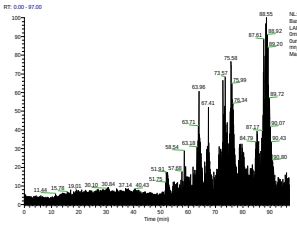	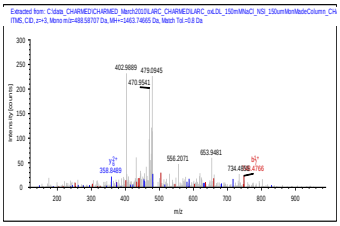

Janus Kinases

	TIC	Base Peak	Spectrum

JAK1

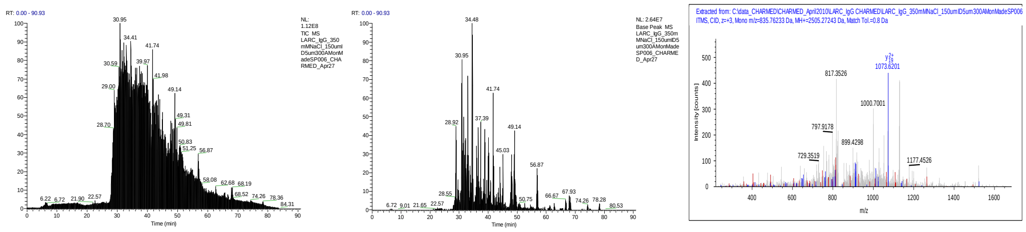

JAK1

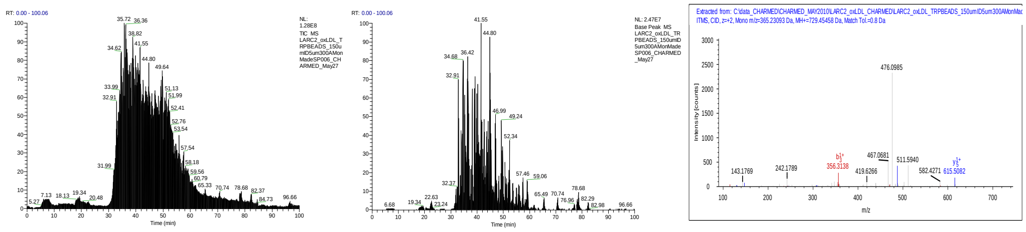

JAK1

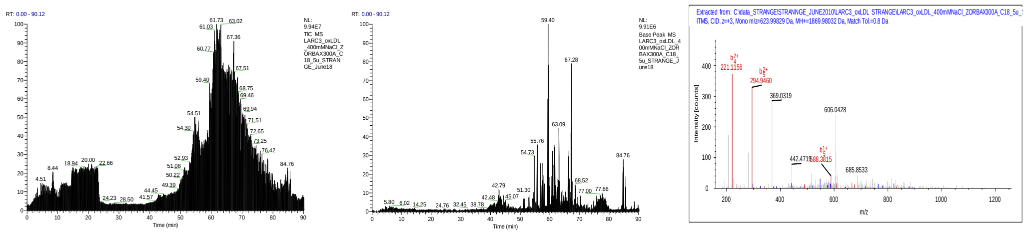

JAK1

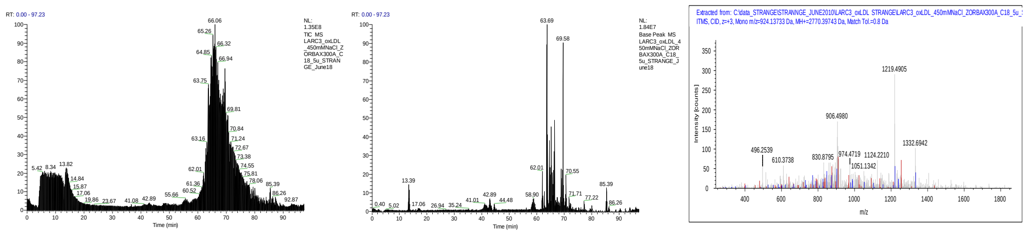

JAK1

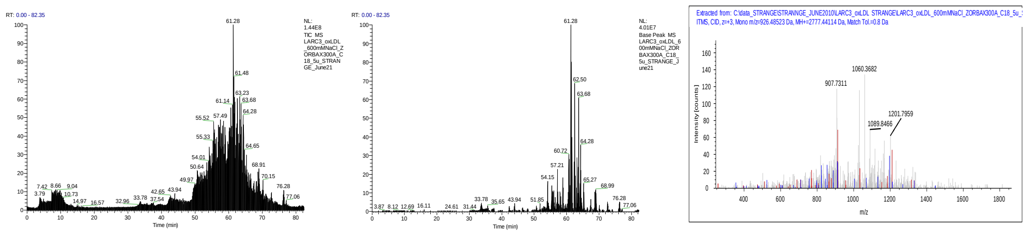

JAK1

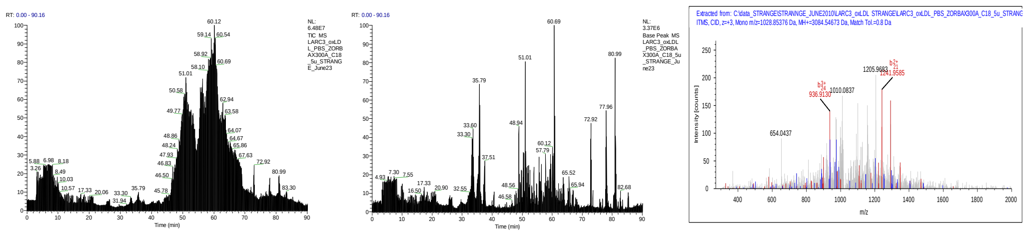

Janus Kinases

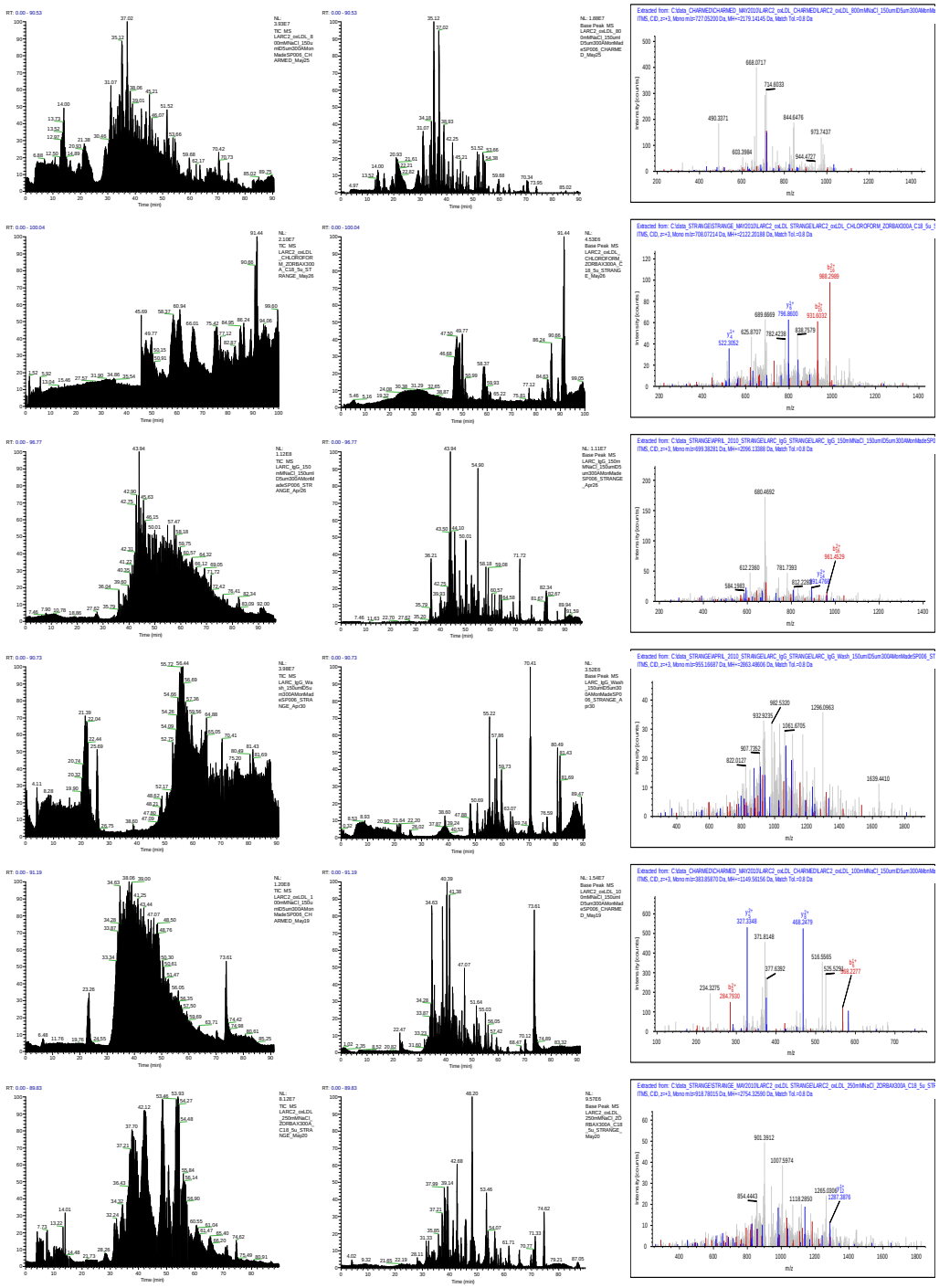

Janus Kinases

	TIC	Base Peak	Spectrum
JAK2	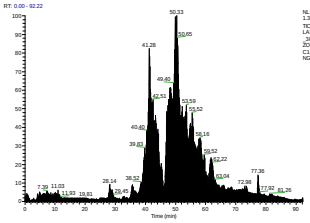	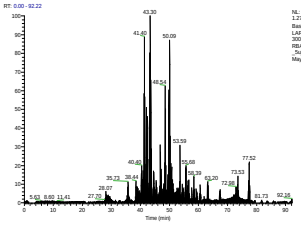	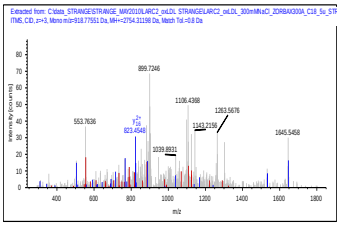
JAK2	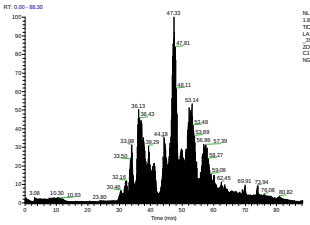	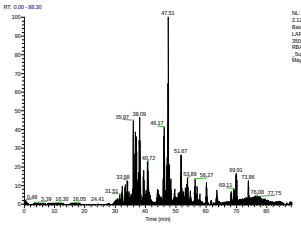	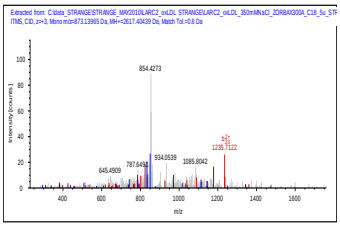
JAK2	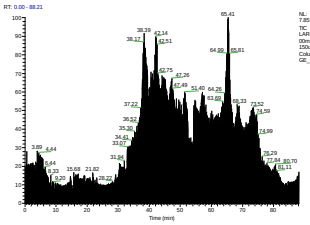	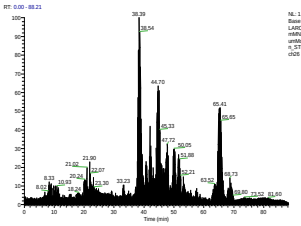	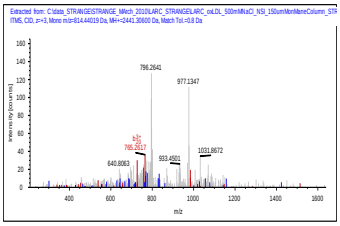
JAK3	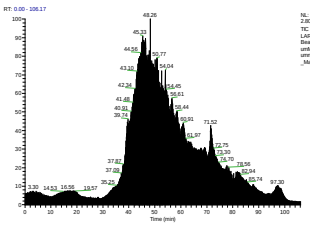	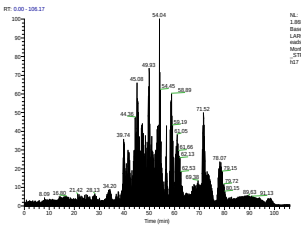	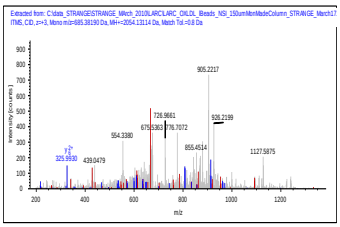

Phospholipase D

	TIC	Base Peak	Spectrum
PLD1	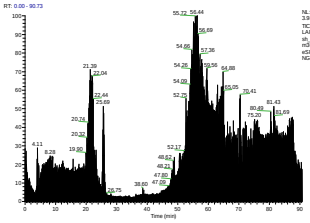	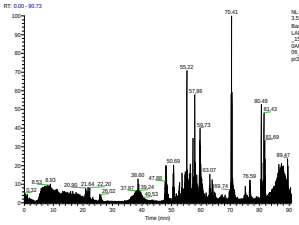	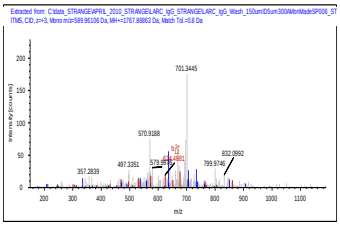
PLD2	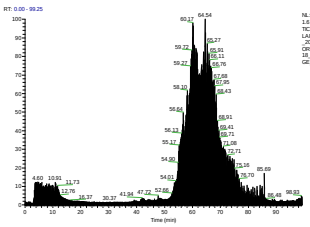	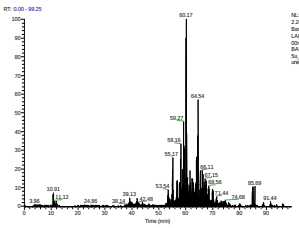	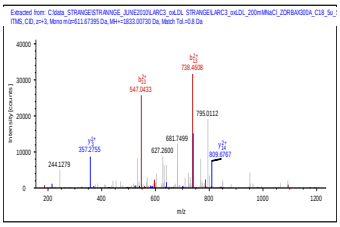
PLD2	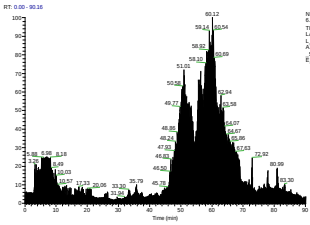	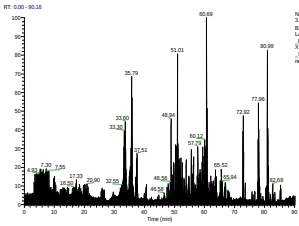	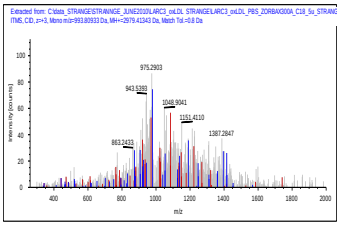
PLD2	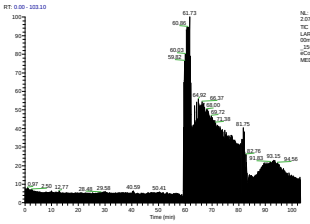	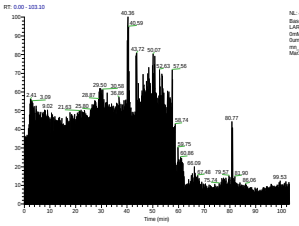	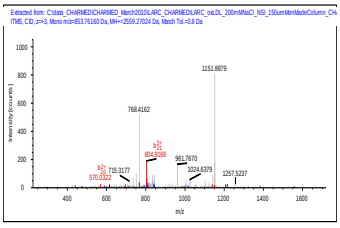
PLD3	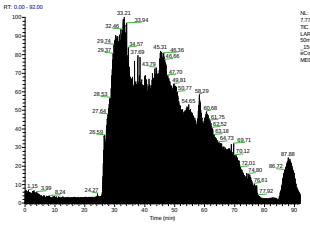	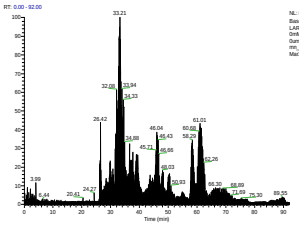	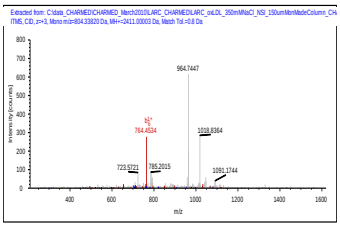
PLD3	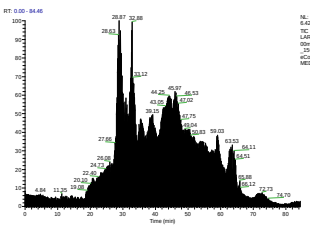	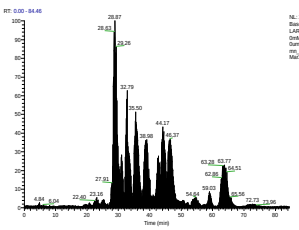	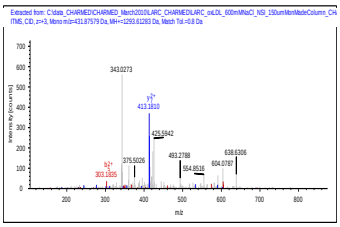

Phospholipase D

	TIC	Base Peak	Spectrum
PLD6	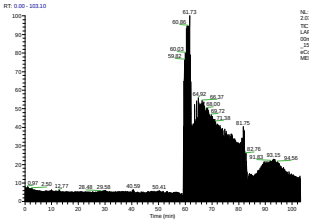	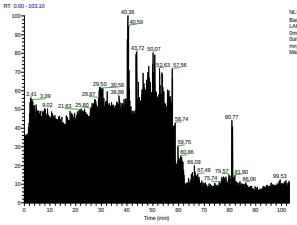	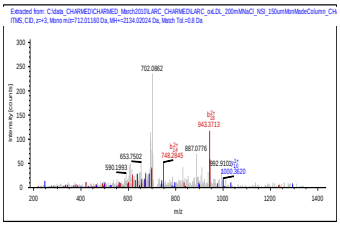
PLD6	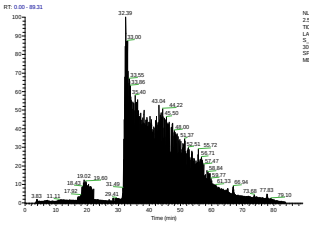	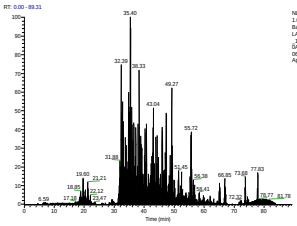	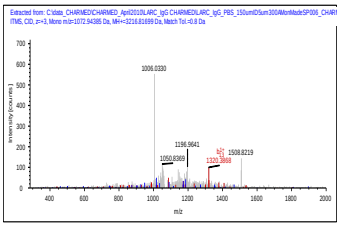

Phosphatidate Phosphatases

	TIC	Base Peak	Spectrum
Lipin1	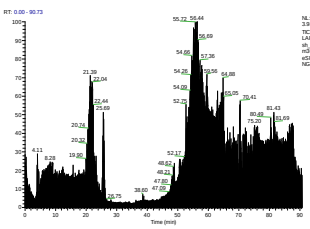	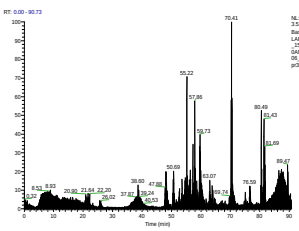	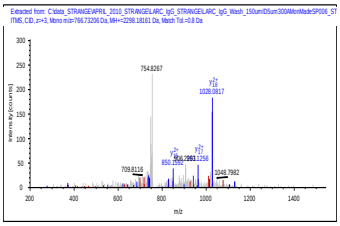
Lipin1	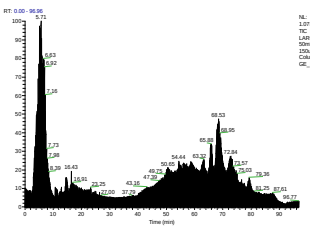	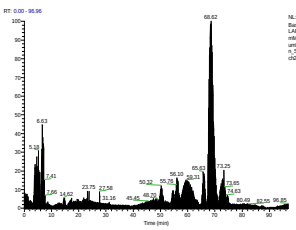	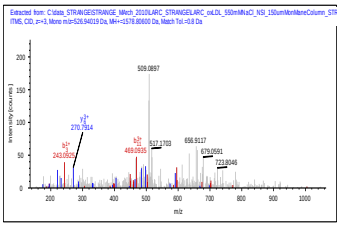
Lipin1	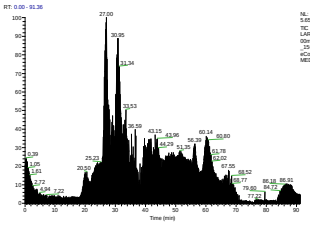	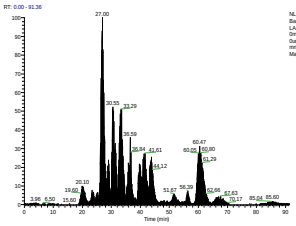	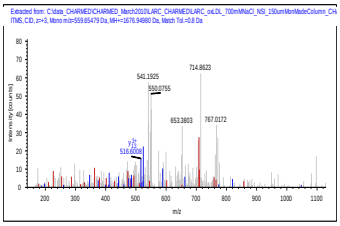
Lipin1	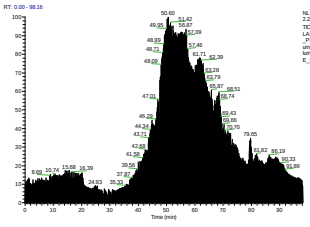	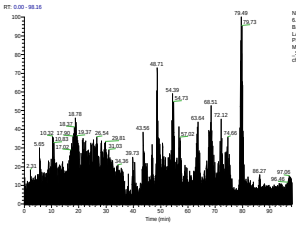	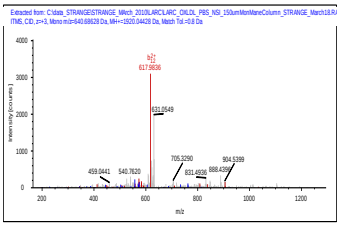
PPAPDC	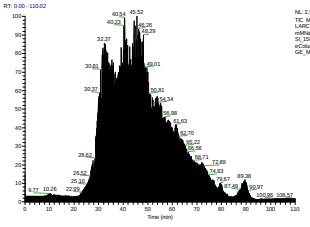	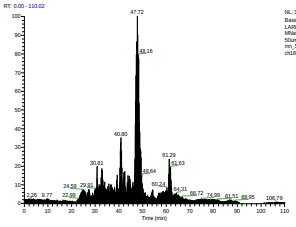	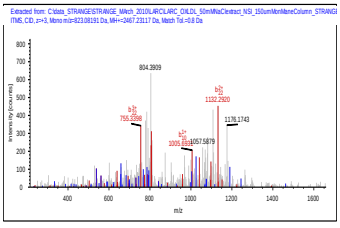

REFERENCES

Aderem, A. & Underhill, D.M. 1999, "Mechanisms of phagocytosis in macrophages", *Annual Review of Immunology,* vol. 17, pp. 593-623.

Aiken, M., Ginsberg, M., Byers-Ward, V. & Plow, E. 1990, "Effects of OKM5, a monoclonal antibody to glycoprotein IV, on platelet aggregation and thrombospondin surface expression", *Blood,* vol. 76, no. 12, pp. 2501-2509.

Akifusa, S., Kamio, N., Shimazaki, Y., Yamaguchi, N., Nonaka, K. & Yamashita, Y. 2010, "Involvement of the JAK-STAT pathway and SOCS3 in the regulation of adiponectin-generated reactive oxygen species in murine macrophage RAW 264 cells", *Journal of cellular biochemistry,* vol. 111, no. 3, pp. 597-606.

Aviram, M. 1993, "Modified Forms of Low-Density-Lipoprotein and Atherosclerosis", *Atherosclerosis,* vol. 98, no. 1, pp. 1-9.

Bamberger, M.E., Harris, M.E., McDonald, D.R., Husemann, J. & Landreth, G.E. 2003, "A Cell Surface Receptor Complex for Fibrillar β-Amyloid Mediates Microglial Activation", *The Journal of Neuroscience,* vol. 23, no. 7, pp. 2665-2674.

Bhatt, K.H., Pandey, R.K., Dahiya, Y. & Sodhi, A. 2010, "Protein kinase Cδ and protein tyrosine kinase regulate peptidoglycan-induced nuclear factor-κB activation and inducible nitric oxide synthase expression in mouse peritoneal macrophages in vitro", *Molecular immunology,* vol. 47, no. 4, pp. 861-870.

Bobryshev, Y.V. 2006, "Monocyte recruitment and foam cell formation in atherosclerosis", *Micron,* vol. 37, no. 3, pp. 208-222.

Boekhoudt, G.H., Frazier-Jessen, M.R. & Feldman, G.M. 2007, "Immune complexes suppress IFN-gamma signaling by activation of the Fc-gamma RI pathway", *Journal of leukocyte biology,* vol. 81, no. 4, pp. 1086-1092.

Bull, H.A., Brickell, P.M. & Dowd, P.M. 1994, "src-related protein tyrosine kinases are physically associated with the surface antigen CD36 in human dermal microvascular endothelial cells", *FEBS letters,* vol. 351, no. 1, pp. 41-44.

Calvo, D., Gomez-Coronado, D., Suarez, Y., Lasuncion, M.A. & Vega, M.A. 1998, "Human CD36 is a high affinity receptor for the native lipoproteins HDL, LDL, and VLDL", *J.Lipid Res.,* vol. 39, no. 4, pp. 777-788.

Cammer, M., Gevrey, J., Lorenz, M., Dovas, A., Condeelis, J. & Cox, D. 2009, "The Mechanism of CSF-1-induced Wiskott-Aldrich Syndrome Protein Activation in Vivo", *Journal of Biological Chemistry,* vol. 284, no. 35, pp. 23302-23311.

Chan, G., Bivins-Smith, E.R., Smith, M.S. & Yurochko, A.D. 2009, "NF-κB and phosphatidylinositol 3-kinase activity mediates the HCMV-induced atypical M1/M2 polarization of monocytes", *Virus research,* vol. 144, no. 1-2, pp. 329-333.

Chen, K., Febbraio, M., Li, W. & Silverstein, R.L. 2008, "A Specific CD36-Dependent Signaling Pathway Is Required for Platelet Activation by Oxidized Low-Density Lipoprotein", *Circulation research,* vol. 102, no. 12, pp. 1512-1519.

Chiou, W., Don, M., Liao, J. & Wei, B. "Psoralidin inhibits LPS-induced iNOS expression via repressing Syk-mediated activation of PI3K-IKK-IκB signaling pathways", *European journal of pharmacology,* vol. In Press, Uncorrected Proof.

Cho, M., Moon, Y., Heo, Y., Woo, Y., Ju, J., Park, K., Kim, S., Park, S., Kim, H. & Min, J. 2009, "NF-κB inhibition leads to increased synthesis and secretion of MIF in human CD4+ T cells", *Immunology letters,* vol. 123, no. 1, pp. 21-30.

Chou, M., Fogelstrand, L., Hartvigsen, K., Hansen, L.F., Woelkers, D., Shaw, P.X., Choi, J., Perkmann, T., Bäckhed, F., Miller, Y.I., Hörkkö, S., Corr, M., Witztum, J.L. & Binder, C.J. 2009, "Oxidation-specific epitopes are dominant targets of innate natural antibodies in mice and humans", *The Journal of clinical investigation,* vol. 119, no. 5, pp. 1335-1349.

Collins, R.F., Touret, N., Kuwata, H., Tandon, N.N., Grinstein, S. & Trimble, W.S. 2009, "Uptake of oxLDL by CD36 occurs by an actin-dependent pathway distinct from macropinocytosis", *Journal of Biological Chemistry,* .

Collot-Teixeira, S., Martin, J., McDennott-Roe, C., Poston, R. & McGregor, J.L. 2007, "CD36 and macrophages in atherosclerosis", *Cardiovascular research,* vol. 75, no. 3, pp. 468-477.

Coraci, I.S., Husemann, J., Berman, J.W., Hulette, C., Dufour, J.H., Campanella, G.K., Luster, A.D., Silverstein, S.C. & El Khoury, J.B. 2002, "CD36, a Class B Scavenger Receptor, Is Expressed on Microglia in Alzheimer's Disease Brains and Can Mediate Production of Reactive Oxygen Species in Response to β-Amyloid Fibrils", *The American Journal of Pathology,* vol. 160, no. 1, pp. 101-112.

Corrotte, M., Chasserot-Golaz, S., Huang, P., Du, G., Ktistakis, N.T., Frohman, M.A., Vitale, N., Bader, M. & Grant, N.J. 2006, "Dynamics and Function of Phospholipase D and Phosphatidic Acid During Phagocytosis", *Traffic,* vol. 7, no. 3, pp. 365-377.

Cuschieri, J., Sakr, S., Bulger, E., Knoll, M., Arbabi, S. & Maier, R.V. 2009, "Oxidant Alterations in Cd16 Expression are Cytoskeletal Induced", *Shock,* vol. 32, no. 6, pp. 572-577.

Dalvai, M. & Bystricky, K. 2010, "Cell Cycle and Anti-Estrogen Effects Synergize to Regulate Cell Proliferation and ER Target Gene Expression", *PLoS ONE,* vol. 5, no. 6, pp. e11011.

Daoud, A.S., Jarmolych, J., Augustyn, J.M. & Fritz, K.E. 1981, "Sequential Morphologic Studies of Regression of Advanced Atherosclerosis", *Archives of Pathology & Laboratory Medicine,* vol. 105, no. 5, pp. 233-239.

Daviet, L., Malvoisin, E., Wild, T.F. & McGregor, J.L. 1997, "Thrombospondin induces dimerization of membrane-bound, but not soluble CD36", *Journal of Thrombosis and Haemostasis,* vol. 78, no. 2, pp. 897-901.

Davis, R.S. 2007, "Fc Receptor-Like Molecules", *Annual Review of Immunology,* vol. 25, no. 1, pp. 525-560.

de Kruif, M.D., van Gorp, E.C.M., Keller, T.T., Ossewaarde, J.M. & ten Cate, H. 2005, "Chlamydia pneumoniae infections in mouse models: relevance for atherosclerosis research", *Cardiovascular research,* vol. 65, no. 2, pp. 317-327.

Drage, M.G., Pecora, N.D., Hise, A.G., Febbraio, M., Silverstein, R.L., Golenbock, D.T., Boom, W.H. & Harding, C.V. 2009, "TLR2 and its co-receptors determine responses of macrophages and dendritic cells to lipoproteins of Mycobacterium tuberculosis", *Cellular immunology,* vol. 258, no. 1, pp. 29-37.

Endemann, G., Stanton, L.W., Madden, K.S., Bryant, C.M., White, R.T. & Protter, A.A. 1993, "Cd36 is a Receptor for Oxidized Low-Density-Lipoprotein", *Journal of Biological Chemistry,* vol. 268, no. 16, pp. 11811-11816.

Endo, A. 1979, "Monacolin K, a new hypocholesterolemic agent that specifically inhibits 3-hydroxy-3-methylglutaryl coenzyme A reductase", *The Journal of Antibiotics,* vol. 33, no. 3, pp. 334-336.

Engelmann, B. & Wiedmann, M.K.H. 2010, "Cellular phospholipid uptake: Flexible paths to coregulate the functions of intracellular lipids", *Biochimica et Biophysica Acta (BBA) - Molecular and Cell Biology of Lipids,* vol. 1801, no. 6, pp. 609-616.

Epstein, D., Rowlette, L. & Roberts, B. 1999, "Acto-myosin drug effects and aqueous outflow function", *Investigative Ophthalmology Visual Science,* vol. 40, no. 1, pp. 74-81.

Etienne-Manneville, S. & Hall, A. 2002, "Rho GTPases in cell biology", *Nature,* vol. 420, no. 6916, pp. 629-635.

Febbraio, M., Hajjar, D.P. & Silverstein, R.L. 2001, "CD36: a class B scavenger receptor involved in angiogenesis, atherosclerosis, inflammation, and lipid metabolism", *Journal of Clinical Investigation,* vol. 108, no. 6, pp. 785-791.

Febbraio, M., Podrez, E.A., Smith, J.D., Hajjar, D.P., Hazen, S.L., Hoff, H.F., Sharma, K. & Silverstein, R.L. 2000, "Targeted disruption of the class B scavenger receptor CD36 protects against atherosclerotic lesion development in mice", *Journal of Clinical Investigation,* vol. 105, no. 8, pp. 1049-1056.

Feldman, G., Chuang, E. & Finbloom, D. 1995, "IgG immune complexes inhibit IFN-gamma-induced transcription of the Fc gamma RI gene in human monocytes by preventing the tyrosine phosphorylation of the p91 (Stat1) transcription factor", *The Journal of Immunology*, vol. 154, no. 1, pp. 318-325.

Fulton, D., Condro, M.C., Pearce, K. & Glanzman, D.L. 2008, "The Potential Role of Postsynaptic Phospholipase C Activity in Synaptic Facilitation and Behavioral Sensitization in Aplysia", *Journal of neurophysiology*, vol. 100, no. 1, pp. 108-116.

Garcia, C.K., Wilund, K., Arca, M., Zuliani, G., Fellin, R., Maioli, M., Calandra, S., Bertolini, S., Cossu, F., Grishin, N., Barnes, R., Cohen, J.C. & Hobbs, H.H. 2001, "Autosomal Recessive Hypercholesterolemia Caused by Mutations in a Putative LDL Receptor Adaptor Protein", *Science*, vol. 292, no. 5520, pp. 1394-1398.

Georgakopoulos, T., Moss, S.T. & Kanagasundaram, V. "Integrin CD11c contributes to monocyte adhesion with CD11b in a differential manner and requires Src family kinase activity", *Molecular immunology*, vol. 45, no. 13, pp. 3671-3681.

Ghosh, S., Gepstein, S., Heikkila, J.J. & Dumbroff, E.B. 1988, "Use of a scanning densitometer or an ELISA plate reader for measurement of nanogram amounts of protein in crude extracts from biological tissues", *Analytical Biochemistry*, vol. 169, no. 2, pp. 227-233.

Glass, C.K. & Witztum, J.L. 2001, "Atherosclerosis: The Road Ahead", *Cell*, vol. 104, no. 4, pp. 503-516.

Gousset, K., Tsvetkova, N.M., Crowe, J.H. & Tablin, F. 2004, "Important role of raft aggregation in the signaling events of cold-induced platelet activation", *Biochimica et Biophysica Acta (BBA) - Biomembranes*, vol. 1660, no. 1-2, pp. 7-15.

Gralczyk, K., Soszyńska, K., Haus, O., Bielis, R. & Rość, D. 2009, *The influence of lovastatin on thrombomodulin gene expression in vascular endothelial cells--in vitro study.*

Greenberg, S., Chang, P. & Silverstein, S.C. 1994, "Tyrosine phosphorylation of the gamma subunit of Fc gamma receptors, p72syk, and paxillin during Fc receptor-mediated phagocytosis in macrophages.", *Journal of Biological Chemistry*, vol. 269, no. 5, pp. 3897-3902.

Greenberg, S., Chang, P. & Silverstein, S.C. 1993, "Tyrosine phosphorylation is required for Fc receptor-mediated phagocytosis in mouse macrophages.", *The Journal of experimental medicine*, vol. 177, no. 2, pp. 529-534.

Grkovich, A., Armando, A., Quehenberger, O. & Dennis, E.A. 2009, "TLR-4 mediated group IVA phospholipase A2 activation is phosphatidic acid phosphohydrolase 1 and protein kinase C dependent", *BBA - Molecular and Cell Biology of Lipids*, vol. 1791, no. 10, pp. 975-982.

Groves, E., Dart, A., Covarelli, V. & Caron, E. 2008, *Molecular mechanisms of phagocytic uptake in mammalian cells*, Birkhäuser Basel.

Ha, H., Lee, J., Kim, H., Kwak, H.B., Kim, H., Lee, S.E., Rhee, J.H., Kim, H. & Lee, Z.H. 2008, "Stimulation by TLR5 Modulates Osteoclast Differentiation through STAT1/IFN-{beta}", *The Journal of Immunology*, vol. 180, no. 3, pp. 1382-1389.

Han, C., Fu, J., Liu, Z., Huang, H., Luo, L. & Yin, Z. 2010, *Dipyrithione inhibits IFN-γ-induced JAK/STAT1 signaling pathway activation and IP-10/CXCL10 expression in RAW264.7 cells*, Birkhäuser Basel.

Hatta, M., Matsuzaki, T., Morioka, Y., Yoshida, Y. & Noda, M. 2009, "Density- and serum-dependent regulation of the Reck tumor suppressor in mouse embryo fibroblasts", *Cellular signalling*, vol. 21, no. 12, pp. 1885-1893.

Hillyard, D.Z., Jardine, A.G., McDonald, K.J. & Cameron, A.J.M. 2004, "Fluvastatin inhibits raft dependent Fc gamma receptor signalling in human monocytes", *Atherosclerosis*, vol. 172, no. 2, pp. 219-228.

Hirano, K., Kuwasako, T., Nakagawa-Toyama, Y., Janabi, M., Yamashita, S. & Matsuzawa, Y. 2003, "Pathophysiology of Human Genetic CD36 Deficiency", *Trends in cardiovascular medicine*, vol. 13, no. 4, pp. 136-141.

Hoebe, K., Georgel, P., Rutschmann, S., Du, X., Mudd, S., Crozat, K., Sovath, S., Shamel, L., Hartung, T., Zahringer, U. & Beutler, B. 2005, "CD36 is a sensor of diacylglycerides", *Nature*, vol. 433, no. 7025, pp. 523-527.

Hoosdally, S.J., Andress, E.J., Wooding, C., Martin, C.A. & Linton, K.J. 2009, "The Human Scavenger Receptor CD36", *Journal of Biological Chemistry*, vol. 284, no. 24, pp. 16277-16288.

Hu, X., Chen, J., Wang, L. & Ivashkiv, L.B. 2007, "Crosstalk among Jak-STAT, Toll-like receptor, and ITAM-dependent pathways in macrophage activation", *Journal of leukocyte biology*, vol. 82, no. 2, pp. 237-243.

Huang, M.M., Bolen, J.B., Barnwell, J.W., Shattil, S.J. & Brugge, J.S. 1991, "Membrane glycoprotein IV (CD36) is physically associated with the Fyn, Lyn, and Yes protein-tyrosine kinases in human platelets", *Proceedings of the National Academy of Sciences of the United States of America*, vol. 88, no. 17, pp. 7844-7848.

Huang, Y., Yan, M., Collins, R.F., DiCiccio, J.E., Grinstein, S. & Trimble, W.S. 2008, "Mammalian Septins Are Required for Phagosome Formation", *Molecular biology of the cell*, vol. 19, no. 4, pp. 1717-1726.

Imagawa, N., Nagasawa, K., Nagai, K., Kawakami-Honda, N. & Fujimoto, S. "Protein kinase C-independent pathway for NADPH oxidase activation in guinea pig peritoneal polymorphonuclear leukocytes by cytochalasin D", *Archives of Biochemistry and Biophysics,* vol. 438, no. 2, pp. 119-124.

Ishibashi, S., Brown, M.S., Goldstein, J.L., Gerard, R.D., Hammer, R.E. & Herz, J. 1993, "Hypercholesterolemia in Low-Density-Lipoprotein Receptor Knockout Mice and its Reversal by Adenovirus-Mediated Gene Delivery", *Journal of Clinical Investigation,* vol. 92, no. 2, pp. 883-893.

Ivashkiv, L.B. 2009, "Cross-regulation of signaling by ITAM-associated receptors", *Nature immunology,* vol. 10, no. 4, pp. 340-347.

Janabi, M., Yamashita, S., Hirano, K., Matsumoto, K., Sakai, N., Hiraoka, H., Kashiwagi, H., Tomiyama, Y., Nozaki, S. & Matsuzawa, Y. 2001, "Reduced Adhesion of Monocyte-Derived Macrophages from CD36-Deficient Patients to Type I Collagen", *Biochemical and biophysical research communications,* vol. 283, no. 1, pp. 26-30.

Janabi, M., Yamashita, S., Hirano, K., Sakai, N., Hiraoka, H., Matsumoto, K., Zhang, Z., Nozaki, S. & Matsuzawa, Y. 2000, "Oxidized LDL-Induced NF-{kappa}B Activation and Subsequent Expression of Proinflammatory Genes Are Defective in Monocyte-Derived Macrophages From CD36-Deficient Patients", *Arteriosclerosis, Thrombosis, and Vascular Biology,* vol. 20, no. 8, pp. 1953-1960.

Jankowski, A., Zhu, P. & Marshall, J.G. 2008, "Capture of an activated receptor complex from the surface of live cells by affinity receptor chromatography", *Analytical Biochemistry,* vol. 380, no. 2, pp. 235-248.

Jimenez, B., Volpert, O.V., Crawford, S.E., Febbraio, M., Silverstein, R.L. & Bouck, N. 2000, "Signals leading to apoptosis-dependent inhibition of neovascularization by thrombospondin-1", *Nature medicine,* vol. 6, no. 1, pp. 41-48.

Jing Chen-Roetling, Li, Z. & Regan, R.F. 2008, "Hemoglobin Neurotoxicity is Attenuated by Inhibitors of the Protein Kinase CK2 Independent of Heme Oxygenase Activity", *Current Neurovascular Research,* vol. 5, no. 3, pp. 193-198.

Jones, M.L., Shawe-Taylor, A.J., Williams, C.M. & Poole, A.W. 2009, "Characterization of a novel focal adhesion kinase inhibitor in human platelets", *Biochemical and biophysical research communications,* vol. 389, no. 1, pp. 198-203.

Jones, N.L., Reagan, J.W. & Willingham, M.C. 2000, "The Pathogenesis of Foam Cell Formation : Modified LDL Stimulates Uptake of Co-Incubated LDL Via Macropinocytosis", *Arteriosclerosis, Thrombosis, and Vascular Biology,* vol. 20, no. 3, pp. 773-781.

Jones, N.L. & Willingham, M.C. 1999, "Modified LDLs are internalized by macrophages in part via macropinocytosis", *The Anatomical Record,* vol. 255, no. 1, pp. 57-68.

Kavanagh, I.C., Symes, C.E., Renaudin, P., Nova, E., Mesa, M.D., Boukouvalas, G., Leake, D.S. & Yaqoob, P. 2003, "Degree of oxidation of low density lipoprotein affects expression of CD36 and PPARγ, but not cytokine production, by human monocyte-macrophages", *Atherosclerosis,* vol. 168, no. 2, pp. 271-282.

Kazerounian, S., Duquette, M., Reyes, M.A., Lawler, J.T., Song, K., Perruzzi, C., Primo, L., Khosravi-Far, R., Bussolino, F., Rabinovitz, I. & Lawler, J. 2011, "Priming of the vascular endothelial growth factor signaling pathway by thrombospondin-1, CD36, and spleen tyrosine kinase", *Blood,* .

Kim, D.-., Lee, S.C. & Lee, H.-. 2009, "CD137 ligand-mediated reverse signals increase cell viability and cytokine expression in murine myeloid cells: Involvement of mTOR/p70S6 kinase and Akt", *European journal of immunology,* vol. 39, no. 9, pp. 2617-2628.

Koenigsknecht, J. & Landreth, G. 2004, "Microglial Phagocytosis of Fibrillar β-Amyloid through a β1 Integrin-Dependent Mechanism", *The Journal of Neuroscience,* vol. 24, no. 44, pp. 9838-9846.

Kruth, H.S., Jones, N.L., Huang, W., Zhao, B., Ishii, I., Chang, J., Combs, C.A., Malide, D. & Zhang, W. 2005, "Macropinocytosis Is the Endocytic Pathway That Mediates Macrophage Foam Cell Formation with Native Low Density Lipoprotein", *Journal of Biological Chemistry,* vol. 280, no. 3, pp. 2352-2360.

Kuchibhotla, S., Vanegas, D., Kennedy, D.J., Guy, E., Nimako, G., Morton, R.E. & Febbraio, M. 2008, "Absence of CD36 protects against atherosclerosis in ApoE knock-out mice with no additional protection provided by absence of scavenger receptor A I/II", *Cardiovascular research,* vol. 78, no. 1, pp. 185-196.

Kunjathoor, V.V., Febbraio, M., Podrez, E.A., Moore, K.J., Andersson, L., Koehn, S., Rhee, J.S., Silverstein, R., Hoff, H.F. & Freeman, M.W. 2002, "Scavenger Receptors Class A-I/II and CD36 Are the Principal Receptors Responsible for the Uptake of Modified Low Density Lipoprotein Leading to Lipid Loading in Macrophages", *Journal of Biological Chemistry,* vol. 277, no. 51, pp. 49982-49988.

Kusner, D., Hall, C. & Schlesinger, L. 1996, "Activation of phospholipase D is tightly coupled to the phagocytosis of Mycobacterium tuberculosis or opsonized zymosan by human macrophages", *The Journal of experimental medicine,* vol. 184, no. 2, pp. 585-595.

Lafrenaye, A.D. & Fuss, B. 2010, "Focal adhesion kinase can play unique and opposing roles in regulating the morphology of differentiating oligodendrocytes", *Journal of Neurochemistry,* vol. 115, no. 1, pp. 269-282.

Laitinen, L., Takala, E., Vuorela, H., Vuorela, P., Kaukonen, A.M. & Marvola, M. "Anthranoid laxatives influence the absorption of poorly permeable drugs in human intestinal cell culture model (Caco-2)", *European Journal of Pharmaceutics and Biopharmaceutics,* vol. 66, no. 1, pp. 135-145.

Larsen, E.C., DiGennaro, J.A., Saito, N., Mehta, S., Loegering, D.J., Mazurkiewicz, J.E. & Lennartz, M.R. 2000, "Differential Requirement for Classic and Novel PKC Isoforms in Respiratory Burst and Phagocytosis in RAW 264.7 Cells", *The Journal of Immunology,* vol. 165, no. 5, pp. 2809-2817.

Larsen, E.C., Ueyama, T., Brannock, P.M., Shirai, Y., Saito, N., Larsson, C., Loegering, D., Weber, P.B. & Lennartz, M.R. 2002, "A role for PKC-ε in FcγR-mediated phagocytosis by RAW 264.7 cells", *The Journal of cell biology,* vol. 159, no. 6, pp. 939-944.

Lee, K.J., Kim, H.A., Kim, P.H., Lee, H.S., Ma, K.R., Park, J.H., Kim, D.J. & Hahn, J.H. 2004, "Ox-LDL suppresses PMA-induced MMP-9 expression and activity through CD36-mediated activation of PPAR-gamma", *EXPERIMENTAL and MOLECULAR MEDICINE,* vol. 36, no. 6, pp. 534-544.

Lennartz, M.R. 1999, "Phospholipases and phagocytosis: the role of phospholipid-derived second messengers in phagocytosis", *The international journal of biochemistry & cell biology,* vol. 31, no. 3-4, pp. 415-430.

Li, G., Xie, J., Lei, X. & Zhang, L. 2009, "Macrophage migration inhibitory factor regulates proliferation of gastric cancer cells via the PI3K/Akt pathway", *World Journal of Gastroenterology,* vol. 15, no. 44, pp. 5541-5548.

Lipsky, R.H., Eckert, D.M., Tang, Y. & Ockenhouse, C.F. 1997, "The carboxyl-terminal cytoplasmic domain of CD36 is required for oxidized low-density lipoprotein modulation of NF-kappaB activity by tumor necrosis factor-alpha", *RECEPTORS & SIGNAL TRANSDUCTION,* vol. 7, no. 1, pp. 1-11.

Llodrá, J., Angeli, V., Liu, J., Trogan, E., Fisher, E.A. & Randolph, G.J. 2004, "Emigration of monocyte-derived cells from atherosclerotic lesions characterizes regressive, but not progressive, plaques", *Proceedings of the National Academy of Sciences of the United States of America,* vol. 101, no. 32, pp. 11779-11784.

Loike, J.D., Shabtai, D.Y., Neuhut, R., Malitzky, S., Lu, E., Husemann, J., Goldberg, I.J. & Silverstein, S.C. 2004, "Statin Inhibition of Fc Receptor-Mediated Phagocytosis by Macrophages Is Modulated by Cell Activation and Cholesterol", *Arteriosclerosis, Thrombosis, and Vascular Biology,* vol. 24, no. 11, pp. 2051-2056.

Maa, M., Chang, M.Y., Chen, Y., Lin, C., Yu, C.J., Yang, Y.L., Li, J., Chen, P., Tang, C., Lei, H. & Leu, T. 2008, "Requirement of Inducible Nitric-oxide Synthase in Lipopolysaccharide-mediated Src Induction and Macrophage Migration", *Journal of Biological Chemistry,* vol. 283, no. 46, pp. 31408-31416.

Mallants, R., Vlaeminck, V., Jorissen, M. & Augustijns, P. 2009, "An improved primary human nasal cell culture for the simultaneous determination of transepithelial transport and ciliary beat frequency", *Journal of Pharmacy and Pharmacology,* vol. 61, no. 7, pp. 883-890.

Mandal, C.C., Ghosh-Choudhury, N., Yoneda, T., Choudhury, G.G. & Ghosh-Choudhury, N. "Simvastatin prevents skeletal metastasis of breast cancer by an antagonistic interplay between p53 and CD44", *Journal of Biological Chemistry,* .

Marshall, J.G., Booth, J.W., Stambolic, V., Mak, T., Balla, T., Schreiber, A.D., Meyer, T. & Grinstein, S. 2001, "Restricted Accumulation of Phosphatidylinositol 3-Kinase Products in a Plasmalemmal Subdomain during Fcγ Receptor-Mediated Phagocytosis", *The Journal of cell biology,* vol. 153, no. 7, pp. 1369-1380.

Mathers, C.D., Boerma, T. & Ma Fat, D. 2009, "Global and regional causes of death", *British medical bulletin,* vol. 92, no. 1, pp. 7-32.

Maxeiner, H., Husemann, J., Thomas, C.A., Loike, J.D., Khoury, J.E. & Silverstein, S.C. 1998, "Complementary Roles for Scavenger Receptor A and CD36 of Human Monocyte–derived Macrophages in Adhesion to Surfaces Coated with Oxidized Low-Density Lipoproteins and in Secretion of H2O2", *The Journal of experimental medicine,* vol. 188, no. 12, pp. 2257-2265.

Medeiros, L.A., Khan, T., El Khoury, J.B., Pham, C.L.L., Hatters, D.M., Howlett, G.J., Lopez, R., O'Brien, K.D. & Moore, K.J. 2004, "Fibrillar Amyloid Protein Present in Atheroma Activates CD36 Signal Transduction", *Journal of Biological Chemistry,* vol. 279, no. 11, pp. 10643-10648.

Metzler, B., Hu, Y., Dietrich, H. & Xu, Q. 2000, "Increased Expression and Activation of Stress-Activated Protein Kinases/c-Jun NH2-Terminal Protein Kinases in Atherosclerotic Lesions Coincide with p53", *American Journal of Pathology,* vol. 156, no. 6, pp. 1875-1886.

Miao, W., Vasile, E., Lane, W.S. & Lawler, J. 2001a, "CD36 associates with CD9 and integrins on human blood platelets", *Blood,* vol. 97, no. 6, pp. 1689-1696.

Miki, S., Horikawa, K., Nishizumi, H., Suemura, M., Sato, B., Yamamoto, M., Takatsu, K., Yamamoto, T. & Miki, Y. 2001, "Reduction of atherosclerosis despite hypercholesterolemia in lyn-deficient mice fed a high-fat diet", *Genes to Cells,* vol. 6, no. 1, pp. 37-42.

Miksa, M., Wu, R., Cui, X., Dong, W., Das, P., Simms, H.H., Ravikumar, T.S. & Wang, P. 2007, "Vasoactive Hormone Adrenomedullin and Its Binding Protein: Anti-Inflammatory Effects by Up-Regulating Peroxisome Proliferator-Activated Receptor-{gamma}", *The Journal of Immunology,* vol. 179, no. 9, pp. 6263-6272.

Mogami, H., Mills, C.L. & Gallagher, D.V. 1997, "Phospholipase C inhibitor, U73122, releases intracellular Ca2+, potentiates Ins(1,4,5)P-3-mediated Ca2+ release and directly activates ion channels in mouse pancreatic acinar cells", *Biochemical Journal,* vol. 324, pp. 645-651.

Mohty, D., Pibarot, P., Despres, J., Cote, C., Arsenault, B., Cartier, A., Cosnay, P., Couture, C. & Mathieu, P. 2008, "Association between plasma LDL particle size, valvular accumulation of oxidized LDL, and inflammation in patients with aortic stenosis", *Arteriosclerosis Thrombosis and Vascular Biology,* vol. 28, no. 1, pp. 187-193.

Munteanu, A., Taddei, M., Tamburini, I., Bergamini, E., Azzi, A. & Zingg, J. 2006, "Antagonistic Effects of Oxidized Low Density Lipoprotein and α-Tocopherol on CD36 Scavenger Receptor Expression in Monocytes", *Journal of Biological Chemistry,* vol. 281, no. 10, pp. 6489-6497.

Nakata, A., Nakagawa, Y., Nishida, M., Nozaki, S., Miyagawa, J., Nakagawa, T., Tamura, R., Matsumoto, K., Kameda-Takemura, K., Yamashita, S. & Matsuzawa, Y. 1999, "CD36, a Novel Receptor for Oxidized Low-Density Lipoproteins, Is Highly Expressed on Lipid-Laden Macrophages in Human Atherosclerotic Aorta", *Arteriosclerosis, Thrombosis, and Vascular Biology,* vol. 19, no. 5, pp. 1333-1339.

Nikkhah, M., Strobl, J., Peddi, B. & Agah, M. 2009, "Cytoskeletal role in differential adhesion patterns of normal fibroblasts and breast cancer cells inside silicon microenvironments", *Biomedical Microdevices,* vol. 11, no. 3, pp. 585-595.

Nozaki, S., Kashiwagi, H., Yamashita, S., Nakagawa, T., Kostner, B., Tomiyama, Y., Nakata, A., Ishigami, M., Miyagawa, J. & Kameda-Takemura, K. 1995, "Reduced uptake of oxidized low density lipoproteins in monocyte-derived macrophages from CD36-deficient subjects", *The Journal of clinical investigation,* vol. 96, no. 4, pp. 1859-1865.

Olakowska, E. & Olakowski, M. 2006, "Propranolol--a place in the modern therapy", *Wiadomości Lekarskie,* vol. 59, no. 5-6, pp. 388-391.

O'Luanaigh, N., Pardo, R., Fensome, A., Allen-Baume, V., Jones, D., Holt, M.R. & Cockcroft, S. 2002, "Continual Production of Phosphatidic Acid by Phospholipase D Is Essential for Antigen-stimulated Membrane Ruffling in Cultured Mast Cells", *Molecular biology of the cell,* vol. 13, no. 10, pp. 3730-3746.

Pan, X., Darby, C., Indik, Z.K. & Schreiber, A.D. 1999, "Activation of Three Classes of Nonreceptor Tyrosine Kinases Following Fc[gamma] Receptor Crosslinking in Human Monocytes,", *Clinical Immunology,* vol. 90, no. 1, pp. 55-64.

Pang, Y., Zheng, B., Fan, L., Rhodes, P.G. & Cai, Z. "IGF-1 protects oligodendrocyte progenitors against TNFα-induced damage by activation of PI3K/Akt and interruption of the mitochondrial apoptotic pathway", *Glia,* vol. 55, no. 11, pp. 1099-1107.

Park, Y.M., Febbraio, M. & Silverstein, R.L. 2009, *CD36 modulates migration of mouse and human macrophages in response to oxidized LDL and may contribute to macrophage trapping in the arterial intima.(Research article)(Report).*

Pentikainen, M.O., Oksjoki, R., Oorni, K. & Kovanen, P.T. 2002, "Lipoprotein Lipase in the Arterial Wall: Linking LDL to the Arterial Extracellular Matrix and Much More", *Arteriosclerosis, Thrombosis, and Vascular Biology*, vol. 22, no. 2, pp. 211-217.

Podrez, E.A., Febbraio, M., Sheibani, N., Schmitt, D., Silverstein, R.L., Hajjar, D.P., Cohen, P.A., Frazier, W.A., Hoff, H.F. & Hazen, S.L. 2000, "Macrophage scavenger receptor CD36 is the major receptor for LDL modified by monocyte-generated reactive nitrogen species", *The Journal of clinical investigation*, vol. 105, no. 8, pp. 1095-1108.

Podrez, E.A., Poliakov, E., Shen, Z., Zhang, R., Deng, Y., Sun, M., Finton, P.J., Shan, L., Febbraio, M., Hajjar, D.P., Silverstein, R.L., Hoff, H.F., Salomon, R.G. & Hazen, S.L. 2002, "A Novel Family of Atherogenic Oxidized Phospholipids Promotes Macrophage Foam Cell Formation via the Scavenger Receptor CD36 and Is Enriched in Atherosclerotic Lesions", *Journal of Biological Chemistry*, vol. 277, no. 41, pp. 38517-38523.

Prieto, J., Eklund, A. & Patarroyo, M. 1994, "Regulated Expression of Integrins and Other Adhesion Molecules during Differentiation of Monocytes into Macrophages", *Cellular immunology*, vol. 156, no. 1, pp. 191-211.

Qiao, J., Tripathi, J., Mishra, N., Cai, Y., Tripathi, S., Wang, X., Imes, S., Fishbein, M., Clinton, S., Libby, P., Lusis, A. & Rajavashisth, T. 1997, "Role of macrophage colony-stimulating factor in atherosclerosis: studies of osteopetrotic mice", *American Journal of Pathology*, vol. 150, no. 5, pp. 1687-1699.

Rahaman, S.O., Lennon, D.J., Febbraio, M., Podrez, E.A., Hazen, S.L. & Silverstein, R. 2006, "A CD36-dependent signaling cascade is necessary for macrophage foam cell formation", *Cell Metabolism*, vol. 4, no. 3, pp. 211-221.

Rahaman, S.O., Swat, W., Febbraio, M. & Silverstein, R.L. 2011, "Vav Family Rho Guanine Nucleotide Exchange Factors Regulate CD36-mediated Macrophage Foam Cell Formation", *Journal of Biological Chemistry*, vol. 286, no. 9, pp. 7010-7017.

Ricci, R., Sumara, G., Sumara, I., Rozenberg, I., Kurrer, M., Akhmedov, A., Hersberger, M., Eriksson, U., Eberli, F.R., Becher, B., Boren, J., Chen, M., Cybulsky, M.I., Moore, K.J., Freeman, M.W., Wagner, E.F., Matter, C.M. & Luscher, T.F. 2004, "Requirement of JNK2 for Scavenger Receptor A-Mediated Foam Cell Formation in Atherogenesis", *Science*, vol. 306, no. 5701, pp. 1558-1561.

Ross, R. 1999, "Atherosclerosis — An Inflammatory Disease", *New England Journal of Medicine*, vol. 340, no. 2, pp. 115-126.

Roy, B. & Rai, U. 2008, "Role of adrenoceptor-coupled second messenger system in sympatho-adrenomedullary modulation of splenic macrophage functions in live fish Channa punctatus", *General and comparative endocrinology*, vol. 155, no. 2, pp. 298-306.

Ruiz-Velasco, N., Domínguez, A. & Vega, M.A. 2004, "Statins upregulate CD36 expression in human monocytes, an effect strengthened when combined with PPAR-γ ligands Putative contribution of Rho GTPases in statin-induced CD36 expression", *Biochemical pharmacology*, vol. 67, no. 2, pp. 303-313.

Rusiñol, A.E., Yang, L., Thewke, D., Panini, S.R., Kramer, M.F. & Sinensky, M.S. 2000, *Isolation of a Somatic Cell Mutant Resistant to the Induction of Apoptosis by Oxidized Low Density Lipoprotein*.

Sanderson, M.P., Gelling, S.J., Rippmann, J.F. & Schnapp, A. 2010, "Comparison of the anti-allergic activity of Syk inhibitors with optimized Syk siRNAs in FcεRI-activated RBL-2H3 basophilic cells", *Cellular immunology*, vol. 262, no. 1, pp. 28-34.

Santy, L.C. & Casanova, J.E. 2001, "Activation of ARF6 by ARNO stimulates epithelial cell migration through downstream activation of both Rac1 and phospholipase D", *The Journal of cell biology*, vol. 154, no. 3, pp. 599-610.

Scott, C.C., Dobson, W., Botelho, R.J., Coady-Osberg, N., Chavrier, P., Knecht, D.A., Heath, C., Stahl, P. & Grinstein, S. 2005, "Phosphatidylinositol-4,5-bisphosphate hydrolysis directs actin remodeling during phagocytosis", *The Journal of cell biology*, vol. 169, no. 1, pp. 139-149.

Segal, G., Lee, W., Arora, P., McKee, M., Downey, G. & McCulloch, C. 2001, "Involvement of actin filaments and integrins in the binding step in collagen phagocytosis by human fibroblasts", *Journal of cell science*, vol. 114, no. 1, pp. 119-129.

Segrest, J.P., Jones, M.K., De Loof, H. & Dashti, N. 2001, "Structure of apolipoprotein B-100 in low density lipoproteins", *Journal of lipid research*, vol. 42, no. 9, pp. 1346-1367.

Seizer, P.F., Schiemann, S.F., Merz, T.F., Daub, K.F., Bigalke, B.F., Stellos, K.F., Muller, I.F., Stockle, C.F., Muller, K.F., Gawaz M FAU - May, Andreas,E. & May, A.E. 2010, *CD36 and macrophage scavenger receptor a modulate foam cell formation via inhibition of lipid-laden platelet phagocytosis*.

Serghides, L., Smith, T.G., Patel, S.N. & Kain, K.C. 2003, "CD36 and malaria: friends or foes?", *Trends in parasitology*, vol. 19, no. 10, pp. 461-469.

Shen, L., Zhou, L., Wang, B., Pu, J., Hu, L., Chai, D., Wang, L., Zeng, J. & He, B. 2008, "Oxidized low-density lipoprotein induces differentiation of RAW264.7 murine macrophage cell line into dendritic-like cells", *Atherosclerosis*, vol. 199, no. 2, pp. 257-264.

Silverstein, R.L. & Febbraio, M. 2000, "CD36 and atherosclerosis", *Current opinion in lipidology*, vol. 11, no. 5, pp. 483-491.

Singh, U., Dasu, M.R., Yancey, P.G., Afify, A., Devaraj, S. & Jialal, I. 2008, "Human C-reactive protein promotes oxidized low density lipoprotein uptake and matrix metalloproteinase-9 release in Wistar rats", *Journal of lipid research,* vol. 49, no. 5, pp. 1015-1023.

Slomiany, A., Nishikawa, H. & Slomiany, B.L. 2002, "Screening and modulation of extracellular signals by mucous barrier. Serum glycosylphosphatidylinositol phospholipase D (gpi-pld) releases protective mucous barrier from oral mucosa", *Journal of Physiology and Pharmacology,* vol. 53, no. 1, pp. 21-38.

Smith, J.D., Trogan, E., Ginsberg, M., Grigaux, C., Tian, J. & Miyata, M. 1995, "Decreased atherosclerosis in mice deficient in both macrophage colony-stimulating factor (op) and apolipoprotein E", *Proceedings of the National Academy of Sciences*, vol. 92, no. 18, pp. 8264-8268.

Srivastava, R.A., Ito, H., Hess, M., Srivastava, N. & Schonfeld, G. 1995, "Regulation of low density lipoprotein receptor gene expression in HepG2 and Caco2 cells by palmitate, oleate, and 25-hydroxycholesterol.", *Journal of lipid research,* vol. 36, no. 7, pp. 1434-1446.

Stadanlick, J.E., Kaileh, M., Karnell, F.G., Scholz, J.L., Miller, J.P., Quinn III, W.,J., Brezski, R.J., Treml, L.S., Jordan, K.A., Monroe, J.G., Sen, R. & Cancro, M.P. 2008, "Tonic B cell antigen receptor signals supply an NF-[kappa]B substrate for prosurvival BLyS signaling", *Nature immunology,* vol. 9, no. 12, pp. 1379-1387.

Stewart, C.R., Stuart, L.M., Wilkinson, K., van Gils, J.,M., Deng, J., Halle, A., Rayner, K.J., Boyer, L., Zhong, R., Frazier, W.A., Lacy-Hulbert, A., Khoury, J.E., Golenbock, D.T. & Moore, K.J. 2010, "CD36 ligands promote sterile inflammation through assembly of a Toll-like receptor 4 and 6 heterodimer", *Nature immunology,* vol. 11, no. 2, pp. 155-161.

Stuart, L.M., Bell, S.A., Stewart, C.R., Silver, J.M., Richard, J., Goss, J.L., Tseng, A.A., Zhang, A., Khoury, J.B.E. & Moore, K.J. 2007, "CD36 Signals to the Actin Cytoskeleton and Regulates Microglial Migration via a p130Cas Complex", *Journal of Biological Chemistry,* vol. 282, no. 37, pp. 27392-27401.

Sulahian, T., Imrich, A., DeLoid, G., Winkler, A. & Kobzik, L. 2008, "Signaling pathways required for macrophage scavenger receptor-mediated phagocytosis: analysis by scanning cytometry", *Respiratory Research,* vol. 9, no. 1, pp. 59.

Sun, X., He, X., Tzipori, S., Gerhard, R. & Feng, H. 2009, "Essential role of the glucosyltransferase activity in Clostridium difficile toxin-induced secretion of TNF-α by macrophages", *Microbial pathogenesis,* vol. 46, no. 6, pp. 298-305.

Suzuki, H., Kurihara, Y., Takeya, M., Kamada, N., Kataoka, M., Jishage, K., Ueda, O., Sakaguchi, H., Higashi, T., Suzuki, T., Takashima, Y., Kawabe, Y., Cynshi, O., Wada, Y., Honda, M., Kurihara, H., Aburatani, H., Doi, T., Matsumoto, A., Azuma, S., Noda, T., Toyoda, Y., Itakura, H., Yazaki, Y., Horiuchi, S., Takahashi, K., Kruijt, J.K., van Berkel, Theo J. C., Steinbrecher, U.P., Ishibashi, S., Maeda, N., Gordon, S. & Kodama, T. 1997, "A role for macrophage scavenger receptors in atherosclerosis and susceptibility to infection", *Nature*, vol. 386, no. 6622, pp. 292-296.

Swanson, J.A. & Hoppe, A.D. 2004, "The coordination of signaling during Fc receptor-mediated phagocytosis", *Journal of leukocyte biology*, vol. 76, no. 6, pp. 1093-1103.

Tandon, N.N., Kralisz, U. & Jamieson, G.A. 1989, "Identification of glycoprotein IV (CD36) as a primary receptor for platelet-collagen adhesion.", *Journal of Biological Chemistry*, vol. 264, no. 13, pp. 7576-7583.

Tandon, N., Lipsky, R., Burgess, W. & Jamieson, G. 1989, "Isolation and characterization of platelet glycoprotein IV (CD36)", *Journal of Biological Chemistry*, vol. 264, no. 13, pp. 7570-7575.

Tao, N., Wagner, S.J. & Lublin, D.M. 1996, "CD36 Is Palmitoylated on Both N- and C-terminal Cytoplasmic Tails", *Journal of Biological Chemistry*, vol. 271, no. 37, pp. 22315-22320.

Tatara, Y., Ohishi, M., Yamamoto, K., Shiota, A., Hayashi, N., Iwamoto, Y., Takeda, M., Takagi, T., Katsuya, T., Ogihara, T. & Rakugi, H. 2009, "Macrophage inflammatory protein-1β induced cell adhesion with increased intracellular reactive oxygen species", *Journal of Molecular and Cellular Cardiology*, vol. 47, no. 1, pp. 104-111.

Thorne, R.F., Marshall, J.F., Shafren, D.R., Gibson, P.G., Hart, I.R. & Burns, G.F. 2000, "The Integrins α3β1 and α6β1 Physically and Functionally Associate with CD36 in Human Melanoma Cells", *Journal of Biological Chemistry*, vol. 275, no. 45, pp. 35264-35275.

Thorne, R.F., Mhaidat, N.M., Ralston, K.J. & Burns, G.F. 2007, "Shed gangliosides provide detergent-independent evidence for Type-3 glycosynapses", *Biochemical and biophysical research communications*, vol. 356, no. 1, pp. 306-311.

Tripathi, A. & Sodhi, A. 2008, "Prolactin-induced production of cytokines in macrophages in vitro involves JAK/STAT and JNK MAPK pathways", *International immunology*, vol. 20, no. 3, pp. 327-336.

Tsimikas, S., Brilakis, E.S., Lennon, R.J., Miller, E.R., Witztum, J.L., McConnell, J.P., Kornman, K.S. & Berger, P.B. 2007, "Relationship of IgG and IgM autoantibodies to oxidized low density lipoprotein with coronary artery disease and cardiovascular events", *Journal of lipid research*, vol. 48, no. 2, pp. 425-433.

Underhill, D.M. & Goodridge, H.S. 2007, "The many faces of ITAMs", *Trends in immunology*, vol. 28, no. 2, pp. 66-73.

van der Vusse, G.J., van Bilsen, M., Glatz, J.F.C., Hasselbaink, D.M. & Luiken, J.J.F.P. 2002, *Critical steps in cellular fatty acid uptake and utilization*, Springer Netherlands.

Varret, M., Abifadel, M., Rabès, J. & Boileau, C. 2008, "Genetic heterogeneity of autosomal dominant hypercholesterolemia", *Clinical genetics,* vol. 73, no. 1, pp. 1-13.

Wang, W., Wu, Y. & Wu, C. 2006, "Prevention of Platelet Glycoprotein IIb/IIIa Activation by 3,4-Methylenedioxy-β-Nitrostyrene, A Novel Tyrosine Kinase Inhibitor", *Molecular pharmacology,* vol. 70, no. 4, pp. 1380-1389.

Wendt, M. & Schiemann, W. 2009, "Therapeutic targeting of the focal adhesion complex prevents oncogenic TGF-beta signaling and metastasis", *Breast Cancer Research,* vol. 11, no. 5, pp. R68.

Wilkinson, B., Koenigsknecht-Talboo, J., Grommes, C., Lee, C.Y.D. & Landreth, G. 2006, "Fibrillar β-Amyloid-stimulated Intracellular Signaling Cascades Require Vav for Induction of Respiratory Burst and Phagocytosis in Monocytes and Microglia", *Journal of Biological Chemistry,* vol. 281, no. 30, pp. 20842-20850.

Xue, Q., Jenkins, S.A., Gu, C., Smeds, E., Liu, Q., Vasan, R., Russell, B.H. & Xu, Y. 2010, "*Bacillus anthracis* Spore Entry into Epithelial Cells Is an Actin-Dependent Process Requiring c-Src and PI3K", *PLoS ONE,* vol. 5, no. 7, pp. e11665.

Yamada, Y., Doi, T., Hamakubo, T. & Kodama, T. 1998, "Scavenger receptor family proteins: roles for atherosclerosis, host defence and disorders of the central nervous system", *Cellular and Molecular Life Sciences,* vol. 54, no. 7, pp. 628-640.

Yamamoto, N., Ikeda, H., Tandon, N., Herman, J., Tomiyama, Y., Mitani, T., Sekiguchi, S., Lipsky, R., Kralisz, U. & Jamieson, G. 1990, "A platelet membrane glycoprotein (GP) deficiency in healthy blood donors: Naka- platelets lack detectable GPIV (CD36)", *Blood,* vol. 76, no. 9, pp. 1698-1703.

Yang, W.S., Seo, J.W., Han, N.J., Choi, J., Lee, K., Ahn, H., Lee, S.K. & Park, S. 2008, "High glucose-induced NF-{kappa}B activation occurs via tyrosine phosphorylation of I{kappa}B{alpha} in human glomerular endothelial cells: involvement of Syk tyrosine kinase", *AJP - Renal Physiology,* vol. 294, no. 5, pp. F1065-1075.

Yu, Y., Huang, Z., Yang, P., Rui, Y. & Yang, P. 2003, "Proteomic Studies of Macrophage-derived Foam Cell from Human U937 Cell Line Using Two-dimensional Gel Electrophoresis and Tandem Mass Spectrometry", *Journal of cardiovascular pharmacology,* vol. 42, no. 6, pp. 782-789.

Zeng, Y., Tao, N., Chung, K., Heuser, J.E. & Lublin, D.M. 2003b, "Endocytosis of Oxidized Low Density Lipoprotein through Scavenger Receptor CD36 Utilizes a Lipid Raft Pathway That Does Not Require Caveolin-1", *Journal of Biological Chemistry,* vol. 278, no. 46, pp. 45931-45936.

Zheleznyak, A. & Brown, E.J. 1992, "Immunoglobulin-mediated phagocytosis by human monocytes requires protein kinase C activation. Evidence for protein kinase C translocation to phagosomes.", *Journal of Biological Chemistry*, vol. 267, no. 17, pp. 12042-12048.

Zingg, J.M., Ricciarelli, R. & Azzi, A. 2000, "Scavenger receptors and modified lipoproteins: Fatal attractions?", *IUBMB life*, vol. 49, no. 5, pp. 397-403.

Zu, L., Shen, Z., Wesley, J. & Cai, Z.P. "PTEN inhibitors cause a negative inotropic and chronotropic effect in mice", *European journal of pharmacology*, vol. In Press, Uncorrected Proof.